

5-2008

## Using ANSYS Workbench Computer Environment in Turbomachinery Design Process

Patricia Lynn Bowlds

*Embry-Riddle Aeronautical University - Daytona Beach*

Follow this and additional works at: <https://commons.erau.edu/db-theses>



Part of the [Aerodynamics and Fluid Mechanics Commons](#)

---

### Scholarly Commons Citation

Bowlds, Patricia Lynn, "Using ANSYS Workbench Computer Environment in Turbomachinery Design Process" (2008). *Theses - Daytona Beach*. 16.

<https://commons.erau.edu/db-theses/16>

This thesis is brought to you for free and open access by Embry-Riddle Aeronautical University – Daytona Beach at ERAU Scholarly Commons. It has been accepted for inclusion in the Theses - Daytona Beach collection by an authorized administrator of ERAU Scholarly Commons. For more information, please contact [commons@erau.edu](mailto:commons@erau.edu).

**USING ANSYS WORKBENCH COMPUTER ENVIRONMENT IN  
TURBOMACHINERY DESIGN PROCESS**

by

Patricia Lynn Bowlds

A Thesis Submitted to the  
Department of Aerospace Engineering  
in Partial Fulfillment of the Requirements for the Degree of  
Master of Science in Aerospace Engineering

Embry-Riddle Aeronautical University

Daytona Beach, Florida

May 2008

UMI Number: EP32013

### INFORMATION TO USERS

The quality of this reproduction is dependent upon the quality of the copy submitted. Broken or indistinct print, colored or poor quality illustrations and photographs, print bleed-through, substandard margins, and improper alignment can adversely affect reproduction.

In the unlikely event that the author did not send a complete manuscript and there are missing pages, these will be noted. Also, if unauthorized copyright material had to be removed, a note will indicate the deletion.

UMI<sup>®</sup>

---

UMI Microform EP32013  
Copyright 2011 by ProQuest LLC  
All rights reserved. This microform edition is protected against  
unauthorized copying under Title 17, United States Code.

---

ProQuest LLC  
789 East Eisenhower Parkway  
P.O. Box 1346  
Ann Arbor, MI 48106-1346

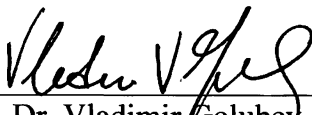
**USING ANSYS WORKBENCH COMPUTER ENVIRONMENT IN  
TURBOMACHINERY DESIGN PROCESS**

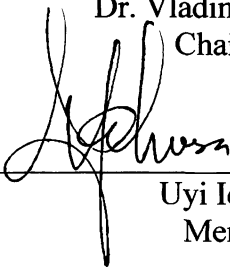
by


Patricia Lynn Bowlds

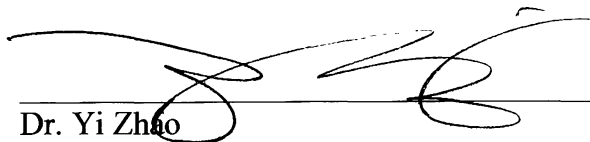
This thesis was prepared under the direction of the candidate's thesis committee chairman, Dr. Vladimir Golubev, Department of Aerospace Engineering, and has been approved by the members of the thesis committee. It was submitted to the Department of Aerospace Engineering and was accepted in partial fulfillment of the requirements for the degree of Master of Science in Aerospace Engineering.

THESIS COMMITTEE:

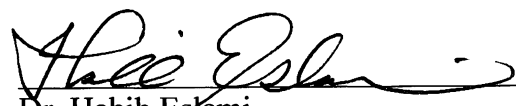
  
\_\_\_\_\_  
Dr. Vladimir Golubev  
Chairman

  
\_\_\_\_\_  
Uyi Idahosa  
Member


  
\_\_\_\_\_  
Dr. Eric Perrell  
Member

  
\_\_\_\_\_  
Dr. Yi Zhao  
Graduate Program Coordinator, Aerospace Engineering

5/19/08  
Date

  
\_\_\_\_\_  
Dr. Habib Estami  
Department Chair, Aerospace Engineering

5/15/08  
Date

  
\_\_\_\_\_  
Dr. Christina Frederick-Recascino  
Vice President for Research and Federal Programs

5-19-08  
Date



## **ACKNOWLEDGEMENTS**

First and foremost, I would like to thank my family and friends for their encouragement throughout this project. Without their reassurance, I would not have finished. I would also like to thank my thesis advisor, Dr. Vladimir Golubev, and Uyi Idahosa for their help on this project when I was struggling for answers and to Dr. Eric Perrell for his time as one of my committee members. Special thanks goes out to Ryan Holt for his help in understanding new computer programs and his fresh outlooks on the project when things were not going according to plan.

## **ABSTRACT**

Author: Patricia Lynn Bowlds  
Title: Using ANSYS Workbench Computer Environment in Turbomachinery Design Process  
Institution: Embry-Riddle Aeronautical University  
Degree: Master of Science in Aerospace Engineering  
Year: 2008

The main focus of designing turbomachinery is to analyze and optimize the aerodynamic efficiency and structural integrity of the machine. The preferred way to perform aerodynamic and structural analysis is to connect the analyses and shorten the analysis time as much as possible. ANSYS, Inc. provides a comprehensive approach to model fluid structure interaction phenomenon in turbomachinery within the ANSYS Workbench environment. This environment combines a number of software components that conduct blade design, fluid dynamic and structural analyses, and pre- and post-processing including mesh generation and overall performance estimation.

The focus of this study is to apply the ANSYS Workbench environment to two turbomachinery applications: a low speed fan design and a propeller design for high altitude flight. The entire process is successfully implemented for the low speed fan analysis and provides verification that the ANSYS Workbench environment works properly, with CFD predictions obtained within 1% of the previous research. On the other hand, the environment fails for the high altitude propeller blade analysis because the blade creation program in ANSYS Workbench does not support creating highly twisted propeller blades, and some essential design information is missing from the blade design source. Overall, it appears that the ANSYS Workbench environment is a highly useful tool for connecting CFD and structural analysis in the turbomachinery design process.

# TABLE OF CONTENTS

ACKNOWLEDGEMENTS.....	iii
ABSTRACT.....	iv
NOMENCLATURE .....	xii
1. INTRODUCTION .....	1
2. METHODOLOGY .....	5
2.1. BladeModeler.....	7
2.1.1. BladeGen.....	7
2.1.2. BladeEditor .....	7
2.2. CFX-Mesh.....	7
2.3. TurboGrid .....	7
2.4. CFX.....	8
2.4.1. CFX-Pre .....	8
2.4.2. CFX-Solver .....	8
2.4.3. CFX-Post.....	8
2.5. DesignModeler.....	9
2.6. Simulation.....	9
3. LOW SPEED FAN APPLICATION .....	10
3.1. BladeModeler.....	12
3.2. CFX-Mesh.....	13
3.3. CFX.....	15
3.3.1. CFD Analysis Comparison .....	18
3.4. DesignModeler.....	18
3.5. Simulation.....	19

4.	HIGH ALTITUDE PROPELLER BLADE APPLICATION.....	25
4.1.	Introduction.....	25
4.1.1.	Propeller Blade Design Information .....	26
4.2.	Preliminary Design Analysis using Blade Element Theory Spreadsheet .....	32
4.2.1.	Minor Changes to Spreadsheet .....	35
4.2.2.	Results and Conclusions .....	36
4.3.	ANSYS Workbench Analysis.....	38
4.3.1.	Propeller Blade Creation.....	39
4.3.2.	Importing Blade File .....	47
4.3.2.1.	Data Import Wizard .....	47
4.3.2.2.	Meanline File .....	50
4.3.3.	Importing 3D CAD Model.....	53
4.3.3.1.	DesignModeler for CFD Analysis .....	55
4.3.3.2.	CFX-Mesh.....	56
4.3.3.3.	CFX.....	59
4.3.3.4.	DesignModeler for Structural Analysis .....	61
4.3.3.5.	Simulation.....	62
5.	CONCLUSIONS AND RECOMMENDATIONS .....	64
	REFERENCES .....	68
	APPENDIX A – LOW SPEED FAN BLADE CFD RESULTS .....	A1
	APPENDIX B – ATMOSPHERE SOURCE.....	B1
	APPENDIX C – BLADE ELEMENT THEORY SPREADSHEET .....	C1
	APPENDIX D – ANSYS, INC. BLADEGEN EMAIL.....	D1

## LIST OF FIGURES

Figure 1: ANSYS Workbench Turbomachinery Flow Chart .....	6
Figure 2: Alternate ANSYS Workbench Turbomachinery Flow Chart.....	6
Figure 3: Low Speed Fan Blade Model 1 in BladeGen with Default Display .....	12
Figure 4: Low Speed Fan Blade Model 1 in BladeGen with 3D Fan Displayed.....	13
Figure 5: Automatic CFD Mesh Created using BladeEditor and CFX-Mesh – Low Speed Fan Blade .....	14
Figure 6: Low Speed Fan Blade CFX Results – Blade Pressure Loading at (a) 20% Span, (b) 50% Span, and (c) 80% Span .....	16
Figure 7: Low Speed Fan Blade CFX Results – Blade Mesh at 50% Span.....	17
Figure 8: Low Speed Fan Blade CFX Results – Blade Velocity Streamlines at Blade Trailing Edge .....	17
Figure 9: Blade Geometry in DesignModeler – Low Speed Fan Blade .....	19
Figure 10: Structural Mesh Created in Simulation – Low Speed Fan Blade.....	21
Figure 11: Total Deformation of Polyethylene Fan Blade.....	22
Figure 12: Total Deformation of ABS Fan Blade.....	24
Figure 13: Chord vs. Radial Position – High Altitude Propeller Blade.....	28
Figure 14: Blade Pitch Angle vs. Radial Position – High Altitude Propeller Blade .....	28
Figure 15: Sample of Original Eppler 387 Coordinates Spreadsheet [13] .....	39
Figure 16: Airfoil Profile with Angle Labels [10].....	40
Figure 17: Eppler 387 Airfoil using Original Coordinates .....	40
Figure 18: Rotated and Translated Eppler 387 Airfoil .....	42
Figure 19: Eppler 387 Airfoil with Pitch Angle .....	43
Figure 20: Eppler 387 Airfoil with Corrected Pitch Angle.....	45
Figure 21: Sample of Eppler 387 Coordinates Spreadsheet including Pitch and Correction Angles .....	45

Figure 22: High Altitude Propeller Blade Drawn in CATIA.....	47
Figure 23: BladeGen Data Import Wizard Opening Window .....	48
Figure 24: BladeGen Data Import Wizard Blade Creation Options .....	49
Figure 25: High Altitude Propeller Blade File in BladeGen Data Import Wizard .....	49
Figure 26: Meanline File Template [15].....	50
Figure 27: Meanline File Error in BladeGen – High Altitude Propeller Blade .....	52
Figure 28: ANSYS Workbench Flow Chart – High Altitude Propeller Blade .....	53
Figure 29: High Altitude Propeller Blade with Fluid Domain .....	54
Figure 30: High Altitude Propeller Blade Filled Fluid Domain .....	55
Figure 31: High Altitude Propeller Blade Fluid Domain in DesignModeler.....	56
Figure 32: Fluid Domain Mesh in CFX-Mesh – High Altitude Propeller Blade.....	58
Figure 33: High Altitude Propeller Blade Mesh in CFX-Mesh .....	58
Figure 34: High Altitude Propeller Blade in DesignModeler.....	61
Figure 35: Structural Mesh Created in Simulation – High Altitude Propeller Blade .....	63
Figure 36: Low Speed Fan Blade CFX Results – Streamwise Plots: (a) Pt and P, (b) Tt and T, (c) Absolute and Relative Mach Number, and (d) Static Entropy.....	A1
Figure 37: Low Speed Fan Blade CFX Results – Spanwise Plots: (a) Alpha and Beta at LE, (b) Relative Mach Number at LE, (c) Alpha and Beta at TE, (d) Relative Mach Number at TE, (e) Absolute Mach Number at TE, and (f) Meridional Velocity at TE .....	A2
Figure 38: Low Speed Fan Blade CFX Results – Contour of Relative Mach Number at (a) 20% Span, (b) 50% Span, and (c) 80% Span .....	A3
Figure 39: Low Speed Fan Blade CFX Results – Velocity Vectors at (a) 20% Span, (b) 50% Span, and (c) 80% Span.....	A3
Figure 40: Low Speed Fan Blade CFX Results – Contour of Specific Entropy at (a) 20% Span, (b) 50% Span, and (c) 80% Span .....	A4
Figure 41: Low Speed Fan Blade CFX Results – Contour on Meridional Surface of (a) Mass Averaged Pressure and (b) Mass Averaged Relative Mach Number ...	A4

Figure 42: Low Speed Fan Blade CFX Results – Contour at Blade LE of (a) Pressure, (b) Relative Mach Number, and (c) Specific Entropy.....	A5
Figure 43: Low Speed Fan Blade CFX Results – Contour at Blade TE of (a) Pressure, (b) Relative Mach Number, and (c) Specific Entropy.....	A5
Figure 44: Sample of Atmospheric Data Table .....	B1
Figure 45: Propeller Blade Importing Error Email Explanation from ANSYS, Inc.....	D1

## LIST OF TABLES

Table 1: Low Speed Fan Blade Model 1 Parameters.....	11
Table 2: CFD Results from Reference [5] for Low Speed Fan Blade .....	11
Table 3: Face Spacing Parameters from Automatic Meshing – Low Speed Fan Blade ..	13
Table 4: Inflation Parameters from Automatic Meshing – Low Speed Fan Blade.....	14
Table 5: Input Parameters and Boundary Conditions for CFX – Low Speed Fan Blade	15
Table 6: CFX CFD Results – Low Speed Fan Blade.....	16
Table 7: Comparison of CFD Results – Low Speed Fan Blade .....	18
Table 8: General Settings for Structural Mesh – Low Speed Fan Blade .....	20
Table 9: Mesh Method Settings for Structural Mesh – Low Speed Fan Blade .....	21
Table 10: Face Sizing Settings for Structural Mesh – Low Speed Fan Blade .....	21
Table 11: Structural Analysis Results for Polyethylene Fan Blade.....	22
Table 12: ABS Material Properties.....	23
Table 13: Structural Analysis Results for ABS Fan Blade .....	23
Table 14: Comparison of Structural Results for Polyethylene and ABS Plastic .....	24
Table 15: High Altitude Propeller Blade Design Parameters .....	27
Table 16: Pitch Angle and Chord Data – High Altitude Propeller Blade.....	29
Table 17: Corrected Chord and Pitch Angle Data – High Altitude Propeller Blade .....	30
Table 18: Atmosphere Properties at 85,000 ft .....	30
Table 19: High Altitude Propeller Blade Results from Reference [9].....	31
Table 20: Results from Blade Element Theory Spreadsheet – High Altitude Propeller Blade .....	36
Table 21: Preliminary Design Results Comparison – High Altitude Propeller Blade.....	37
Table 22: Facing Spacing Parameters – High Altitude Propeller Blade.....	57
Table 23: Inflation Parameters – High Altitude Propeller Blade.....	57



Table 24: Input Parameters and Boundary Conditions for CFX – High Altitude Propeller Blade ..... 60

Table 25: General Settings for Structural Mesh – High Altitude Propeller Blade ..... 62

Table 26: Mesh Method Settings for Structural Mesh – High Altitude Propeller Blade. 62

Table 27: Face Sizing Settings for Structural Mesh – High Altitude Propeller Blade .... 63

## NOMENCLATURE

$a$	=	speed of sound
$A$	=	blade surrounding area
$B$	=	tip loss distance
$c$	=	chord
$c_{avg}$	=	average chord along span
$c_{shr}/c_h$	=	hub-to-shroud chord ratio
$C_{cf}$	=	compressibility correction factor
$C_d$	=	coefficient of drag
$(C_d)_{com}$	=	compressible drag coefficient
$(C_d)_{incom}$	=	incompressible drag coefficient
$(C_d)_{Rn}$	=	compressible drag coefficient with Reynolds number correction
$C_j$	=	coefficient of $j$
$C_L$	=	coefficient of lift
$(C_{L\alpha})_{com}$	=	compressible 3D coefficient of lift slope
$(C_{L\alpha})_{incom.2D}$	=	incompressible 2D coefficient of lift slope
$(C_{L\alpha})_{incom.3D}$	=	incompressible 3D coefficient of lift slope
$C_Q$	=	torque coefficient
$C_{Q_i}$	=	induced torque coefficient
$(C_{Q_i})_{no\ loss}$	=	induced torque coefficient with no tip loss

$(\Delta C_{Q_i})_{tip\ loss}$	=	induced torque coefficient tip loss
$C_{Q_i}$	=	profile torque coefficient
$C_T$	=	thrust coefficient
$(C_T)_{no\ loss}$	=	thrust coefficient with no tip loss
$D$	=	diameter of blade
$\frac{dC_j}{dr}$	=	coefficient per unit radius for $j$
$\left(\frac{dC_j}{dr}\right)_{trap}$	=	trapezoidal rule coefficient per unit radius for $j$
$\frac{dC_{Q_i}}{dr}$	=	coefficient per unit radius for induced torque
$\frac{dC_{Q_i}}{dr}$	=	coefficient per unit radius for profile torque
$\frac{dC_T}{dr}$	=	coefficient per unit radius for thrust
$\left(\frac{dC_T}{dr}\right)_{r=0.9}$	=	coefficient per unit radius for thrust at 0.9 radial position
$\left(\frac{dC_T}{dr}\right)_{r=1.0}$	=	coefficient per unit radius for thrust at 1.0 radial position
$h_{LE}$	=	hub leading edge
$h_{TE}$	=	hub trailing edge
$(HP)_e$	=	engine horsepower
$(HP)_{Total}$	=	total power
$i$	=	span increment ( $i = 1 : k - 1$ )

$I$	=	first intermediate calculation for induced velocity
$II$	=	second intermediate calculation for induced velocity
$III$	=	third intermediate calculation for induced velocity
$IV$	=	fourth intermediate calculation for induced velocity
$j$	=	coefficient subscript ( $j = T)_{no\ loss}$ , $Q_o$ , or $Q_i)_{no\ loss}$ )
$k$	=	number of span increments
$M$	=	Mach number
$M_c$	=	cruise Mach number
$N$	=	number of blades in turbomachinery (fan/propeller)
$p_o$	=	total pressure
$p_s$	=	static pressure
P-Static	=	static pressure
P-Total	=	total pressure
$Q_i)_{no\ loss}$	=	subscript for induced torque with no loss
$Q_o$	=	subscript for profile torque
$r$	=	non-dimensional radial position / span location
$r_i$	=	radial position for $i$ span increment
$r_{i+1}$	=	radial position for $i + 1$ span increment
$r_{0.9}$	=	0.9 radial position
$r_{1.0}$	=	1.0 radial position
$R$	=	blade radius
$R_h/R_{shr}$	=	hub-to-shroud radius ratio

$R_p$	=	Reynolds number
$shr_{LE}$	=	shroud leading edge
$shr_{TE}$	=	shroud trailing edge
$t_{LE}/t_{TE}$	=	leading edge to trailing edge thickness ratio
$t_{max}/c$	=	maximum thickness to chord ratio
$T$	=	thrust
$T)_{no\ loss}$	=	subscript for thrust with no loss
$T_o$	=	total temperature
$T_{st}$	=	static temperature
T-Total	=	total temperature
$V$	=	tangential velocity
$V_f$	=	cruise velocity / forward speed
$v_i$	=	induced velocity
$x$	=	original x coordinate
$x_o$	=	original trailing edge x coordinate
$x'$	=	rotated and translated x coordinate
$x''$	=	angled x coordinate
$x_c''$	=	angled x coordinate with corrected pitch angle
$y$	=	span radius
$y$	=	original y coordinate
$y'$	=	rotated and translated y coordinate
$y''$	=	angled y coordinate

$y_c''$	=	angled y coordinate with corrected pitch angle
$\%Power$	=	percent of power
$\alpha$	=	angle of attack
$\alpha_{L=0}$	=	zero lift angle of attack
$\beta$	=	pitch angle
$\gamma$	=	specific gas ratio ( $\gamma \approx 1.4$ )
$(\Delta C_T)_{tip\ loss}$	=	thrust coefficient tip loss
$\Delta\theta$	=	pitch angle correction
$\epsilon_{st}$	=	static efficiency
$\epsilon_T$	=	total efficiency
$\eta_{prop}$	=	propeller efficiency
$\theta$	=	corrected pitch angle
$\theta_b$	=	pitch angle (base)
$\theta'$	=	negative blade pitch angle
$\theta_c$	=	negative corrected pitch angle
$\mu$	=	dynamic viscosity
$\nu$	=	kinematic viscosity
$\rho$	=	density
$\sigma$	=	solidity
$\phi$	=	flow angle
$\Omega$	=	angular velocity

## 1. INTRODUCTION

Companies, that use turbomachinery in the machines they make, are always looking for ways to design the turbomachinery for optimal performance. Some companies perform computational fluid dynamics (CFD) on their turbomachinery parts and optimize for aerodynamic performances and perform structural analysis as an afterthought. Even when companies perform both CFD and structural analysis on the turbomachinery parts, the analyses are typically performed separately by two different groups: an aerodynamics group and a structures group. Having the analyses performed by different groups can cause the design time to be very long. A better way to perform CFD and structural analysis is to have one person or group perform both analyses and perform them in the same program environment. ANSYS, Inc. has recently introduced this type of environment through ANSYS Workbench, which is a convenient and user-friendly environment where turbomachinery analysis, CFD and structural, can be performed by one person.

The ANSYS Workbench environment incorporates CFD analysis using the program CFX and structural analysis using the program Simulation. To help make designing the turbomachinery using CFD analysis easier, ANSYS Workbench provides programs that create the turbomachinery components, either from scratch or using three-dimensional computer-aided design (3D CAD) models, and mesh the components and their surrounding fluid regions. Creating the model is easily performed using BladeModeler or DesignModeler. According to ANSYS, BladeModeler “can assist in the design of axial, mixed-flow, and radial blade components in applications such as pumps, compressors, fans, blowers, turbines, expanders, turbochargers, inducers, and

others” [1]. Meshing in ANSYS Workbench is performed by either CFX-Mesh or TurboGrid. The turbomachinery model created in BladeModeler or DesignModeler can be used in both CFX-Mesh and TurboGrid. The mesh is imported into CFX with ANSYS Workbench for CFD analysis.

For structural analysis, ANSYS Workbench uses Simulation. Simulation is a finite element analysis (FEA) program that imports a geometry model from BladeModeler or DesignModeler and performs structural analysis on the model. Within Simulation, the fluid structure interaction is modeled. For turbomachinery, the fluid structure interaction is applied to the model by using the results from the CFD analysis, performed by CFX, in terms of the obtained pressure load on the structure. This creates a direct connection between the CFD and structural analysis that most other analysis programs cannot provide. With the results from the analyses, the model can be modified in BladeModeler or DesignModeler to correct any aerodynamic or structural flaws in the model. The CFD and structural analysis can be run and new designs can be made again and again in ANSYS Workbench until a structurally and aerodynamically optimal design is created.

Many companies are using ANSYS Workbench with great success. For example, PCA Engineers, turbomachinery design engineering consultants, was asked by the Flakt Woods Group, manufacturers of large industrial fans, to design a fan with nearly flat operating conditions, which causes the delivery pressure to rise insignificantly when the volume flow falls [2]. PCA Engineers used CFX-BladeGen, CFX-TurboGrid, and CFX-TASCflow (all of which are programs in ANSYS Workbench) to design, mesh, and perform CFD analysis. Using these programs, PCA Engineers was able to see that the



initial design did not meet the specified requirements and easily redesigned a fan that met the requirements. The fan was built and tested by Flakt Woods, and the fan performed almost as predicted by CFX. PCA Engineers saved time in the design of the fan; they designed and redesigned the fan in one month, which would have taken three months to finish if the build-and-test approach was used.

The company Wood Group Heavy Industrial Turbines used ANSYS programs to perform fluid structure interaction on gas turbine blades to extend the life of the blade by cooling, without affecting their thermal efficiency [3]. Wood Group used ANSYS DesignModeler to import the 3D CAD model of the blade and ANSYS ICEM to mesh the fluid domains and blade. Flowmaster2 was then used to model the cooling channels. The resulting 1D thermal simulation and ANSYS-CFX software was used to perform the CFD analysis on the blade. The temperature field in the blade, calculated in ANSYS-CFX, was used as the thermal load in ANSYS Mechanical for heat transfer analysis. The heat transfer analysis provided thermal and mechanical stress distributions of the blade, which in turn were used to determine the life expectancy of the blade. With the use of the fluid structure interaction capability of ANSYS, Wood Group gained a better understanding of the blade's total performance, which allowed for design modifications to occur early in the analysis process.

PCA Engineers Limited used the fluid structure interaction feature within ANSYS Workbench to study blade flutter as part of high-fidelity turbomachinery analysis [4]. Blade flutter is not easily predicted because it depends on the blade's aerodynamic and structural characteristics. Using the fluid structure interaction analysis capability of ANSYS Workbench, blade flutter was predicted and analyzed. Forced vibration analysis

of the blade was performed in ANSYS Mechanical and the resulting time-dependent deformations were applied to the CFD computational grid. CFX used this deformed grid to perform CFD unsteady flow computations. Analyzing the modal vibration of blades using structural and CFD analysis predicted the existence of flutter and allows the blade design to be modified before it was manufactured and tested or put into production.

The functionality of the ANSYS Workbench environment combining CFD and structural analysis is very important in all turbomachinery design applications. The main focus of this thesis is to examine a process for analyzing different turbomachinery applications using the fluid structure interaction analysis developed within ANSYS Workbench. Two applications are analyzed: a low speed fan blade and a propeller blade used in high altitude flight. The experience developed in this thesis allows future turbomachinery design projects to use the ANSYS Workbench environment more affectively and efficiently.

## 2. METHODOLOGY

When designing any type of turbomachinery blade, computational fluid dynamics (CFD) is typically used to design the blade for the best aerodynamic efficiency. The blades are not only designed for aerodynamic efficiency; they are also designed to withstand the structural loading applied to the blades when they are in use. Most of the time, one analyst designs a blade just looking at the aerodynamics side and then hands off the blade design to a structural analyst to see if the blade design is structurally sound. If the blade is not structurally sound, the blade is redesigned and the whole process is run again. This process continues until the design creates an aerodynamically efficient, structurally sound blade. The process may be very time consuming if the blade design is going back and forth between two analysts or analysis groups to create an optimal blade design. A more efficient way to design a blade with CFD and structural analysis is to have one person perform both analyses within the same program environment.

ANSYS, Inc. provides a way to analyze the design of a blade, or any other object, with CFD and structural analysis using its group of programs contained in ANSYS Workbench. ANSYS-CFX is used for CFD analysis and Simulation is used for structural analysis. Along with ANSYS-CFX and Simulation, some other programs used within ANSYS Workbench to help with the analyses are: BladeModeler, which includes BladeGen and BladeEditor; CFX-Mesh; and DesignModeler. Figure 1 shows a flow chart of the ANSYS Workbench programs and the method in which they are used.

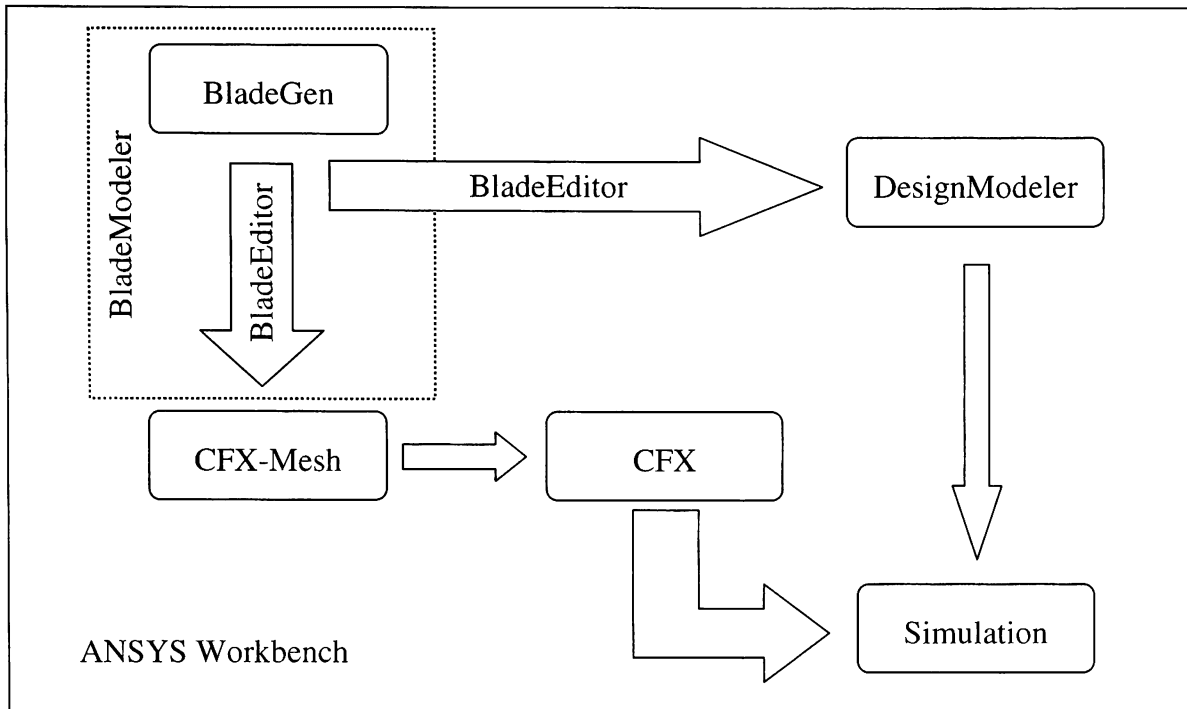


**Figure 1: ANSYS Workbench Turbomachinery Flow Chart**

Figure 2 shows an alternate way to use the ANSYS Workbench environment to combine CFD and structural analysis. Here, TurboGrid is used to mesh the blade and fluid domain in place of BladeEditor and CFX-Mesh.

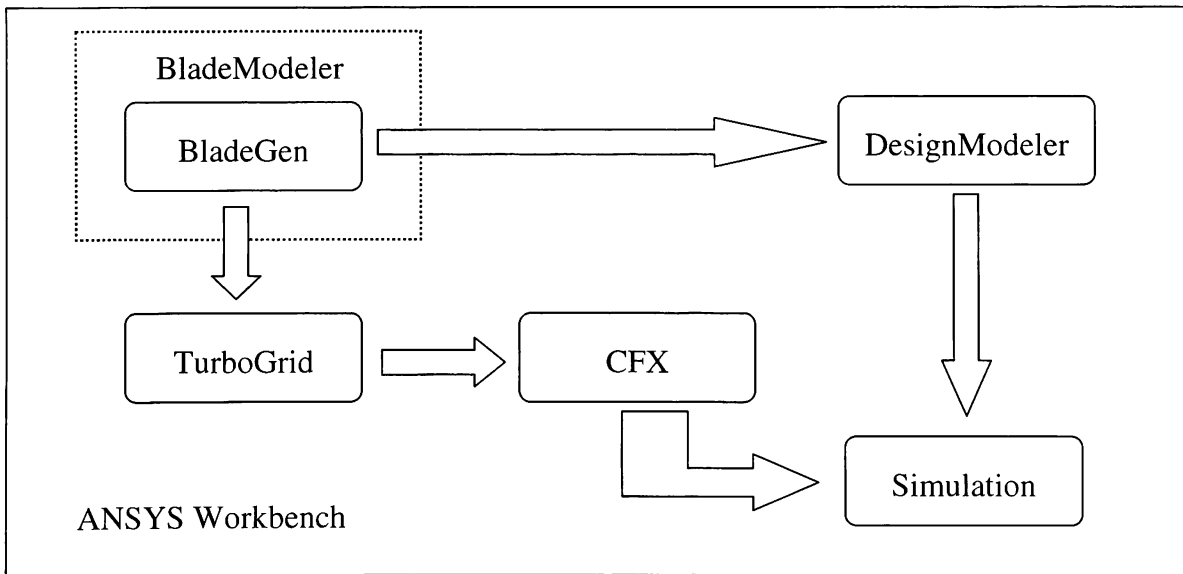


**Figure 2: Alternate ANSYS Workbench Turbomachinery Flow Chart**

## **2.1. BladeModeler**

### **2.1.1. BladeGen**

BladeGen is the main program of BladeModeler within ANSYS Workbench. It is used to create blade models for turbomachinery. Blades are designed using angle/thickness information or pressure/suction information. BladeGen also automatically creates the fluid region for the blade for easy export to a CFD meshing program.

### **2.1.2. BladeEditor**

BladeEditor is the secondary program of BladeModeler. It takes the blade model created in BladeGen, sends it to DesignModeler and CFX-Mesh, and helps automatically create a mesh for CFD analysis.

## **2.2. CFX-Mesh**

CFX-Mesh is one of the CFD meshing programs within ANSYS Workbench. BladeEditor automatically creates a mesh in CFX-Mesh using the geometry of the blade created in BladeGen. If the mesh automatically created is not at the desired quality, it is possible to modify the mesh within CFX-Mesh.

## **2.3. TurboGrid**

TurboGrid is another CFD meshing program within ANSYS Workbench. The mesh is not automatically created if TurboGrid is used for meshing. The blade geometry created in BladeGen has to be exported as TurboGrid input files. Exporting the blade

geometry creates the following files: hub.curve, shroud.curve, and profile.curve. These files create a hub fluid domain, a shroud fluid domain, and the blade profile, respectively. The TurboGrid mesh is created with control points. Moving these control points or adding new ones may help make a better quality mesh.

## **2.4. CFX**

The CFD solver within ANSYS Workbench is CFX. There are three parts to the CFX program: CFX-Pre, CFX-Solver, and CFX-Post.

### **2.4.1. CFX-Pre**

CFX-Pre is the part of CFX where the boundary conditions and input parameters are set up and the fluid domains are checked to make sure they are correct. The mesh created in CFX-Mesh or TurboGrid is uploaded in CFX-Pre.

### **2.4.2. CFX-Solver**

CFX-Solver is the part of CFX that runs the CFD analysis, using the input parameters and boundary conditions set up in CFX-Pre. CFX-Solver allows direct monitoring of convergence parameters as it is running. For fluid structure interaction, the results from CFX-Solver are imported into Simulation as the pressure loading for the structural analysis.

### **2.4.3. CFX-Post**

CFX-Post is the part of CFX that is used for post processing the CFD analysis performed in CFX-Solver. It creates charts and graphs that show the results from CFX-

Solver. These include the blade pressure loading at different spans along the entire blade and the velocity streamlines along the trailing edge of the blade. The blade efficiency can also be found in the results. CFX-Post has the ability to create an analysis report that includes all the important blade results included.

## **2.5. DesignModeler**

DesignModeler is the geometry model program within ANSYS Workbench. A geometry model is made from scratch or it is imported into DesignModeler. Imported models are typically made in BladeGen or a three-dimensional computer-aided design (3D CAD) program and then are imported into DesignModeler. It is possible to modify the model in DesignModeler if changes are needed. Models from DesignModeler are exported to ANSYS Simulation for structural analysis.

## **2.6. Simulation**

Simulation is the finite element analysis (FEA) program within ANSYS Workbench. A geometry model is imported into Simulation from DesignModeler. It is then structurally meshed within Simulation. For fluid-structure interface, the loading applied to the blade is a CFX-generated pressure load.

### **3. LOW SPEED FAN APPLICATION**

Previous research has been conducted on low speed industrial air conditioner fan blades to optimize their aerodynamic performance and total efficiency [5]. Three initial blade models were designed with varying parameters using CFX-BladeGen, and CFX-BladeGen(Plus) to perform CFD analysis on the blade. Both of these programs were created by CFX. In particular, CFX-BladeGen(Plus) was able to pre-process, generate a grid, and post-process the CFD analysis solution of the flow field around the blade. Once the initial CFD analysis was complete, the blades were optimized using VisualDoc, a multidisciplinary optimization program. The CFD analysis and optimization were continually run on the blade models until each blade reached its optimal total efficiency values.

The optimization research on the low speed fan blades did not consider the structural integrity of the blade designs as an optimization parameter, as the structural analysis of the fan blades was not conducted at all. With the help of ANSYS Workbench and its fluid structure interaction feature, structural analysis can now be included in the fan blade optimization. This will help create a blade that is not only optimally efficient but is also able to withstand the operational loading.

The programs used for the previous research, CFX-BladeGen and CFX-BladeGen(Plus), are now incorporated into ANSYS Workbench, and CFX-BladeGen(Plus) has been replaced by BladeEditor, CFX-Mesh, and CFX. Because the programs are not in the exact format as used in the previous research, verification of the new method, by comparing the new CFD results to the previous ones, is necessary. The CFD analysis is verified if the results are similar to each other. Once the verification is



complete, structural analysis is performed. The focus of this research is to develop a process for the ANSYS Workbench environment, to help prepare for future optimization studies to achieve the optimal low speed fan blade design.

In this research, only the blade design prototype Model 1 from the previous research is examined and results are compared with Reference [5]. Table 1 shows the design parameters used for Model 1. The CFD results from the previous research are shown in Table 2.

**Table 1: Low Speed Fan Blade Model 1 Parameters**

Parameter	Model 1	
Angular Velocity, $\Omega$ (RPM)	1140	
Diameter, D	(in)	30
	(mm)	762
# of Blades, N	9	
$R_{tr}/R_{shr}$	0.4	
$c_{shr}/c_h$	2	
Blade Vortex Model	-1	
$t_{max}/c$	0	
$t_{LE}/t_{TE}$	4/1	
$h_{LE}$ Incidence Angle ( $^\circ$ )	2.5	
$shr_{LE}$ Incidence Angle ( $^\circ$ )	-2.5	
$h_{TE}$ Deviation Angle ( $^\circ$ )	5	
$shr_{TE}$ Deviation Angle ( $^\circ$ )	5	
Camber Load	Aft Tip and Mid Load	

**Table 2: CFD Results from Reference [5] for Low Speed Fan Blade**

CFD Results	
Angular Velocity (RPM)	-1140
	(rad/s) -119.381
Number of Blades	9
Mass Flow Rate	4.2861
Volume Flow Rate ( $m^3/s$ )	3.617
Torque (N-m)	14.31
Head Rise (m)	31.14
Static Efficiency ( $\epsilon_{st}$ )	0.526
Total Efficiency ( $\epsilon_T$ )	0.765

The ANSYS Workbench method shown in Figure 1 is used for verification because of its simplicity and automatic mesh capabilities using BladeEditor and CFX-Mesh.

### 3.1. BladeModeler

The same BladeGen file for Model 1, sweeepy.bgd, created in the previous research, is used for verification of the CFD analysis in ANSYS Workbench.

BladeEditor is then used to automatically create mesh around the blade and through the fluid domain in CFX-Mesh. While running BladeEditor, it prompts for desired units; millimeters are used for the blade. Figure 3 and Figure 4 show the default and 3D fan BladeGen displays for Model 1, respectively.

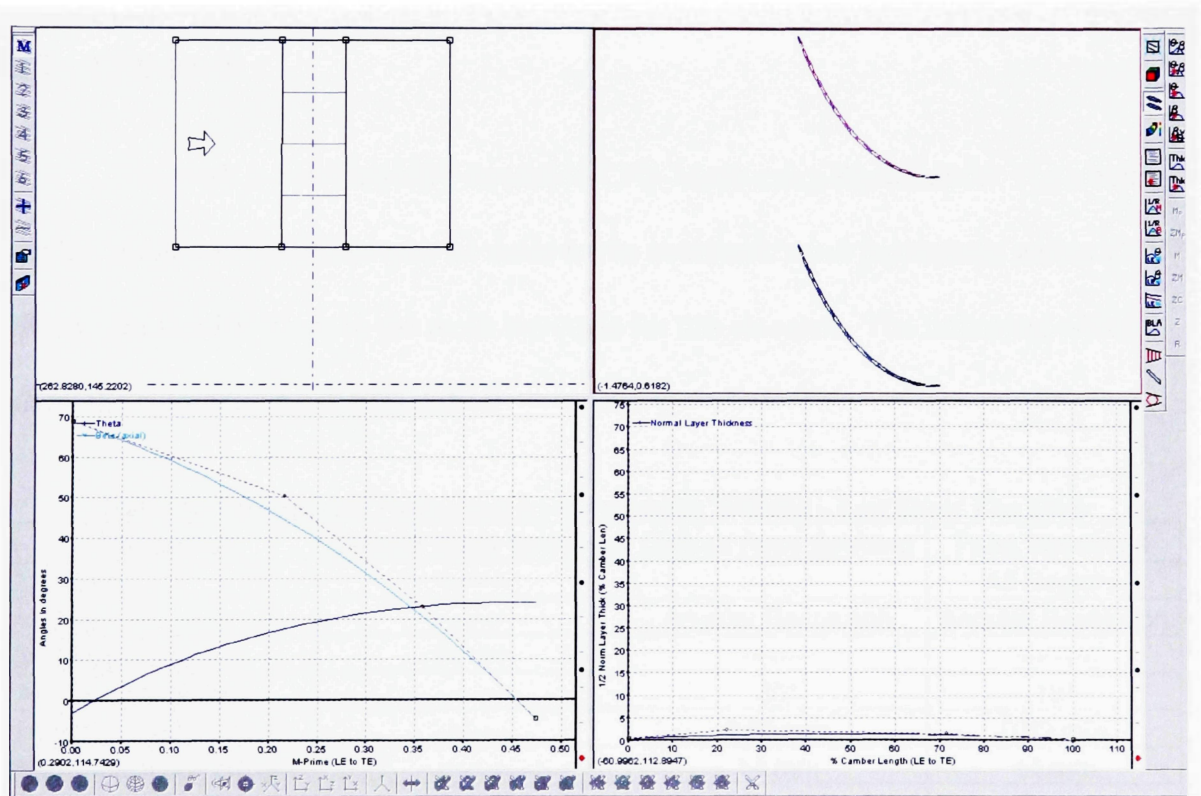


Figure 3: Low Speed Fan Blade Model 1 in BladeGen with Default Display

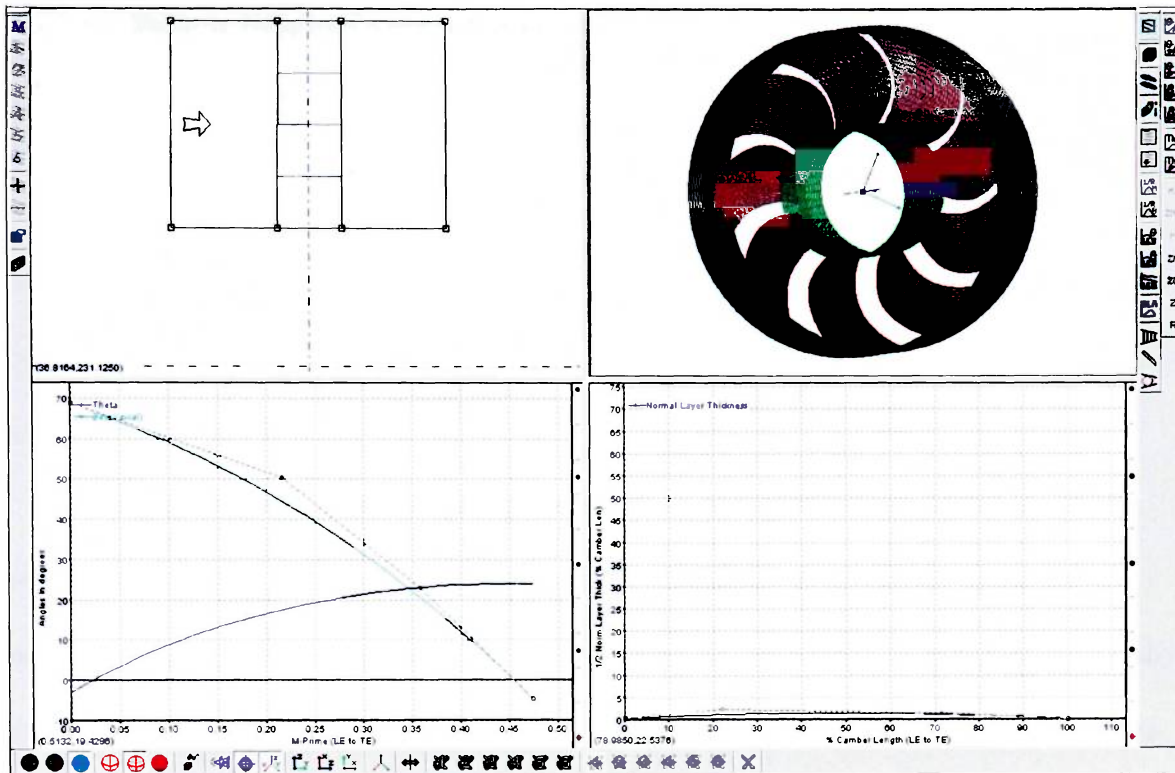


Figure 4: Low Speed Fan Blade Model 1 in BladeGen with 3D Fan Displayed

### 3.2. CFX-Mesh

The mesh is automatically created in CFX-Mesh using BladeEditor. For a better quality mesh, modifications may be made to the automatic mesh parameters within CFX-Mesh. No modifications to the mesh are made for this research. The following tables show the automatic mesh parameters:

Table 3: Face Spacing Parameters from Automatic Meshing – Low Speed Fan Blade

Parameter	Default Body Spacing	Default Face Spacing	Face Spacing 1
Location	-----	-----	All Regions
Option	-----	Angular Resolution	Angular Resolution
Maximum Spacing	14 mm	-----	-----
Angular Resolution	-----	30°	18°
Minimum Edge Length	-----	0.69 mm	0.69 mm
Maximum Edge Length	-----	14 mm	14 mm
Radius of Influence	-----	0 mm	0 mm
Expansion Factor	-----	1.2	1.2

**Table 4: Inflation Parameters from Automatic Meshing – Low Speed Fan Blade**

Inflation	
Location	Hub, Shroud, Blade
Maximum Thickness	14 mm
Number of Inflated Layers	10
Expansion Factor	1.2
Number of Spreading Iterations	0
Minimum Internal Angle	2.5°
Minimum External Angle	10°
Option	Total Thickness
Thickness Multiplier	1.5

The automatic mesh creates a periodic region using Periodic 1 and Periodic 2 regions in rotation. The automatic mesh uses the Delaunay algorithm to mesh the surfaces and the Advancing Front approach for volume meshing. The mesh automatically created by BladeEditor in CFX-Mesh is used in CFX for CFD analysis. Figure 5 shows the automatic mesh created for the low speed fan blade.

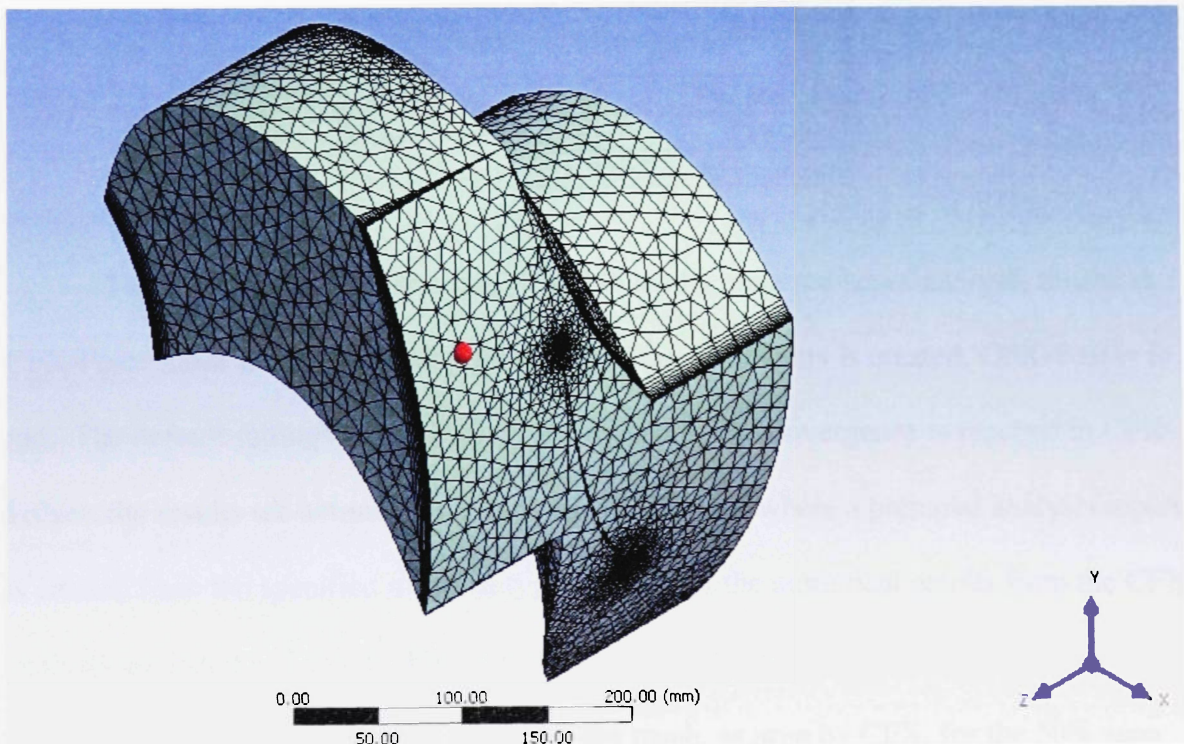


**Figure 5: Automatic CFD Mesh Created using BladeEditor and CFX-Mesh – Low Speed Fan Blade**

### 3.3. CFX

After the mesh is automatically created in CFX-Mesh, a new blade CFD simulation is created from the mesh file in CFX. The input parameters and boundary conditions are applied to the mesh in CFX-Pre. These parameters are the same as used in the previous research [5]. The input parameters and boundary conditions used in CFX are listed in Table 5.

**Table 5: Input Parameters and Boundary Conditions for CFX – Low Speed Fan Blade**

<b>Input Parameters</b>	
Machine Type	Fan
Angular Velocity	-1140 RPM
Fluid	Air Ideal Gas
Reference Pressure	0 Pa
Simulation Type	Steady State
Heat Transfer	Total Energy
Turbulence	k-Epsilon
<b>Boundary Templates</b>	
P-Total In	101325 Pa
T-Total	300 K
Mass Flow	Per Machine
Mass Flow Rate Out	4.286 kg/s
Flow Direction	Normal to Boundary

The machine type is chosen as “Fan” to load a prepared set of analysis results in CFX-Post. Once the CFX-Pre definition file of the parameters is created, CFX-Solver is run. The default settings are used in CFX-Solver. After convergence is reached in CFX-Solver, the results are automatically moved to CFX-Post where a prepared analysis report is created from the specified machine type. Some of the numerical results from the CFX analysis are listed in Table 6. Figure 6 shows the blade pressure loading at 20%, 50%, and 80% span. Figure 7 shows a picture of the mesh, as seen by CFX, for the 50% span.

The velocity streamlines at the blade's trailing edge are shown in Figure 8. More CFD graphical and pictorial results are in Appendix A.

**Table 6: CFX CFD Results – Low Speed Fan Blade**

CFD Results	
Angular Velocity	-119.38 rad/s
Mass Flow Rate	4.2864 kg/s
Inlet Volume Flow Rate	3.6436 m <sup>3</sup> /s
Input Power	1475.67 W
Inlet Flow Coefficient	0.2793
Exit Flow Coefficient	0.2789
Total Isentropic Efficiency (%)	77.1229
Total Polytropic Efficiency (%)	77.121

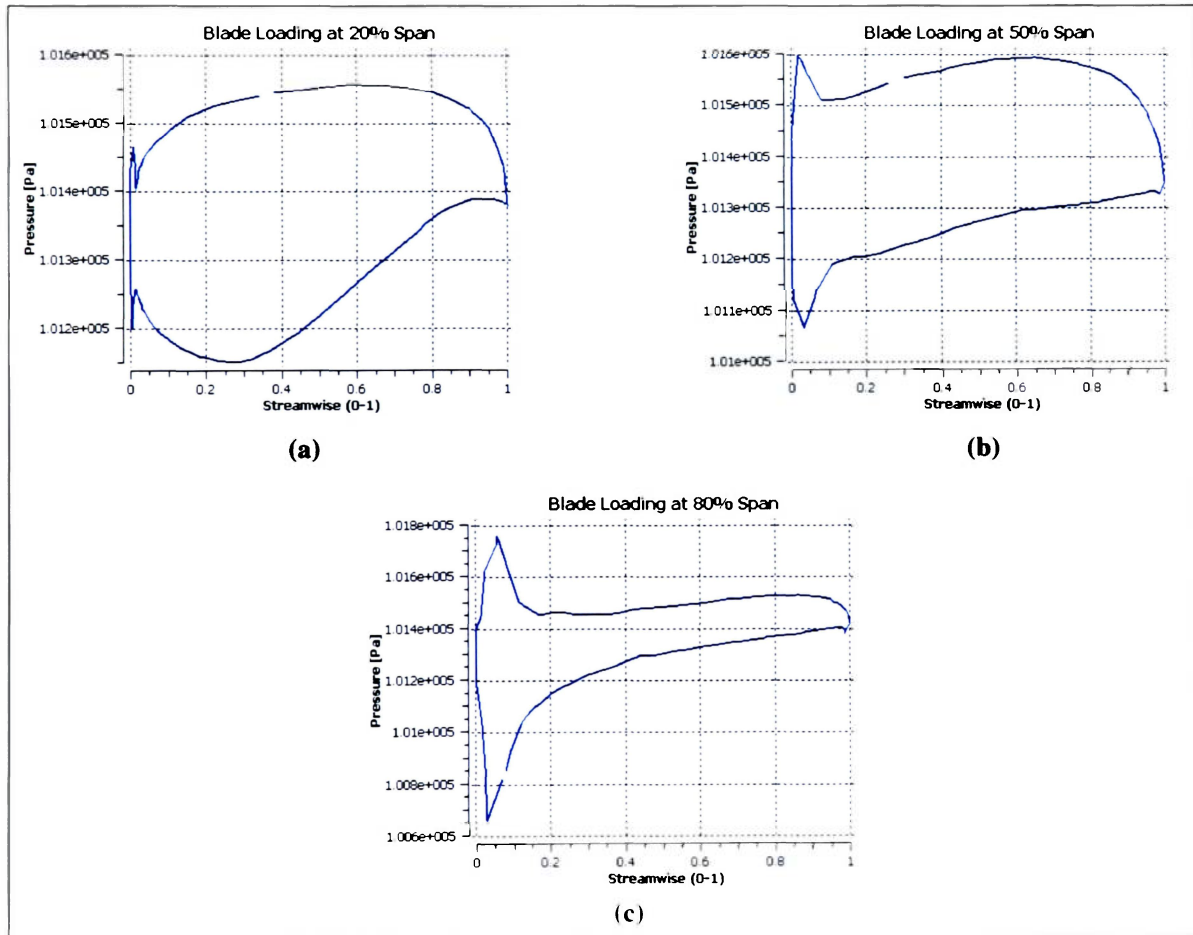


**Figure 6: Low Speed Fan Blade CFX Results – Blade Pressure Loading at (a) 20% Span, (b) 50% Span, and (c) 80% Span**



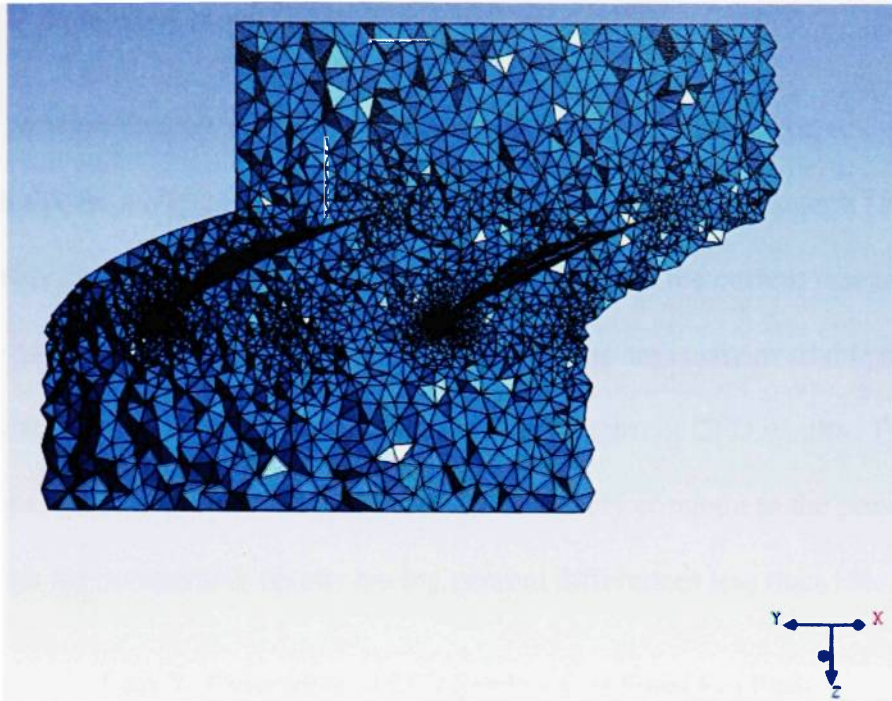


Figure 7: Low Speed Fan Blade CFX Results – Blade Mesh at 50% Span

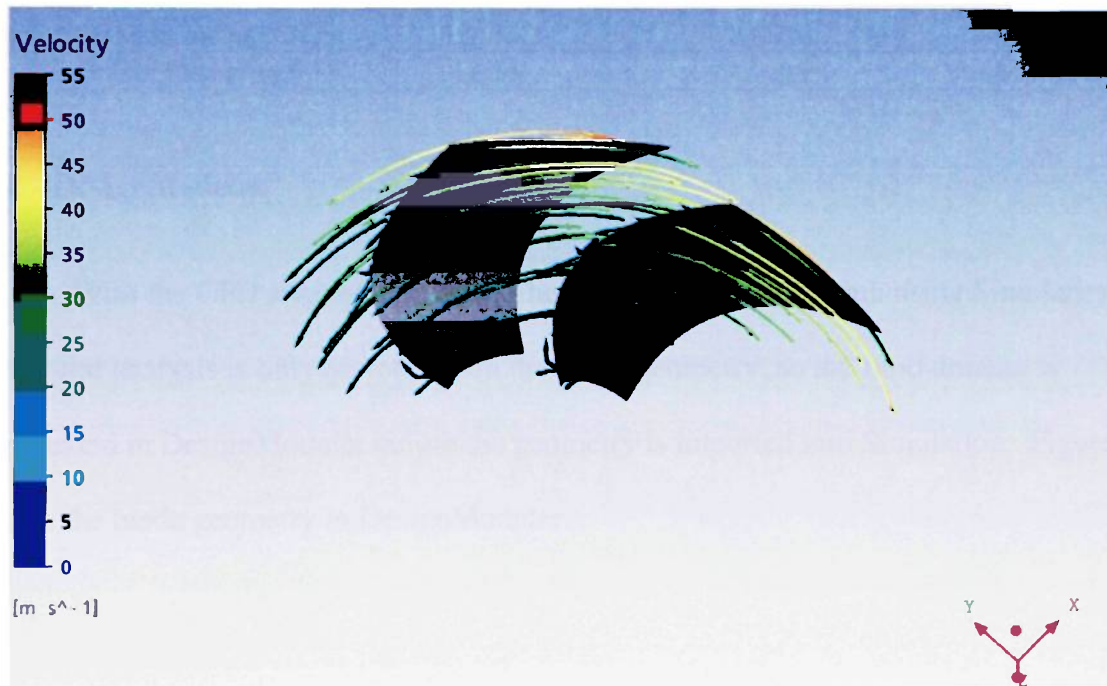


Figure 8: Low Speed Fan Blade CFX Results – Blade Velocity Streamlines at Blade Trailing Edge

### 3.3.1. CFD Analysis Comparison

To confirm that the meshing and boundary condition setup is correct, the CFD analysis results are compared to the CFD results from the previous research [5]. Since the CFD analysis process between the previous research and the current research is not exactly the same, not all the previously calculated results are easily available now.

Table 7 shows a comparison between the previous and current CFD results. From Table 7, the CFD results from the current research closely compare to the previous research with the comparable results having percent differences less than 1%.

**Table 7: Comparison of CFD Results – Low Speed Fan Blade**

	<b>Previous Study</b>	<b>ANSYS Study</b>	<b>Percent Difference</b>
Angular Velocity (rad/s)	-119.381	-119.380	0.0004%
Mass Flow Rate (kg/s)	4.2861	4.2864	-0.0070%
Volume Flow Rate (m <sup>3</sup> /s)	3.6170	3.6436	-0.7327%
Total (Isentropic) Efficiency	76.50%	77.1229%	-0.8109%

### 3.4. DesignModeler

With the CFD analysis complete, the structural analysis is run using Simulation. Structural analysis is only performed on the blade geometry, so the fluid domain is suppressed in DesignModeler before the geometry is imported into Simulation. Figure 9 shows the blade geometry in DesignModeler



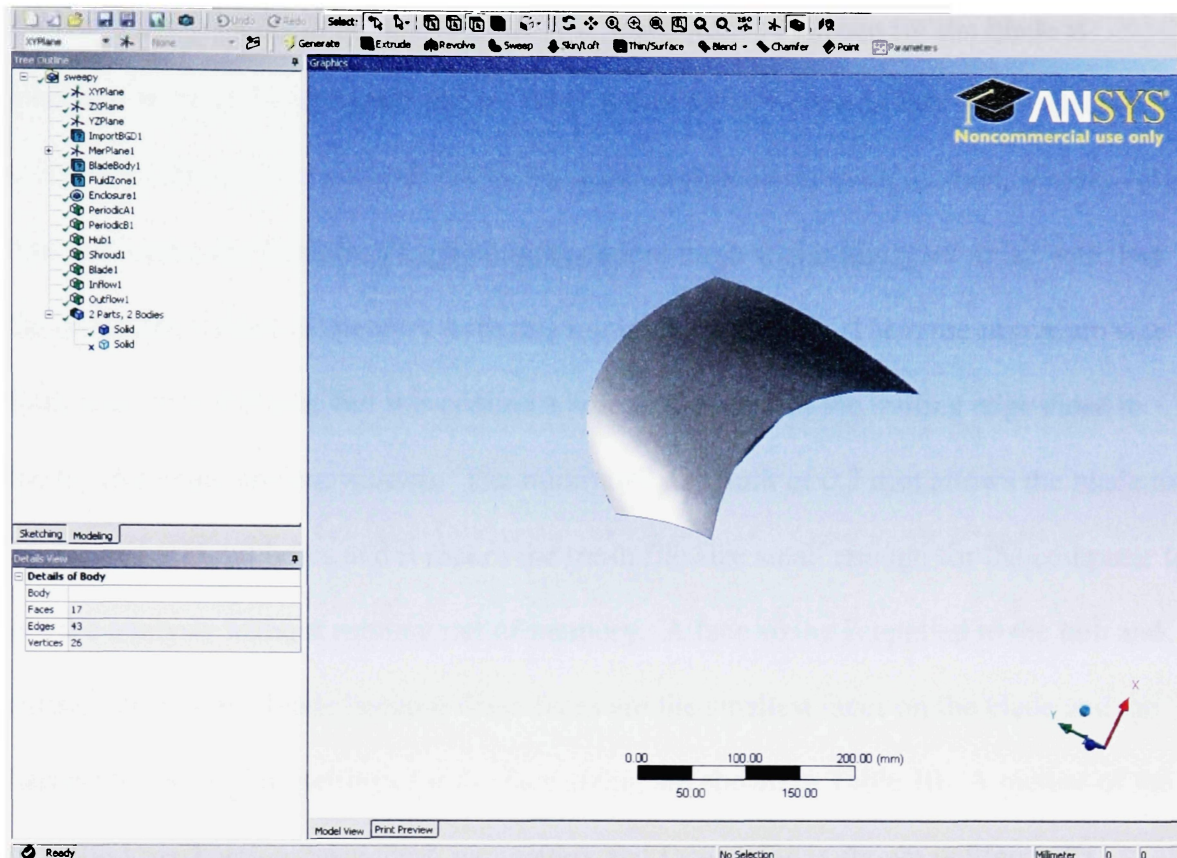


**Figure 9: Blade Geometry in DesignModeler – Low Speed Fan Blade**

### 3.5. Simulation

Once the blade geometry is imported into Simulation, a new static structural analysis is added to the model. The next step is to set the correct blade material. In this study, the blades are assumed to be made of a plastic. The only plastic listed in the available (built-in) material list is polyethylene. For illustration of the process, polyethylene is initially chosen as the blade material. Loadings and constraints are then applied to the blade. A CFX pressure load is added, which uses the blade's CFX results as the loading distribution. A fixed support is placed at the hub and shroud of the blade.

A structural mesh is created in Simulation to run structural analysis on the blade. The shape and size of the blade makes it difficult to create a structural mesh, so the

choice of mesh methods is very limited. The mesh method chosen for the blade is mechanical, patch independent mesh. Table 8 and Table 9 provide lists of the specific settings for the mesh in general and for the patch independent mesh method, respectively. The minimum size limit for the patch independent mesh was initially set to 0.1 mm, but the computer ran out of memory with this minimum size limit. Then, the minimum size limit was set to 0.5 mm, but this created a hole in the mesh at the trailing edge close to the tip (for some unclear reason). The minimum size limit of 0.7 mm allows the blade to be meshed without holes and it makes the mesh file size small enough for the computer to run the analysis without running out of memory. A face sizing is applied to the hub and shroud faces of the blade because these faces are the smallest faces on the blade and the hardest to mesh. The settings for the face sizing are shown in Table 10. A picture of the structural mesh using these mesh parameters and face sizing is shown in Figure 10.

**Table 8: General Settings for Structural Mesh – Low Speed Fan Blade**

<b>General Settings</b>	
Physical Preference	Mechanical
Relevance	100
Relevance Center	Fine
Element Size	5 mm
Shape Checking	Standard Mechanical
Solid Element Midside Nodes	Program Controlled
Straight Sided Elements	No
Initial Size Seed	Part
Smoothing	High
Transition	Fast

**Table 9: Mesh Method Settings for Structural Mesh – Low Speed Fan Blade**

<b>Mesh Method -- Patch Independent</b>	
Method	Tetrahedrons
Algorithm	Patch Independent
Element Midside Nodes	Use Global Setting
Defined By	Max Element Size
Max Element Size	5 mm
Define Defeaturing Tolerance	No
Curvature and Proximity Refinement	Yes
Min Size Limit	0.7 mm
Span Angle	Fine
Minimum Edge Length	0.017381 mm

**Table 10: Face Sizing Settings for Structural Mesh – Low Speed Fan Blade**

<b>Face Sizing</b>	
Location	Hub and Shroud
Type	Element Size
Element Size	1 mm
Edge Behavior	Curv/Proximity Refinement

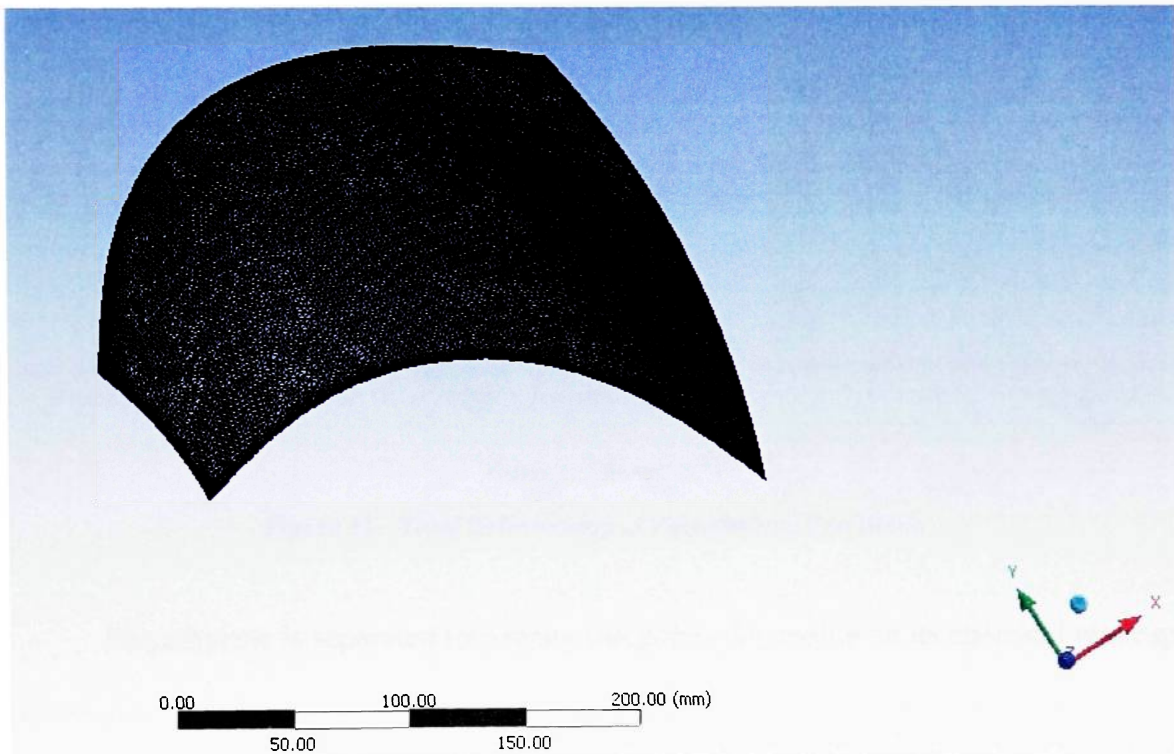


**Figure 10: Structural Mesh Created in Simulation – Low Speed Fan Blade**

The static structural analysis in Simulation is able to calculate several types of structural results, including deformations and stresses. The default results calculated by the analysis are: total deformation, equivalent stress, and shear stress. The results for the fan blade are shown in Table 11. Figure 11 shows the total deformation distributions on the fan blade.

**Table 11: Structural Analysis Results for Polyethylene Fan Blade**

Structural Results	
Maximum Total Deformation	4.4566 mm
Maximum Equivalent Stress	34.967 MPa
Maximum Shear Stress	20.051 MPa

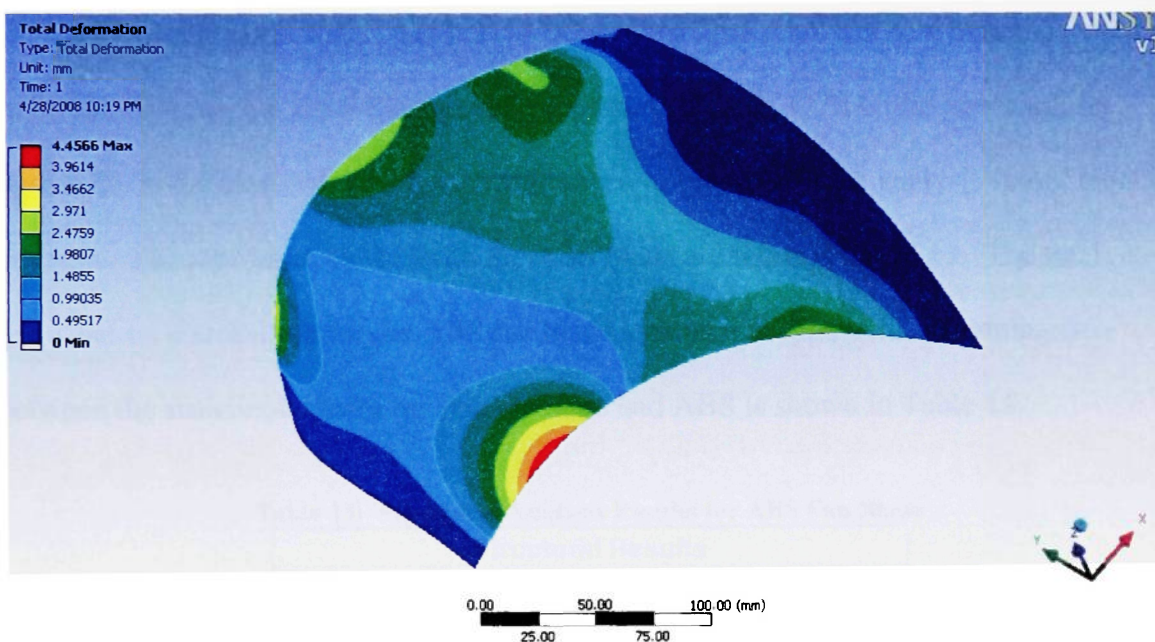


**Figure 11: Total Deformation of Polyethylene Fan Blade**

Polyethylene is separated into many categories depending on its chemical makeup and density. Each category has its own applications. Low density polyethylene is mainly used to make plastic bags and packaging. High density polyethylene is used to make plastic bottles and bottle caps. ANSYS does not specify what type of polyethylene is given. To know exactly what type of material and its properties are used for the blade,

the structural analysis is run again with a new material. The material chosen is acrylonitrile butadiene styrene (ABS), which is a common plastic found in piping, musical instruments, and many toys including LEGOs. The material properties for ABS are listed in Table 12 [6], [7], [8].

**Table 12: ABS Material Properties**

<b>Material Properties</b>	
Young's Modulus	2.758 GPa
Poisson's Ratio	0.35
Density	1.05 g/cm <sup>3</sup>
Tensile Yield Strength	41.368 MPa
Compressive Yield Strength	7.722 MPa

Since Simulation does not have ABS as a material choice, a new material is made in Simulation that has the ABS material properties in Table 12. For the new analysis with ABS as the material, no other changes need to be made to the analysis setup, model, or mesh. The structural results from the ABS blade are listed in Table 13. The total deformation distribution for the ABS fan blade is shown in Figure 12. A comparison between the structural results for Polyethylene and ABS is shown in Table 14.

**Table 13: Structural Analysis Results for ABS Fan Blade**

<b>Structural Results</b>	
Maximum Total Deformation	1.7403 mm
Maximum Equivalent Stress	34.231 MPa
Maximum Shear Stress	19.03 MPa



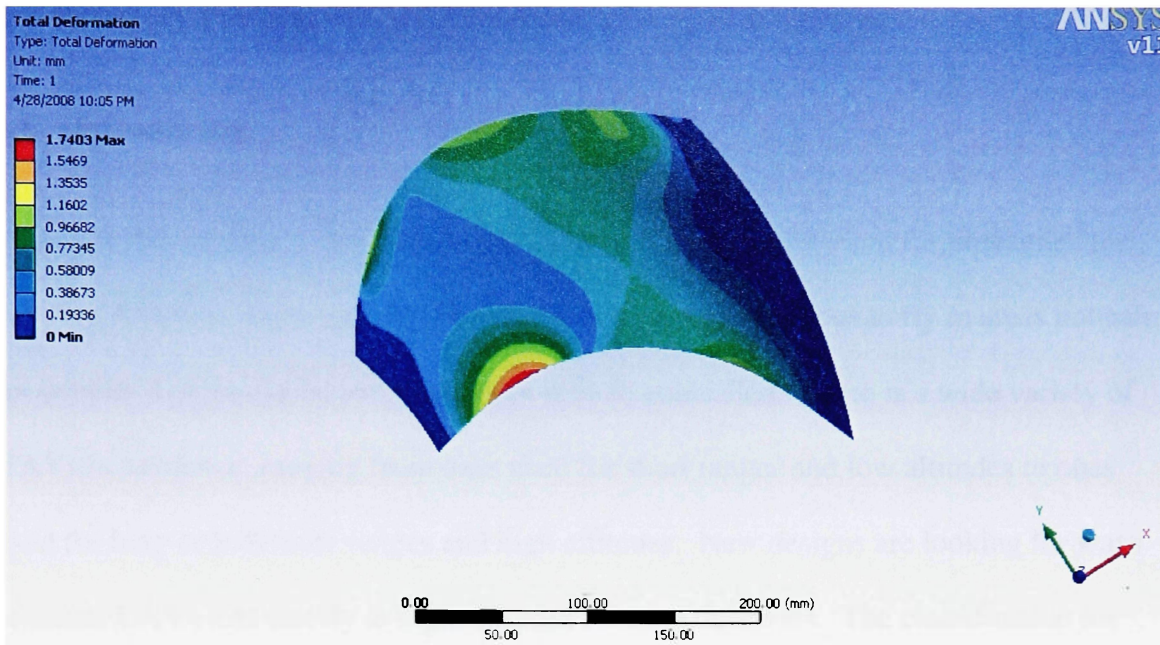


**Figure 12: Total Deformation of ABS Fan Blade**

**Table 14: Comparison of Structural Results for Polyethylene and ABS Plastic**

	<b>Polyethylene</b>	<b>ABS</b>	<b>Percent Difference</b>
Maximum Total Deformation (mm)	4.4566	1.7403	87.67%
Maximum Equivalent Stress (MPa)	34.967	34.231	2.13%
Maximum Shear Stress (MPa)	20.051	19.030	5.23%

Looking at the comparison of structural results in Table 14, the type of plastic does not change the maximum equivalent stress or maximum shear stress very much (2.13% and 5.23%, respectively). However, the maximum total deformation greatly varies when the type of plastic changes; the polyethylene blade's maximum total deformation is 87.67% higher than that for the ABS blade. Even though the magnitude of the total deformation changes with the type of plastic material, the location of the maximum total deformation stays the same, on the leading edge close to the hub of the blade. To get a better structural analysis of the low speed fan blade, the correct plastic material and its corresponding material properties should be found. With the correct plastic, the analysis will give a better approximation of the true total deformation.

## **4. HIGH ALTITUDE PROPELLER BLADE APPLICATION**

### **4.1. Introduction**

In the aerospace industry, there is an ever increasing demand for unmanned air vehicles (UAVs). They are used in military and civil applications to fly in areas not safe for people. UAVs can be autonomous or remote controlled. There is a wide variety of UAVs in existence, ranging from ones used for short ranges and low altitudes to ones used for long or indefinite ranges and high altitudes. New designs are looking for ways to create UAVs that can fly at high altitudes for long durations. The classification for these UAVs is known as High Altitude/ Long Endurance (HALE). With high altitude capabilities, these UAVs can fly over thunderstorms and still be able to perform aerial surveillance on the ground below. The long endurance aspect of HALE UAVs allows the vehicle to stay airborne for long hours, and sometimes days, at a time before they have to find a safe place to land.

NASA's Environmental Research Aircraft and Sensor Technology (ERAST) program has been involved in researching and developing HALE UAVs for many years. In 1998, this program was conducting research on a remote controlled UAV capable of flying at high altitudes (80,000 ft to 100,000 ft) at subsonic speeds. L. Danielle Koch, in Reference [9], conducted research for this project. The study focused on designing a propeller blade that would be capable of creating the thrust and power needed for a UAV to reach and maintain the specified high altitudes.

Since no previous or on-going research is being conducted on HALE UAVs at Embry-Riddle Aeronautical University, Koch's research on high altitude propeller blades is used in this research as a starting point. In the course of this project, it was planned

that CFD and structural analysis would be conducted on Koch's propeller blade design in the ANSYS Workbench environment. Note that in Reference [9], the propeller blade modeling included CFD analysis using Advanced Ducted Propfan Analysis Code (ADPAC), but it did not include structural analysis. The previous research also included theoretical calculations using blade strip theory equations published by Adkins and Liebeck in Reference [10]. The CFD analysis from ANSYS Workbench would be compared to the ADPAC analysis, to help verify the ANSYS Workbench process for propeller design studies. The following sections describe and discuss the success and failures of this effort.

#### **4.1.1. Propeller Blade Design Information**

The high altitude propeller blade research of Reference [9] has two designs for the propeller blade: a base design and a final design. The final design for the blade is used in this research because it is the only design used for 3D analysis in Reference [9]. The information for the selected blade design is given in Table 15.



**Table 15: High Altitude Propeller Blade Design Parameters**

Parameter	Final Design
Airfoil Type	Eppler 387 (constant through span)
Chord	see Figure 13
Pitch Angle	see Figure 14
Corrected Pitch Angle at 0.75 Span Location	44.52°
Power	63.4 kW (85 hp)
Altitude	25.9 km (85,000 ft)
Number of Blades	3
Operational Reynolds Number	60,000 – 100,000
Blade Diameter	4.6 m (15.1 ft)
Torque	703.7 N-m (519.0 ft-lb)
Propeller Angular Velocity*	860.35 RPM
Cruise (Vertical) Velocity	Mach 0.40
Zero Lift Angle of Attack**	-2.30°

\*Propeller Angular Velocity was not given directly, so it was calculated by dividing the given theoretical power by the given theoretical torque.

\*\* Zero Lift Angle of Attack was extrapolated from the coefficient of lift vs. angle of attack curves.

The chord and blade pitch angle for the blade are given in Reference [9] as graphs versus the radial position along the entire span of the blade. Data points from these graphs are extrapolated. The chord and pitch angle graphs are reproduced in Figure 13 and Figure 14.

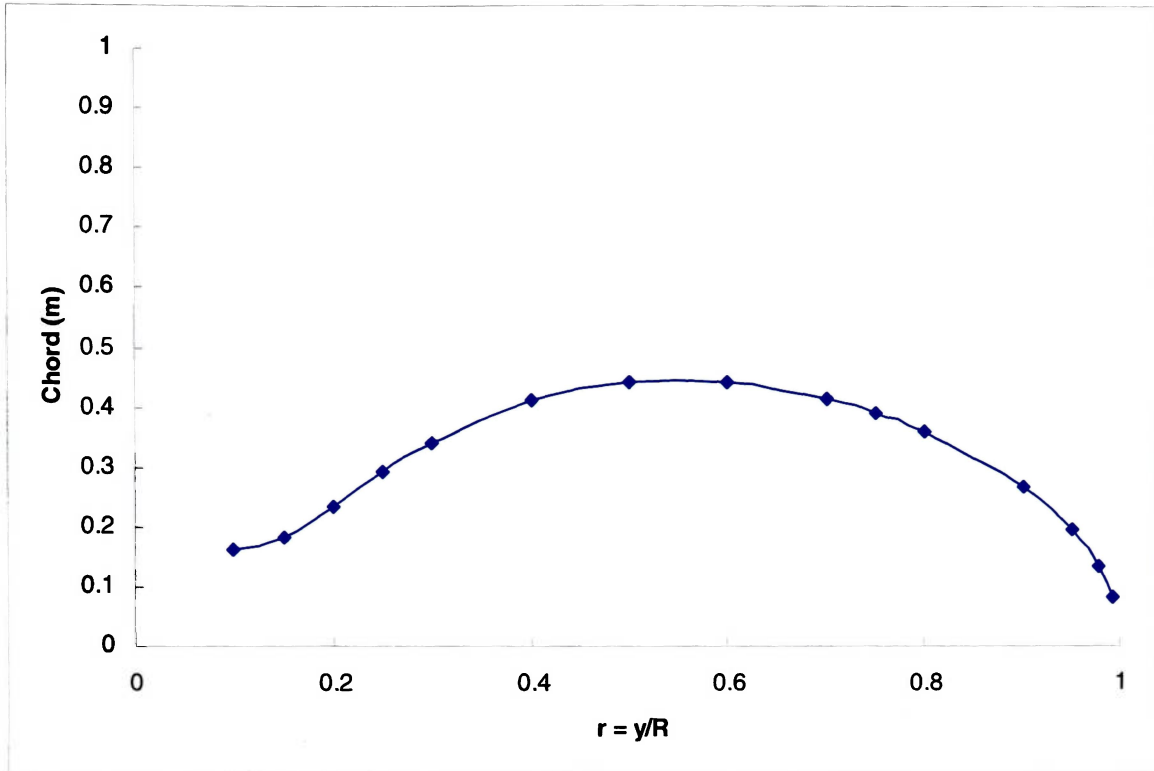


**Figure 13: Chord vs. Radial Position – High Altitude Propeller Blade**

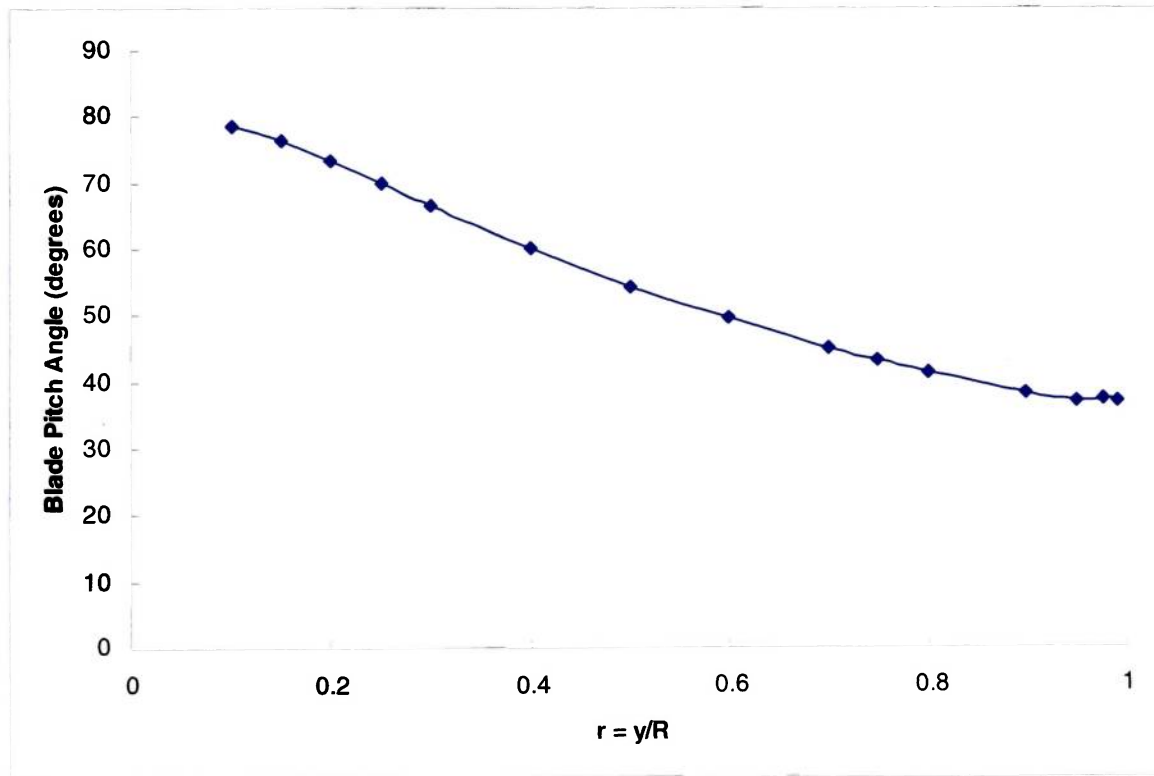


**Figure 14: Blade Pitch Angle vs. Radial Position – High Altitude Propeller Blade**

The data to create Figure 13 and Figure 14 is in the following table:

**Table 16: Pitch Angle and Chord Data – High Altitude Propeller Blade**

<b>r = y/R</b>	<b>Pitch Angle (°)</b>	<b>Chord (m)</b>
0.100	78.54	0.163
0.150	76.46	0.183
0.200	73.33	0.233
0.250	69.79	0.292
0.300	66.46	0.342
0.400	60.00	0.413
0.500	54.17	0.442
0.600	49.58	0.442
0.700	45.00	0.417
0.750	42.92	0.392
0.800	41.25	0.363
0.900	38.13	0.267
0.950	36.67	0.196
0.977	37.08	0.133
0.992	36.67	0.083

The graphs of chord and pitch angle do not include values for 0.0 or 1.0 span locations. The propeller blade hub starts at a span location of 0.1 because it connects to the center ring at this location. For the 1.0 span location, the tip chord is estimated as 30% of the last known value at the 0.992 span location, and the tip pitch angle is kept the same as the angle for 0.992 span location. The corrected chord and pitch angle values are shown in Table 17.

**Table 17: Corrected Chord and Pitch Angle Data – High Altitude Propeller Blade**

<b>r = y/R</b>	<b>Pitch Angle (°)</b>	<b>Chord (m)</b>
0.100	78.54	0.163
0.150	76.46	0.183
0.200	73.33	0.233
0.250	69.79	0.292
0.300	66.46	0.342
0.400	60.00	0.413
0.500	54.17	0.442
0.600	49.58	0.442
0.700	45.00	0.417
0.750	42.92	0.392
0.800	41.25	0.363
0.900	38.13	0.267
0.950	36.67	0.196
0.977	37.08	0.133
0.992	36.67	0.083
1.000	36.67	0.025

As seen in Table 15, the propeller blade is designed to operate at an altitude of 85,000 ft. The atmospheric data at the operational altitude is found using a website that calculates atmosphere properties based on the 1976 Standard Atmosphere Properties [11]. An example of the website layout is shown in Appendix B. Table 18 gives a list of essential atmospheric data at the operational altitude (85,000 ft).

**Table 18: Atmosphere Properties at 85,000 ft**

<b>Atmospheric Data</b>	
Height	85,000 ft
Density	6.74342E-05 slug/ft <sup>3</sup>
Speed of Sound	980.955 ft/s
Dynamic Viscosity	3.0353E-07 slug/ft-s
Temperature	222.4528 K
	394.32 °R
Pressure	45.827 lb/ft <sup>2</sup>
Kinematic Viscosity	4.50117E-03 ft <sup>2</sup> /s
Inverse of Kinematic Viscosity	222.164 s/ft <sup>2</sup>

The results from the high altitude propeller blade analysis for the theoretical strip theory calculations and the ADPAC CFD analysis [9] are shown in Table 19. Comparing the ADPAC and strip theory results, the ADPAC CFD analysis shows an error of 1.5% for efficiency for efficiency. The errors for the thrust, power, and torque coefficients are approximately 5%.

**Table 19: High Altitude Propeller Blade Results from Reference [9]**

<b>Results</b>	<b>Strip Theory</b>	<b>ADPAC</b>
Efficiency	0.8509	0.8624
Thrust Coefficient	0.1411	0.1355
Power Coefficient	0.3007	0.2850
Torque Coefficient	0.04785	0.04536
Thrust	450.9 N	433.0 N
	101.3 lb	97.3 lb
Power	63.4 kW	60.1 kW
	85 hp	80.6 hp
Torque	703.7 N-m	667.0 N-m
	519.0 ft-lb	491.9 ft-lb

## 4.2. Preliminary Design Analysis using Blade Element Theory Spreadsheet

Before any analysis on the high altitude propeller blade is performed in ANSYS Workbench, a preliminary design analysis is completed using blade element theory equations. Professor Charles Eastlake at Embry-Riddle Aeronautical University created a spreadsheet to equate the blade element theory equations at radial positions along the entire span of the blade [12]. This spreadsheet was used to design many blades that, once built, performed close to the spreadsheet's predicted performance. The spreadsheet calculates the thrust, total horsepower, percentage of power, and propeller efficiency for the blade. The inputs for the spreadsheet are:

- engine horsepower,  $(HP)_e$
- number of blades,  $N$
- blade radius (in feet),  $R$
- angular velocity (in RPM),  $\Omega$
- forward speed (in knots),  $V_f$
- atmospheric data:
  - density,  $\rho$
  - speed of sound,  $a$
  - inverse of kinematic viscosity (density divided by dynamic viscosity),  $\frac{1}{\nu} = \frac{\rho}{\mu}$
- pitch angle correction,  $\Delta\theta$
- chord,  $c$ , at varying span locations (in inches)
- pitch angle,  $\theta_b$ , at varying span locations
- zero lift angle of attack,  $\alpha_{L=0}$ , at varying span locations
- incompressible 2D coefficient of lift slope,  $(C_{L\alpha})_{incom.2D}$ , at varying span locations

The blade input values used for the blade element theory spreadsheet are listed in Table 15 through Table 17. Note that some of the input values' units are not the same as the units in the spreadsheet. Unit conversions are made, so the input values are in the correct units in the spreadsheet. The chord and pitch angle values at each radial position are listed in Table 17. Since the blade uses a constant airfoil (Eppler 387) throughout the span, the zero lift angle of attack is taken as the same at all radial positions.

Since  $(C_{L\alpha})_{incom\ 2D}$  does not vary greatly between different airfoil shapes, it is estimated by the following equation:

$$(C_{L\alpha})_{incom\ 2D} \approx 2\pi [1/\text{rad}] \approx 6.28 [1/\text{rad}] \quad (1)$$

The spreadsheet calculates the following values at each span increment:

- corrected pitch angle,  $\theta$
- Mach number,  $M$
- compressibility correction factor,  $C_{cf}$
- incompressible 3D coefficient of lift slope,  $(C_{L\alpha})_{incom\ 3D}$
- compressible 3D coefficient of lift slope,  $(C_{L\alpha})_{com}$
- solidity,  $\sigma$
- flow angle,  $\phi$
- induced velocity,  $v_i$
- tangential velocity,  $V$
- angle of attack,  $\alpha$
- incompressible drag coefficient,  $(C_d)_{incom}$

- compressible drag coefficient,  $(C_d)_{com}$
- Reynolds number,  $R_n$
- compressible drag coefficient with Reynolds number correction,  $(C_d)_{Rn}$
- coefficient of lift,  $C_L$
- coefficient per unit radius for thrust,  $\frac{dC_T}{dr}$
- coefficient per unit radius for profile torque,  $\frac{dC_{Q_p}}{dr}$
- coefficient per unit radius for induced torque,  $\frac{dC_{Q_i}}{dr}$

The spreadsheet also calculates:

- blade surrounding area,  $A$
- tip loss distance,  $B$
- thrust coefficient with no tip loss,  $(C_T)_{no\ loss}$
- thrust coefficient tip loss,  $(\Delta C_T)_{tip\ loss}$
- thrust coefficient,  $C_T$
- thrust,  $T$
- profile torque coefficient,  $C_{Q_p}$
- induced torque coefficient with no tip loss,  $(C_{Q_i})_{no\ loss}$
- induced torque coefficient tip loss,  $(\Delta C_{Q_i})_{tip\ loss}$
- induced torque coefficient,  $C_{Q_i}$



- torque coefficient,  $C_Q$
- total power,  $(HP)_{Total}$
- percent of power,  $\%Power$
- propeller efficiency,  $\eta_{prop}$

The equations used to calculate all the values in the spreadsheet are listed in Appendix C.

#### 4.2.1. Minor Changes to Spreadsheet

There are some minor changes to the blade element theory spreadsheet. First, the spreadsheet starts at 0.1 span location because the blade hub starts at 0.1 span location. The 0.0 span location is deleted. Second, the original spreadsheet uses a constant spanwise increment of 0.1. The data extrapolated from the chord and pitch angle graphs includes some intermediate spanwise locations between the 0.1 increments. These values are inserted into the spreadsheet, so the calculations are as accurate as possible. With the addition of these spanwise locations, the calculations for thrust coefficient with no tip loss,  $(C_T)_{no\ loss}$ , profile torque coefficient,  $C_{Q_p}$ , and induced torque coefficient with no tip loss,  $(C_{Q_i})_{no\ loss}$  are adjusted. These values are calculated using the mathematical trapezoidal rule. The original equation for the trapezoidal rule is correct only if the span increases in constant increments. The additional span locations cause the increments to no longer be constant. Three new columns are created to calculate the trapezoidal rule for each span increment using the following equation:

$$\left(\frac{dC_j}{dr}\right)_{trap} = \frac{1}{2}(r_{i+1} - r_i) \left[ \left(\frac{dC_j}{dr}\right)_{i+1} + \left(\frac{dC_j}{dr}\right)_i \right] \quad (2)$$

where:

$\left(\frac{dC_j}{dr}\right)_{nap}$  is the trapezoidal rule coefficient per unit radius for “j”

$C_j$  is coefficient of “j”

$\frac{dC_j}{dr}$  is coefficient per unit radius for “j”

$j = T)_{no\ loss}$ ,  $Q_o$ , or  $Q_i)_{no\ loss}$  for thrust, profile torque, or induced torque

$r$  is the radial position

$i = 1 : k - 1$  for the entire span of the blade

$k$  is the number of span increments

The values in each new columns are then added together and the resulting values

are  $(C_T)_{no\ loss}$ ,  $C_{Q_o}$ , and  $(C_{Q_i})_{no\ loss}$ .

#### 4.2.2. Results and Conclusions

The calculated results from the blade element theory spreadsheet are shown in Table 20. The comparable results from the blade element theory spreadsheet and Reference [9] are listed in Table 21.

**Table 20: Results from Blade Element Theory Spreadsheet – High Altitude Propeller Blade**

Results	Blade Element Theory
Efficiency	1.0547
Thrust Coefficient	0.01250
Profile Torque Coefficient	0.0004567
Induced Torque Coefficient	0.006386
Torque Coefficient	0.006843
Thrust	69.7 lb
Power	47.15 hp
% Power	55.47%

**Table 21: Preliminary Design Results Comparison – High Altitude Propeller Blade**

	<b>Preliminary Design</b>	<b>Strip Theory (Ref. 9)</b>	<b>ADPAC (Ref. 9)</b>
Efficiency	1.0547	0.8509	0.8624
Thrust Coefficient	0.01250	0.1411	0.1355
Torque Coefficient	0.006843	0.04785	0.04536
Thrust (lb)	69.7	101.3	97.3
Power (hp)	47.15	85	80.6

Thus, comparing with the results of Reference [9] for the high altitude propeller blade analysis, the blade element theory spreadsheet predictions appear drastically different.

There are several possible reasons for such discrepancies. One reason is that the equation for the coefficient of drag ( $C_d$ ) in the spreadsheet is for a NACA 4412 airfoil and not an Eppler 387 airfoil. This equation is used as an approximation because the NACA 4412 airfoil is not a symmetric airfoil. (The Eppler 387 airfoil is not symmetric either.) The  $C_d$  equation is a fourth-order polynomial equation, unlike a second-order polynomial normally used for a symmetric airfoil. Since the  $C_d$  equation is not for an Eppler 387 airfoil, the spreadsheet is not calculating the correct coefficient of drag, which might help increase the errors.

Another possibility for the discrepancies is that the spreadsheet uses a Reynolds number of 3,000,000 in the Reynolds number correction of coefficient of drag ( $C_d$ ) and coefficient of lift ( $C_L$ ). The propeller blade operates at a low Reynolds number (60,000 – 100,000), as stated in Table 15. Correcting for a higher Reynolds number might be causing the errors to be high. Also, as stated previously, the coefficient of lift slope is estimated as  $2\pi$  instead of the true value for the coefficient of lift slope for an Eppler 387 airfoil.

Finally, the high errors may result from incorrect estimation of the tip chord and pitch angle values. As previously stated, the propeller blade research did not specify the chord and pitch angle values at the tip of the blade. The estimation of the tip parameters might have been an over- or under-estimation that contributes to the high errors.

In conclusion, even though the results from the blade element theory spreadsheet do not predict similar results to the strip theory or ADPAC CFD analysis from the propeller blade research, the preliminary analysis may be very informative (if properly adjusted). In the spreadsheet, it is possible to change one input at a time, which shows how this change affects the results. Optimization of the blade is feasible with the spreadsheet by modifying the inputs. This may help save time in running CFD analysis on the blades because not as many analyses have to be run to reach the optimal design.

#### **4.3. ANSYS Workbench Analysis**

Once the preliminary design of the high altitude propeller blade is complete, an analysis using the ANSYS Workbench environment may be performed. Initially, the ANSYS Workbench method in Figure 1 is used for the propeller blade analysis. The first step for this method is to create the blade in BladeGen. Since Reference [9] only provides the chord and pitch angle of the blade, the angle/thickness or pressure/suction information is not available to directly create the blade. BladeGen does provide other ways to import a blade. The blade may be imported through BladeGen's Data Import Wizard or through a meanline file (.rtzt file).

### 4.3.1. Propeller Blade Creation

To create the propeller blade with the Data Import Wizard or using a meanline file, a 3D CAD model of the blade is created. The first step in creating the blade model is to find the exact airfoil shape. The blade has a constant Eppler 387 airfoil cross-section. A spreadsheet created by Colin Usher calculates the normalized coordinates of an Eppler 387 airfoil [13]. Within the spreadsheet, the chord value is allowed to change, which changes shape and size of the airfoil. Since the airfoil coordinates are initially normalized, the units for the chord do not have to be changed. Figure 15 gives a sample of the original spreadsheet with the normalized and chord coordinates manually labeled.

Aerofoil Calculator Eppler 387		Normalized Coordinates		Coordinates with chord		Geodetic	
Enter	Chord	100.000		Enter Rib	Angle in	Degrees	20.000
	Pt.	X	Y	X plot	Y plot	X plot	Y plot
	01	1.0000000	0.0000000	100.000	0.000	106.418	0.000
	02	0.9940200	0.0008120	99.402	0.081	105.781	0.081
	03	0.9819530	0.0026260	98.195	0.263	104.497	0.263
	04	0.9669320	0.0050560	96.693	0.506	102.899	0.506
	05	0.9505750	0.0077460	95.058	0.775	101.158	0.775
	06	0.9339020	0.0104760	93.390	1.048	99.384	1.048
	07	0.9171040	0.0132140	91.710	1.321	97.596	1.321
	08	0.9002700	0.0159510	90.027	1.595	95.805	1.595
When you enter	09	0.8834370	0.0186810	88.344	1.868	94.013	1.868
a number at C4 the	10	0.8665950	0.0214090	86.660	2.141	92.221	2.141
values in columns	11	0.8497440	0.0241380	84.974	2.414	90.428	2.414
G & H change.	12	0.8328910	0.0268690	83.289	2.687	88.634	2.687
Plot these values.	13	0.8160450	0.0295960	81.605	2.960	86.842	2.960
Entering Degrees	14	0.7992070	0.0323170	79.921	3.232	85.050	3.232
in K4 will "stretch"	15	0.7823810	0.0350280	78.238	3.503	83.259	3.503
the aerofoil X axis.	16	0.7655640	0.0377280	76.556	3.773	81.470	3.773
Plot these values.	17	0.7487590	0.0404120	74.876	4.041	79.681	4.041
	18	0.7319680	0.0430760	73.197	4.308	77.894	4.308

Figure 15: Sample of Original Eppler 387 Coordinates Spreadsheet [13]

The original Eppler 387 airfoil spreadsheet does not include a pitch angle in the coordinate calculations, so the pitch angle is added to the airfoil coordinates to get the correct shape and location at different spanwise locations. Figure 16 shows a typical

airfoil shape rotated at an arbitrary pitch angle, which is labelled as  $\beta$  in the figure [10].

The pitch angle is defined as the angle between the plane of rotation and the airfoil chord.

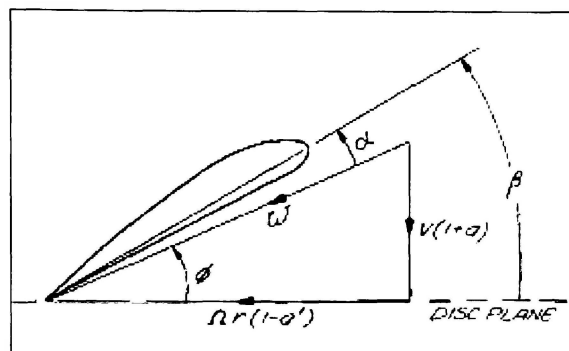


Figure 16: Airfoil Profile with Angle Labels [10]

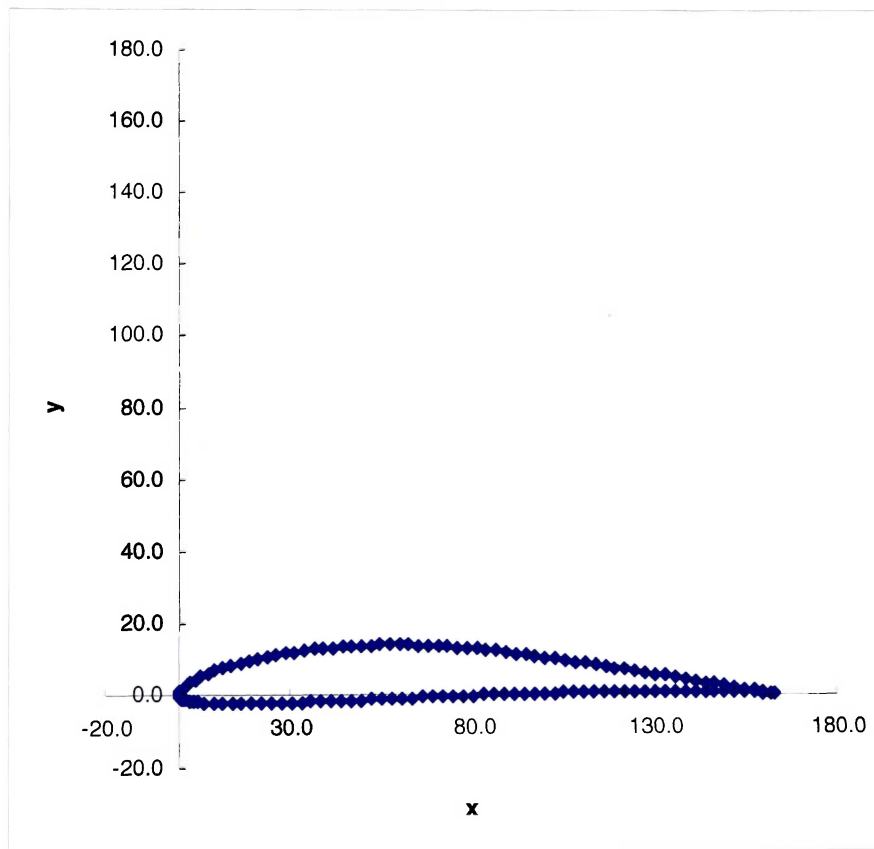


Figure 17: Eppler 387 Airfoil using Original Coordinates

As seen in Figure 17, the original coordinate data has the leading edge of the airfoil lined up along the origin of the x-y axes. To apply the pitch angle correctly and have the airfoil be in the orientation as shown in Figure 16, with the trailing edge at the origin, the coordinates are rotated and translated with the following equations:

$$x' = -x + x_o \quad (3)$$

$$y' = y \quad (4)$$

where:

$x$  is the original x coordinate

$x'$  is the rotated and translated x coordinate

$x_o$  is the original trailing edge x coordinate

$y'$  is the rotated and translated y coordinate

$y$  is the original y coordinate

The rotated and translated airfoil is shown in Figure 18.

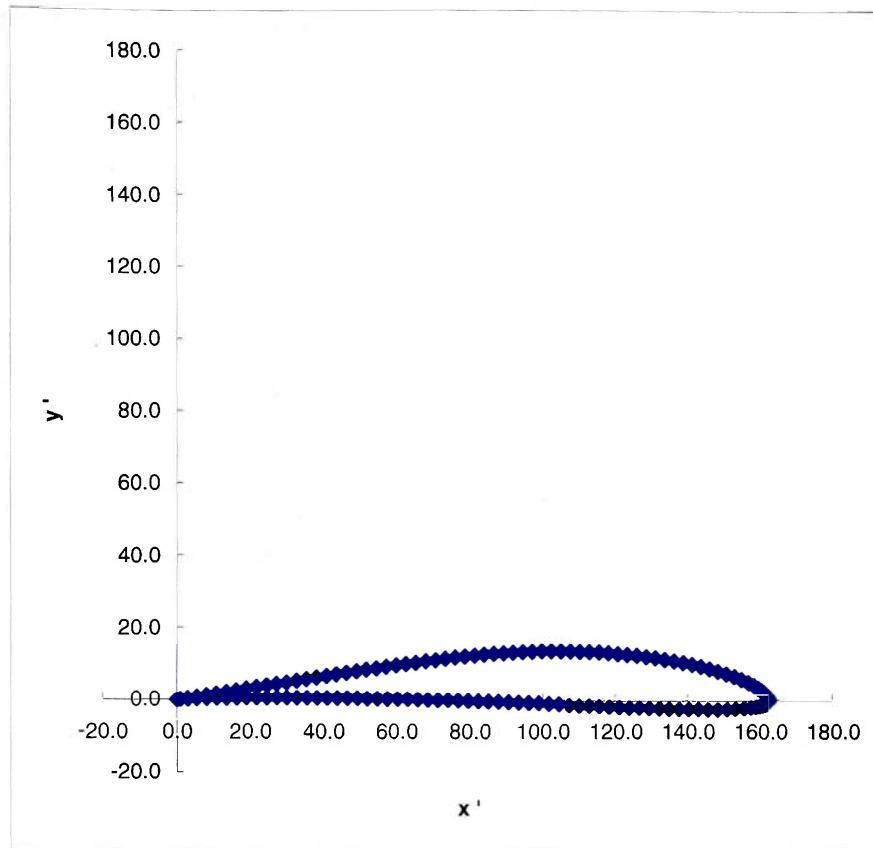


**Figure 18: Rotated and Translated Eppler 387 Airfoil**

Two columns are set up in the spreadsheet to calculate the coordinates that include the blade pitch angle, which is accomplished using the transformation equations (Equation 5 and Equation 6).

$$x'' = x' \cos \theta' + y' \sin \theta' \quad (5)$$

$$y'' = -x' \sin \theta' + y' \cos \theta' \quad (6)$$

where:

$x''$  is the angled x coordinate

$y''$  is the angled y coordinate

$\theta'$  is the negative blade pitch angle



The pitch angle is used as the negative version in the spreadsheet, so the airfoil rotates in the correct direction as shown in Figure 16. The airfoil angled at a given pitch angle is shown in Figure 19.

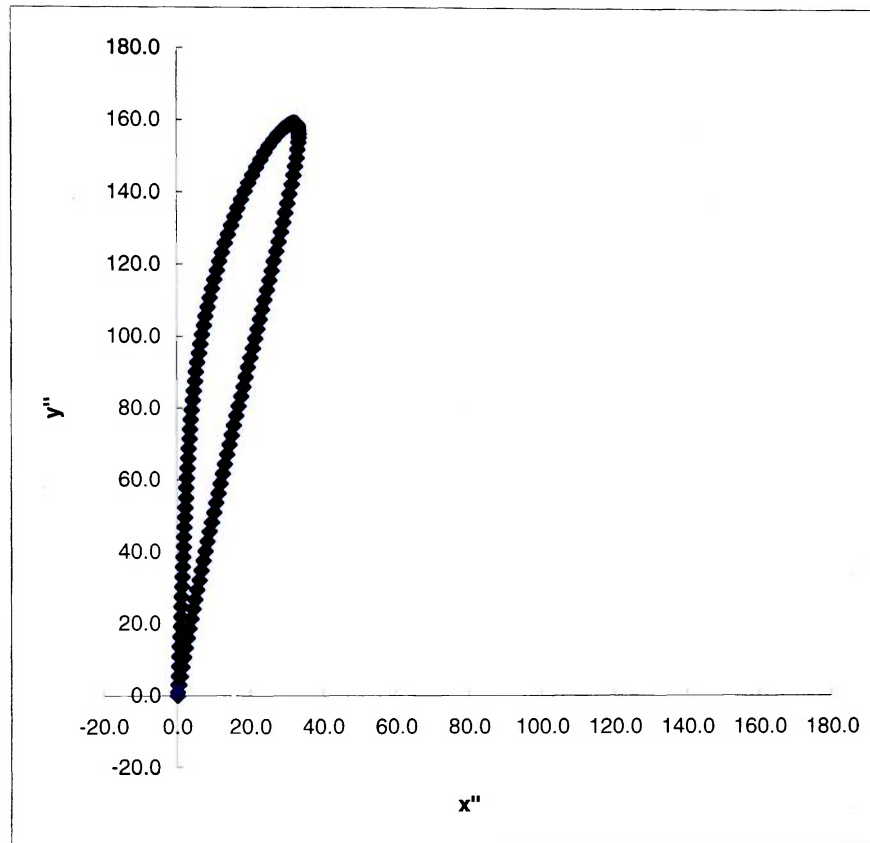


**Figure 19: Eppler 387 Airfoil with Pitch Angle**

According to Reference [9], the entire blade is rotated so the pitch angle at 0.75 span location is at  $42.52^\circ$ . This pitch angle correction is applied to the airfoil at each blade span. Two more columns are created in the airfoil spreadsheet to calculate the airfoil coordinates that includes the pitch angle with the angle correction. Similar to Equation 5 and Equation 6, the following transformation equations are used to calculate the airfoil coordinates with the corrected pitch angle:

$$x_c'' = x' \cos \theta_c' + y' \sin \theta_c' \quad (7)$$

$$y_c'' = -x' \sin \theta_c' + y' \cos \theta_c' \quad (8)$$

where:

$x_c''$  is the angled x coordinate with corrected pitch angle

$y_c''$  is the angled y coordinate with corrected pitch angle

$\theta_c'$  is the negative corrected pitch angle

The corrected pitch angle is still input as a negative value for the same reason it is negative for the initial pitch angle. Figure 20 shows the airfoil at the corrected pitch angle. Figure 21 shows a sample of the updated spreadsheet with the pitch angle and corrected pitch angle coordinates.

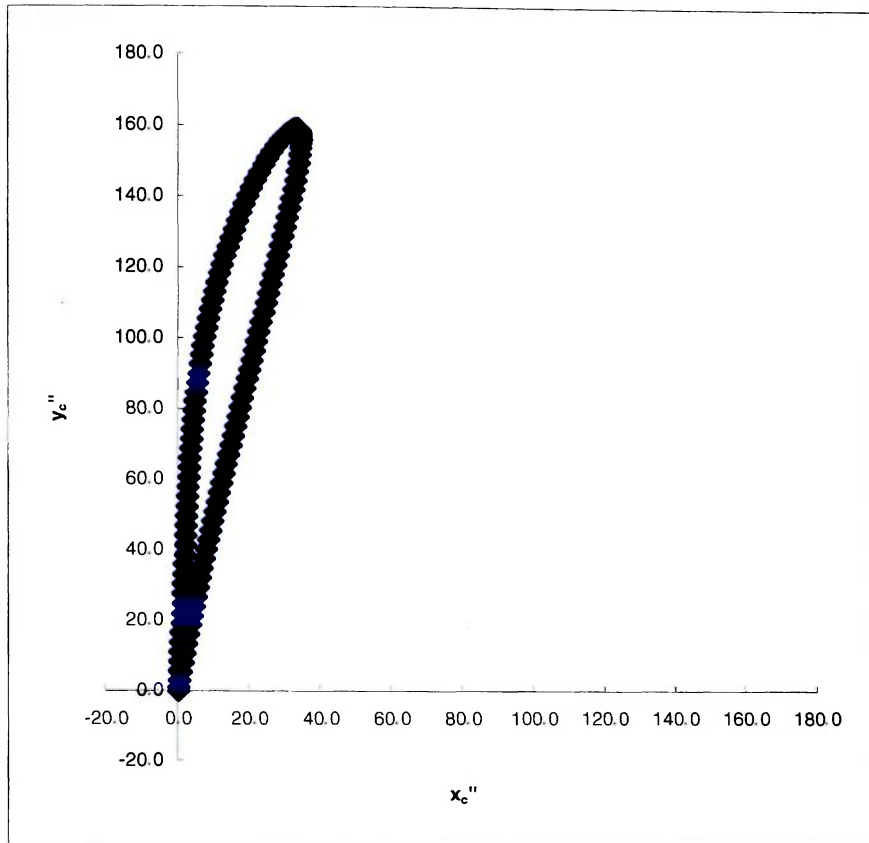


Figure 20: Eppler 387 Airfoil with Corrected Pitch Angle

Aerofoil Calculator  
Eppler 387

Enter Chord 0.163

Pt.	Coordinates with chord		Rotated and Translated Coordinates		Pitch Angle Coordinates		Coordinates with angle correction	
	X plot	Y plot	x'	y'	x''	y''	x <sub>c</sub> ''	y <sub>c</sub> ''
01	0.162500	0.000000	0.000000	0.000000	0.000	0.000	0.000	0.000
02	0.161528	0.000132	0.000972	0.000132	0.064	0.979	0.070	0.978
03	0.159567	0.000427	0.002933	0.000427	0.164	2.959	0.185	2.958
04	0.157126	0.000822	0.005374	0.000822	0.262	5.430	0.300	5.428
05	0.154468	0.001259	0.008032	0.001259	0.362	8.122	0.418	8.119
06	0.151759	0.001702	0.010741	0.001702	0.465	10.865	0.541	10.862
07	0.149029	0.002147	0.013471	0.002147	0.572	13.629	0.666	13.624
08	0.146294	0.002592	0.016206	0.002592	0.679	16.398	0.793	16.393
09	0.143559	0.003036	0.018941	0.003036	0.788	19.167	0.920	19.161
10	0.140822	0.003479	0.021678	0.003479	0.897	21.937	1.049	21.931
11	0.138083	0.003922	0.024417	0.003922	1.006	24.709	1.177	24.702
12	0.135345	0.004366	0.027155	0.004366	1.115	27.481	1.306	27.473
13	0.132607	0.004809	0.029893	0.004809	1.225	30.252	1.434	30.243
14	0.129871	0.005252	0.032629	0.005252	1.335	33.022	1.564	33.012
15	0.127137	0.005692	0.035363	0.005692	1.446	35.789	1.694	35.778
16	0.124404	0.006131	0.038096	0.006131	1.559	38.554	1.826	38.543
17	0.121673	0.006567	0.040827	0.006567	1.674	41.318	1.960	41.305
18	0.118945	0.007000	0.043555	0.007000	1.792	44.078	2.097	44.064

Summary Tables:

0.75 angle	angle cor.
42.917	0.397

Pitch	w/ correction
Angle (°)	78.542
	78.145

Figure 21: Sample of Eppler 387 Coordinates Spreadsheet including Pitch and Correction Angles

Since the axis of rotation is the z-axis, the x-coordinates in the spreadsheet are actually the y-coordinates of the blade and the spreadsheet y-coordinates are the z-coordinates of the blade. The x-coordinates of the blade are the spanwise radius values.

After the Eppler 387 airfoil coordinate spreadsheet is set up to give the correct coordinates in the correct order, the chord and pitch angle are input for each spanwise location. In order to create the entire blade, using the chord and pitch angle values for each span, a list of x-y-z coordinates is populated in a spreadsheet. This list is imported into CATIA using a macro to create points and splines of the airfoils [14]. The CATIA macro also has the ability to connect the airfoils together and create a 3D model of the propeller blade. One limitation to the macro is that it only creates models with units of inches or millimeters. Since the chord values are given in meters, the blade coordinates are changed from meters to millimeters.

The blade coordinates cause the airfoils to line up along the TE, but the blade design from the previous research has the airfoils lined up along their center of gravities (CGs). The easiest way to line up the airfoil CGs is to move them all to the origin of the y-z axes. The CG is found for each airfoil by first running the macro to create the points and splines of the airfoils. The airfoil splines are filled individually and the CG for the airfoil is found using the “Measure Inertia” function in CATIA. In the macro, the y-z coordinates of each airfoil’s CG location are subtracted from the y-z coordinates of the corresponding airfoil, which shifts the airfoil to the origin of the y-z axes.

The macro is run again to create points, splines, and loft, which connects all the airfoils, with the CG shifted coordinates, together and makes the full CG centered blade.

The last adjustment to complete the blade is to fill the hub and tip airfoils to make the blade a solid surface. Figure 22 shows a picture of the blade created in CATIA.

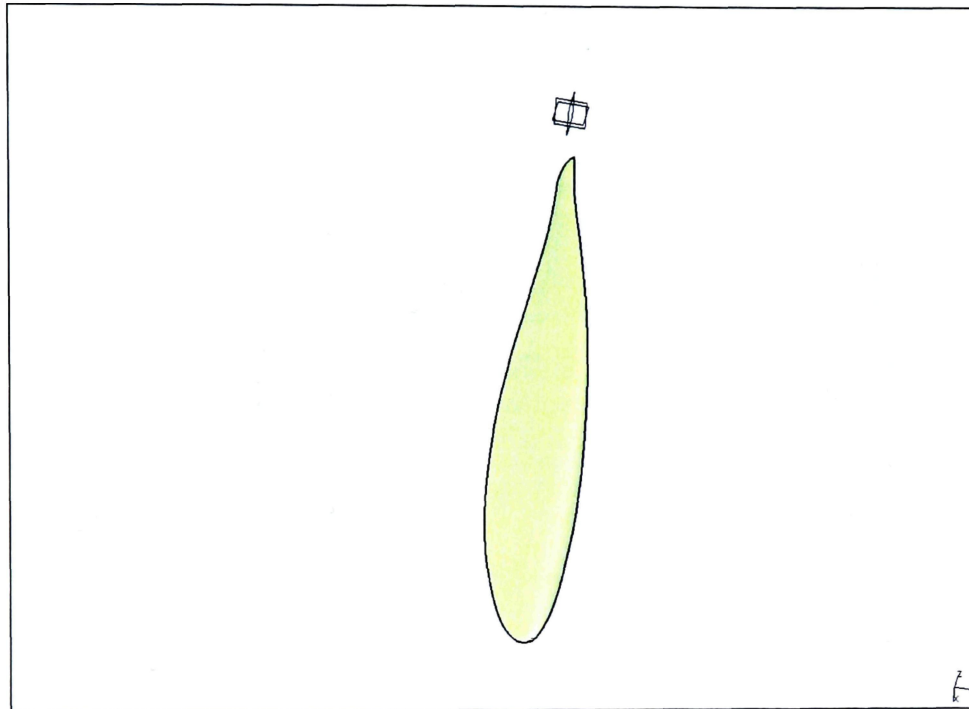


**Figure 22: High Altitude Propeller Blade Drawn in CATIA**

### **4.3.2. Importing Blade File**

#### **4.3.2.1. Data Import Wizard**

After the propeller blade is created, the blade is imported into BladeGen through its Data Import Wizard (Figure 23 and Figure 24). The Data Import Wizard only needs the airfoil profiles of the blade and the outline of the fluid domain in the blade file. To create the fluid domain, the sketching feature is used. Since the propeller is made up of three blades, the fluid domain covers a 120-degree arc (60 degrees on each side) around the blade. These features of the blade and fluid domain are saved as an IGES file (.igs file) in CATIA and imported into the import wizard. Figure 25 shows the blade profiles

and fluid domain in the Data Import Wizard. Once the blade file is loaded into the import wizard, the next step is to select the curves that represent the hub, shroud and blade profiles. After the curves are selected, the tangency points of the blade profiles in the meridional plane are identified.

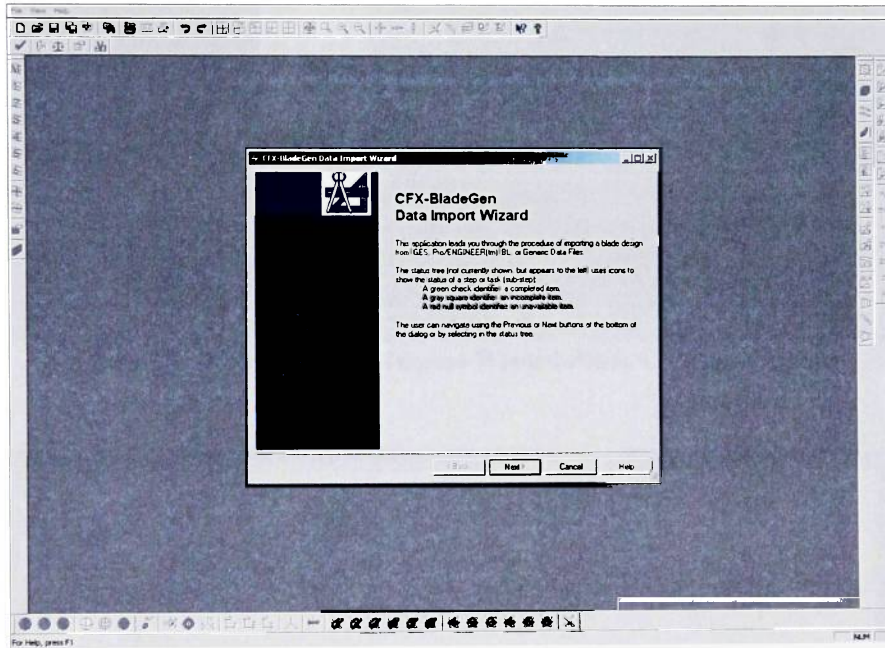


**Figure 23: BladeGen Data Import Wizard Opening Window**

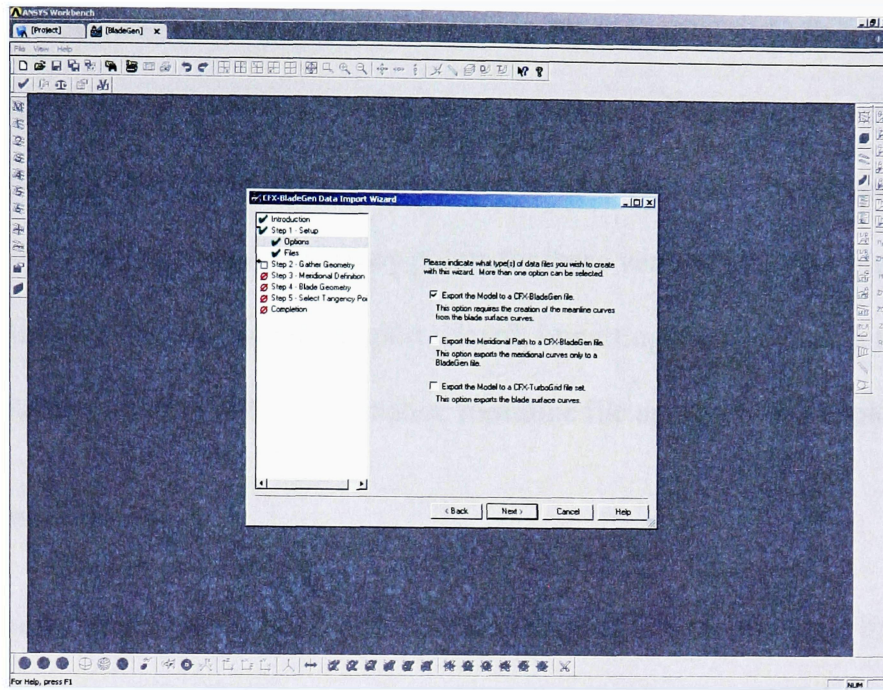


Figure 24: BladeGen Data Import Wizard Blade Creation Options

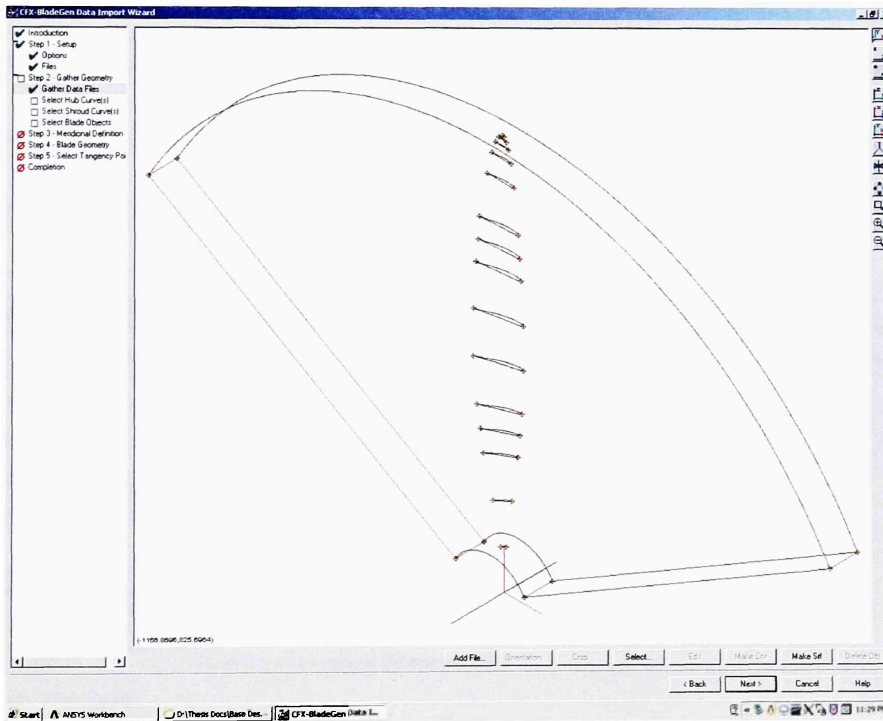


Figure 25: High Altitude Propeller Blade File in BladeGen Data Import Wizard

When selecting the tangency points for each blade profile, an issue appeared in the Data Import Wizard with the propeller blade. The twist of the blade caused some of the blade profiles to be almost vertical in the meridional plane. The Data Import Wizard apparently was unable to create tangency points for these vertical blade profiles. After several continuous failures with the import wizard, importing the blade using this approach was abandoned, and the alternative meanline file approach was explored.

#### 4.3.2.2. Meanline File

A meanline file includes the airfoil's mean camber line radius, angle in radians, and z-coordinate, and the thickness of airfoil. A template for a meanline file is shown in Figure 26 [15]. First, the mean camber line of the normalized airfoil is found to help create the mean camber line for each airfoil. After the normalized airfoil mean camber line is found, it is multiplied by the chord value for each airfoil, which gives the mean camber line for the corresponding airfoil.

```

Meanline Data File Format (rtzt)

This section describes the generic data file format for BladeGen. The file is an ASCII file that uses space separation between values

Note: Angular values must be in radians

Example File

text enclosed in {} is a data item
text enclosed in {} is a comment
text enclosed in [] is optional

(number of blades)
(number of splitters) (0 is main blade only)
(for each blade, main and splitter)
{pitch fraction} (Ignored for main blade)
(number of layers)
[N] [T] (Normal or Tangential Thickness Flag)

(for each layer)
{span fraction} {number of points} [a][t][b]
(for each point)
(r) (theta) (z) {thickness}
:
.

```

Figure 26: Meanline File Template [15]



To find the mean camber line of the normalized airfoil, the coordinates are first rotated and translated using Equation 3 and Equation 4, so the orientation looks like Figure 16. The normalized coordinates are also multiplied by 1,000, so the units are in millimeters when the chord value is multiplied into them. The normalized coordinates are imported into CATIA using the macro, and the points and splines of the airfoil are created. CATIA is also used to create the mean camber line of the normalized airfoil. After the mean camber line for the normalized airfoil is created, the thickness at different points along the mean camber line is measured in CATIA.

Once the mean camber line of the normalized airfoil is created, the x-y-z coordinates are extrapolated and put into a spreadsheet. The blade airfoil mean camber lines are created from these coordinates, using the correct chord value and corrected pitch angle. Once the x-y-z coordinates of the mean camber line for each airfoil is calculated, the coordinates are changed to radius-angle-z coordinates. The thickness values of each airfoil are calculated from the normalized airfoil thickness values and the airfoil's chord value.

The meanline file is created as a text document from the radius-angle-z coordinates and thickness values of the airfoils, using the template in Figure 26. To change the text document into a meanline file, the text document is saved as a .rtzt file. The blade is created by importing the meanline file into BladeGen. However, an error message occurs when the meanline file is opened in BladeGen. The error message states that the control curves cross, which is not allowed in BladeGen. Figure 27 shows the error message that occurs when the meanline file opens in BladeGen.

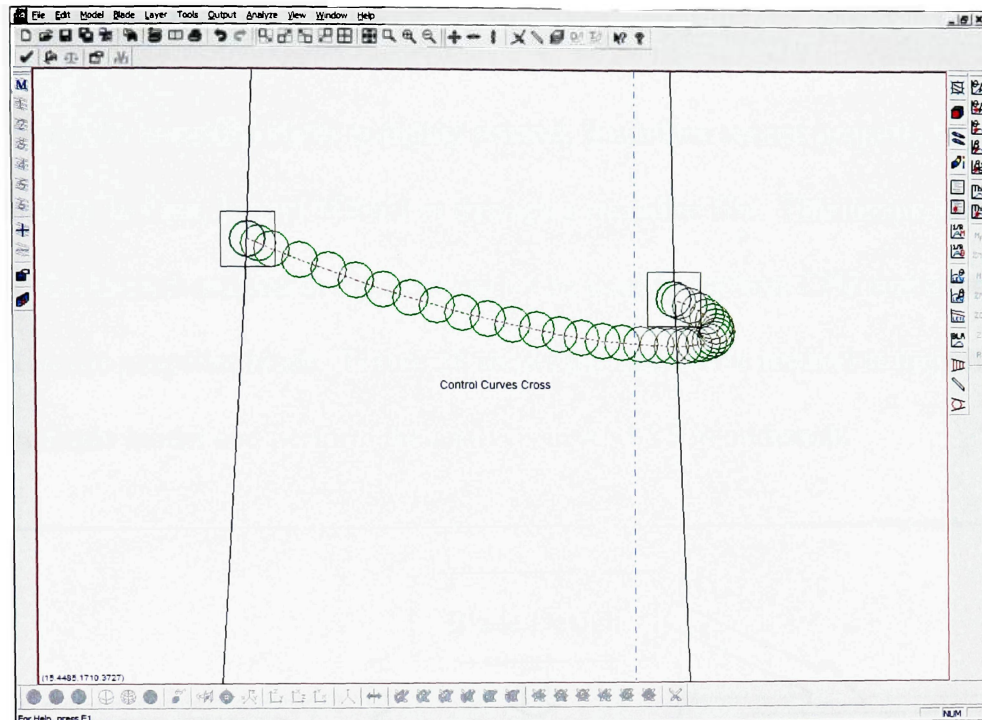


**Figure 27: Meanline File Error in BladeGen – High Altitude Propeller Blade**

For the similar reason the BladeGen Data Import Wizard did not work, the meanline file was also unable to import the propeller blade design because of the blade's large twist. When asked about the problems incurred using BladeGen's Data Import Wizard and meanline file capabilities, an ANSYS, Inc. representative, Mihajlo Ivanovic, responded that BladeGen was not suited for the creation of propeller and wind turbine blades because they are extremely twisted and that the pitch angle,  $\beta$ , must be greater than  $-90^\circ$  and less than  $90^\circ$ . (A copy of this email is in Appendix D.) For this reason, attempts to create or import the blade into BladeGen were abandoned and other methods to import the propeller blade into ANSYS Workbench for CFD and structural analysis were explored.

### 4.3.3. Importing 3D CAD Model

Since the propeller blade is highly twisted, BladeGen cannot properly import the blade through its Data Import Wizard or through a meanline file. This means that the ANSYS Workbench method in Figure 1 cannot be used to perform CFD and structural analysis on the propeller blade. Figure 28 shows the alternative method to import the propeller blade model and perform the analysis in ANSYS Workbench.

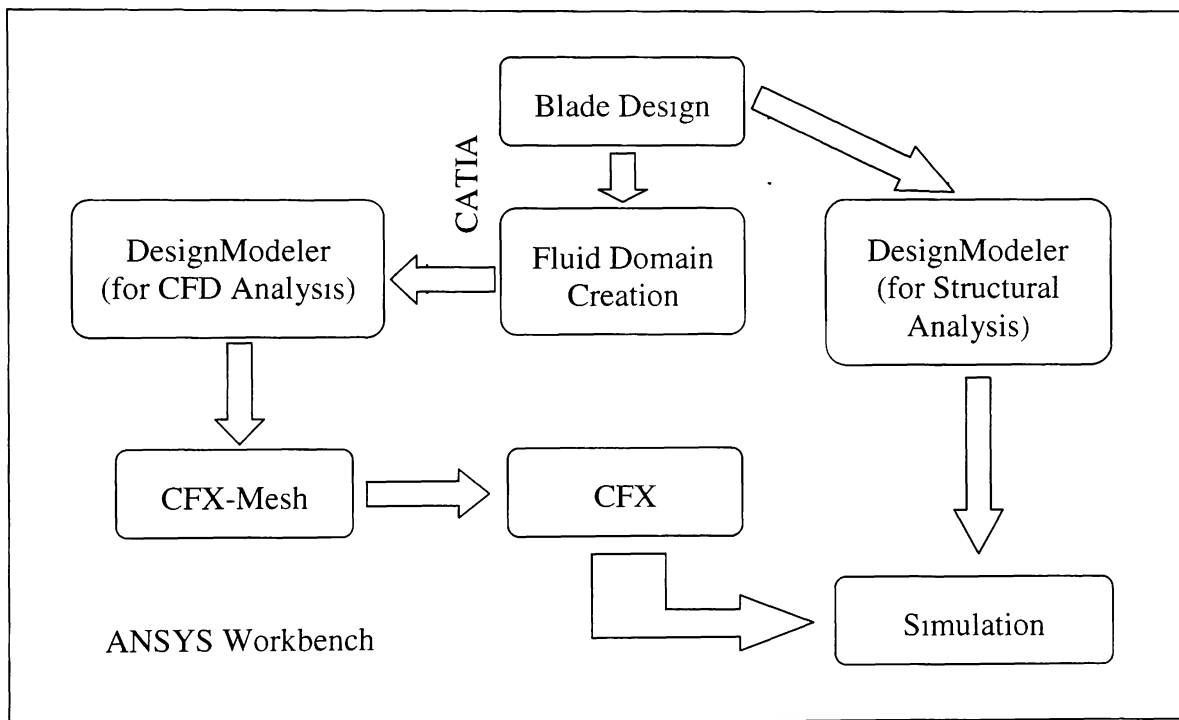
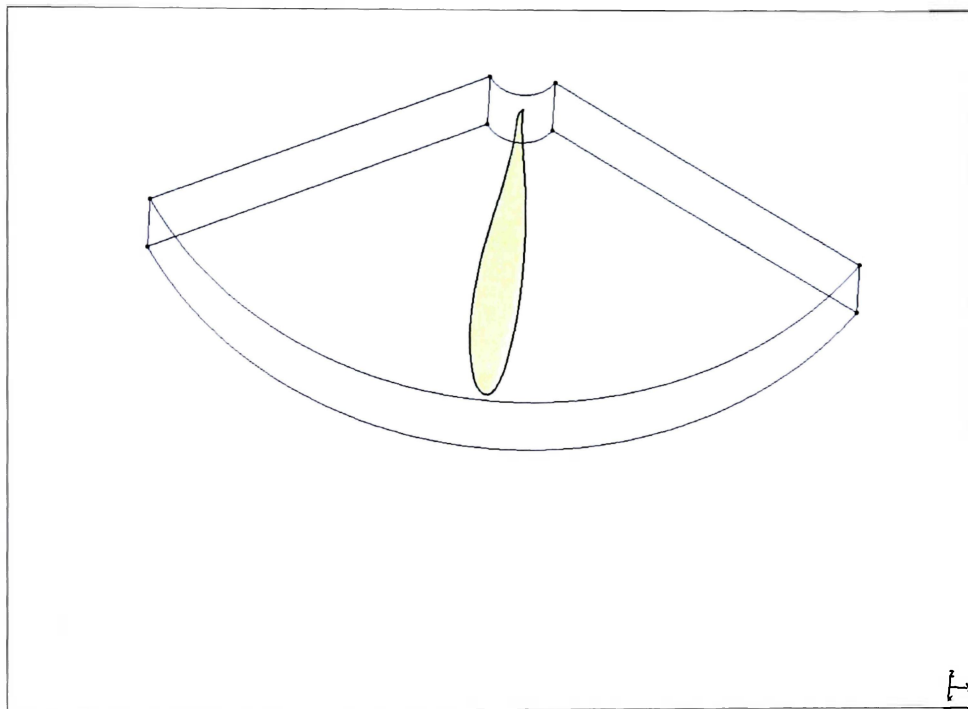


Figure 28: ANSYS Workbench Flow Chart – High Altitude Propeller Blade

The new method to analyze the propeller imports the blade model from CATIA into DesignModeler and then the blade is meshed in CFX-Mesh for CFD analysis and Simulation for structural analysis. To mesh the blade for CFD analysis, some additions are created to the blade model. A fluid domain is created around the blade to make the hub, shroud, inlet, outlet, and two periodic regions. These regions are needed to create the proper mesh for CFD analysis.

The fluid domain is created the same way it is created for the Data Import Wizard file. For this model, the entire blade is used instead of just the blade profiles used in the Data Import Wizard file. Figure 29 shows the blade surrounded by the fluid domain. The fluid domain is filled and joined together in CATIA for meshing in ANSYS. Figure 30 shows a picture of the fluid domain filled and joined together. To import into ANSYS for meshing in CFX-Mesh, the CATIA file is saved as a STEP file (.stp file).



**Figure 29: High Altitude Propeller Blade with Fluid Domain**

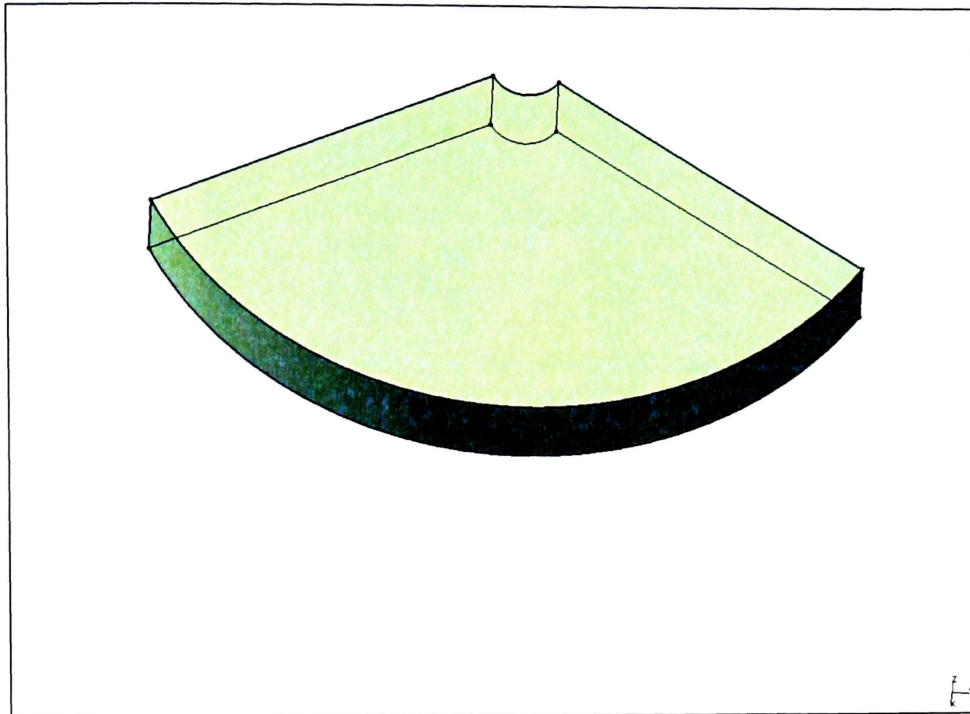


**Figure 30: High Altitude Propeller Blade Filled Fluid Domain**

#### **4.3.3.1. DesignModeler for CFD Analysis**

Once the fluid domain is created around the blade, the model is imported into DesignModeler. When DesignModeler opens, the units are selected as millimeters, since these are the units used in the 3D CAD model. For CFD analysis, the parts imported from the geometry file that are not the fluid domain or blade are suppressed, so they are not transferred with the geometry when it is imported into CFX-Mesh for meshing. Figure 31 shows the propeller blade's fluid domain geometry file in DesignModeler.

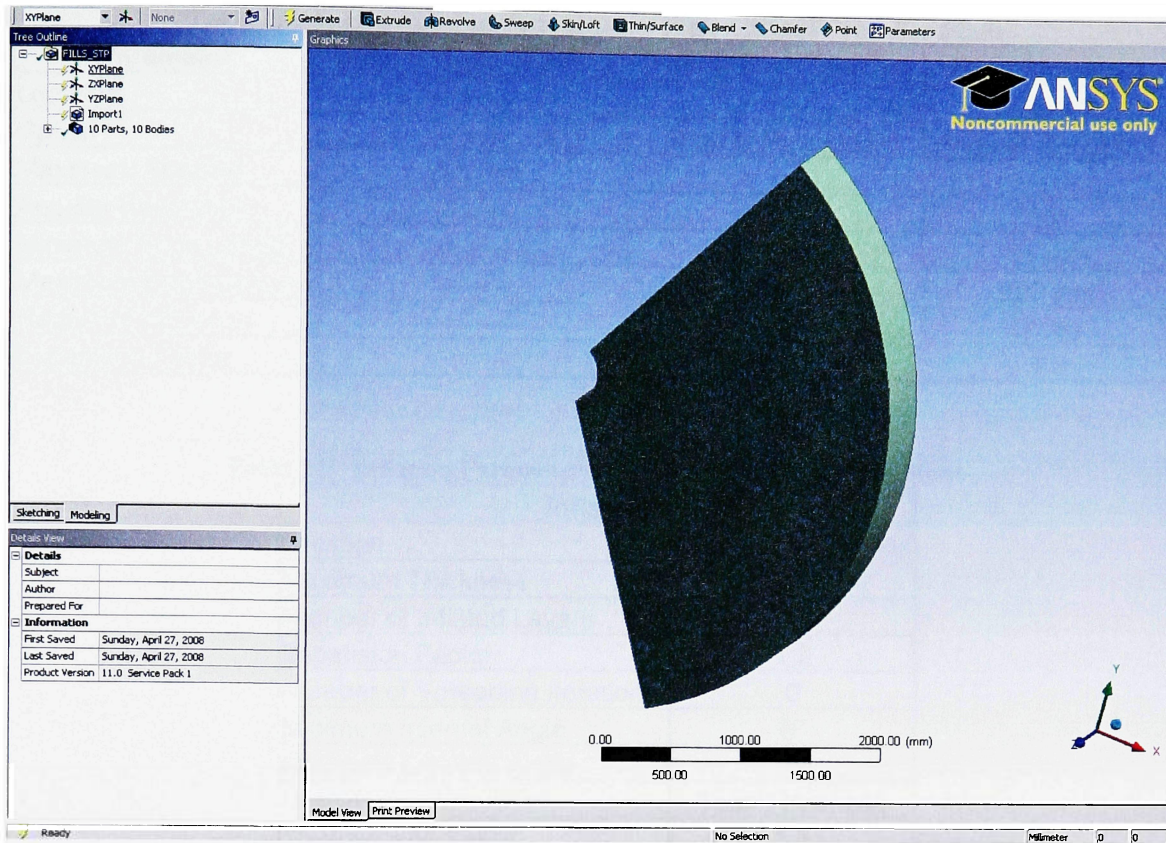


**Figure 31: High Altitude Propeller Blade Fluid Domain in DesignModeler**

#### 4.3.3.2. CFX-Mesh

Since the propeller blade is not created in BladeGen, automatic meshing with BladeEditor and CFX-Mesh for the CFD analysis is not available. Even without the automatic mesh capabilities, the propeller blade is still meshed in CFX-Mesh using the DesignModeler geometry file. The automatic mesh parameters from the low speed fan blade are used as a basis for creating the propeller blade mesh. Since the propeller blade is much larger than the low speed fan blade, the minimum and maximum edge lengths for the face spacings are increased accordingly. The unstructured mesh parameters for the propeller blade are listed in the following tables:

**Table 22: Facing Spacing Parameters – High Altitude Propeller Blade**

Parameter	Default Body Spacing	Default Face Spacing	Face Spacing 1
Location	-----	-----	All Regions
Option	-----	Angular Resolution	Angular Resolution
Maximum Spacing	220 mm	-----	-----
Angular Resolution	-----	30°	18°
Minimum Edge Length	-----	11 mm	11 mm
Maximum Edge Length	-----	220 mm	220 mm
Radius of Influence	-----	-----	0 mm
Expansion Factor	-----	-----	1.2

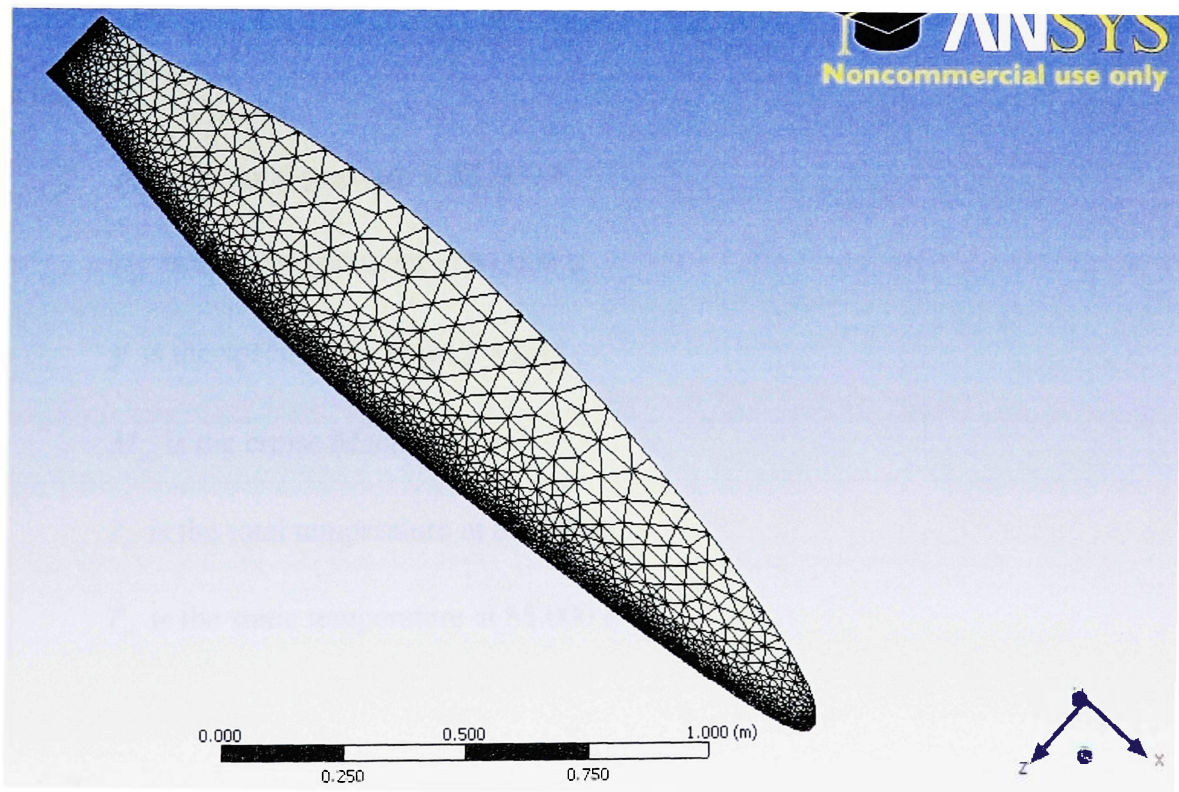
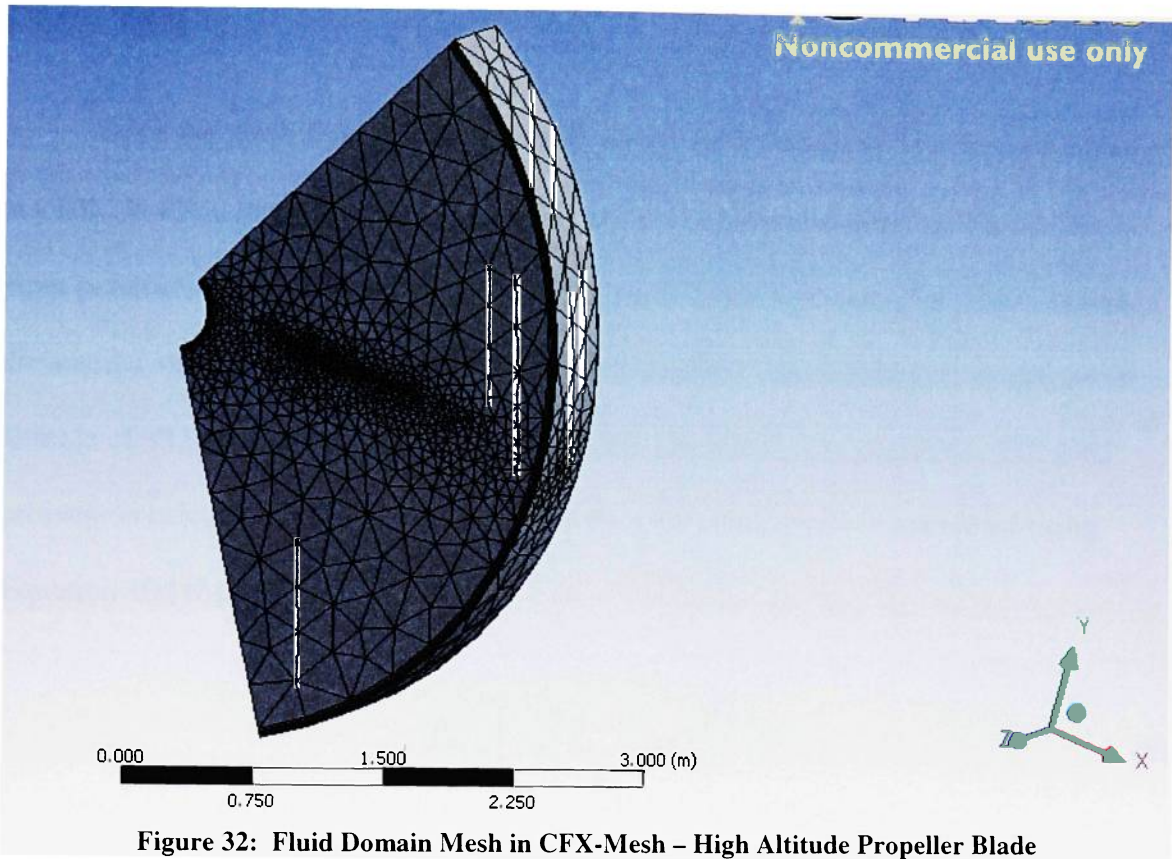
**Table 23: Inflation Parameters – High Altitude Propeller Blade**

Inflation	
Location	Hub, Shroud, Blade
Maximum Thickness	50 mm
Number of Inflated Layers	5
Expansion Factor	1.2
Number of Spreading Iterations	0
Minimum Internal Angle	5°
Minimum External Angle	10°
Option	Total Thickness
Thickness Multiplier	1.5

A periodic region is created using Periodic 1 and Periodic 2 regions in rotation. The surface and volume meshes are created using Delaunay and Advancing Front algorithms, respectively. The mesh created in CFX-Mesh for the propeller blade is used in CFX for CFD analysis.

To get a better mesh quality, the mesh parameters are changed, but there is a limit on the magnitude of the changes because large changes may create a large mesh file. If a large mesh file is created, CFX is not able to run because the computer runs out of memory. Focusing the finer mesh on only the small and highly-curved surfaces helps to keep the mesh file size small. Figure 32 and Figure 33 show the mesh created in CFX-Mesh for the fluid domain and blade, respectively.







### 4.3.3.3. CFX

Once the mesh file is created in CFX-Mesh, a CFD analysis simulation is created in CFX. In CFX-Pre, the machine type chosen for the propeller blade is “Fan”. The input parameters for the blade are the same as used for the low speed fan blade, except the angular velocity (860.35 RPM). Since the propeller blade is designed to operate an altitude of 85,000 ft, the boundary conditions are calculated at this altitude. The total pressure is calculated using Equation 9, and the total temperature is calculated using Equation 10 [16].

$$\frac{p_o}{p_{st}} = \left[ 1 + \left( \frac{\gamma - 1}{2} \right) M_c^2 \right]^{\gamma / \gamma - 1} \quad (9)$$

$$\frac{T_o}{T_{st}} = 1 + \left( \frac{\gamma - 1}{2} \right) M_c^2 \quad (10)$$

where:

$p_o$  is the total pressure at 85,000 ft

$p_{st}$  is the static pressure at 85,000 ft

$\gamma$  is the specific gas ratio ( $\gamma \approx 1.4$ )

$M_c$  is the cruise Mach number

$T_o$  is the total temperature at 85,000 ft

$T_{st}$  is the static temperature at 85,000 ft

The static pressure and static temperature at 85,000 ft are listed in Table 18, and the cruise Mach number is listed in Table 15. The input parameters and boundary conditions used in CFX-Pre are listed in Table 24. The default settings are used in CFX-Solver. Once the CFX-Pre definition file of the parameters is created, CFX-Solver is run.

**Table 24: Input Parameters and Boundary Conditions for CFX – High Altitude Propeller Blade**

<b>Input Parameters</b>	
Machine Type	Fan
Angular Velocity	860.35 RPM
Fluid	Air Ideal Gas
Reference Pressure	0 Pa
Simulation Type	Steady State
Heat Transfer	Total Energy
Turbulence	k-Epsilon
<b>Boundary Templates</b>	
P-Total	51.168 psf
P-Static	45.827 psf
T-Total	406.94 °R
Flow Direction	Normal to Boundary

Unfortunately, an error message continuously occurred when the CFX-Solver was run. The error message stated that there were two isolated volumes, and CFX failed to run the CFD analysis with two isolated volumes. One possible reason for the two isolated volumes is the way the blade and fluid domain 3D CAD model was created, with the blade surface, hub airfoil, and shroud airfoil connected together and then fluid domain surfaces connected together. The blade and fluid domain were not connected together in the 3D CAD model. Another reason for this problem in CFX might come from the boundary conditions set in CFX-Pre. To remove the isolated volumes, some modifications to the blade and fluid domain geometry are needed; and an investigation into the current boundary conditions is needed. With the additional modifications and

investigation needed, CFD analysis was abandoned for the current research and no CFD results were produced.

#### 4.3.3.4. DesignModeler for Structural Analysis

In the effort to test the structural analysis option, the fluid domain geometry is suppressed in DesignModeler before the model is imported into Simulation. No other changes to the model are needed. Figure 34 shows the propeller blade geometry file in DesignModeler.

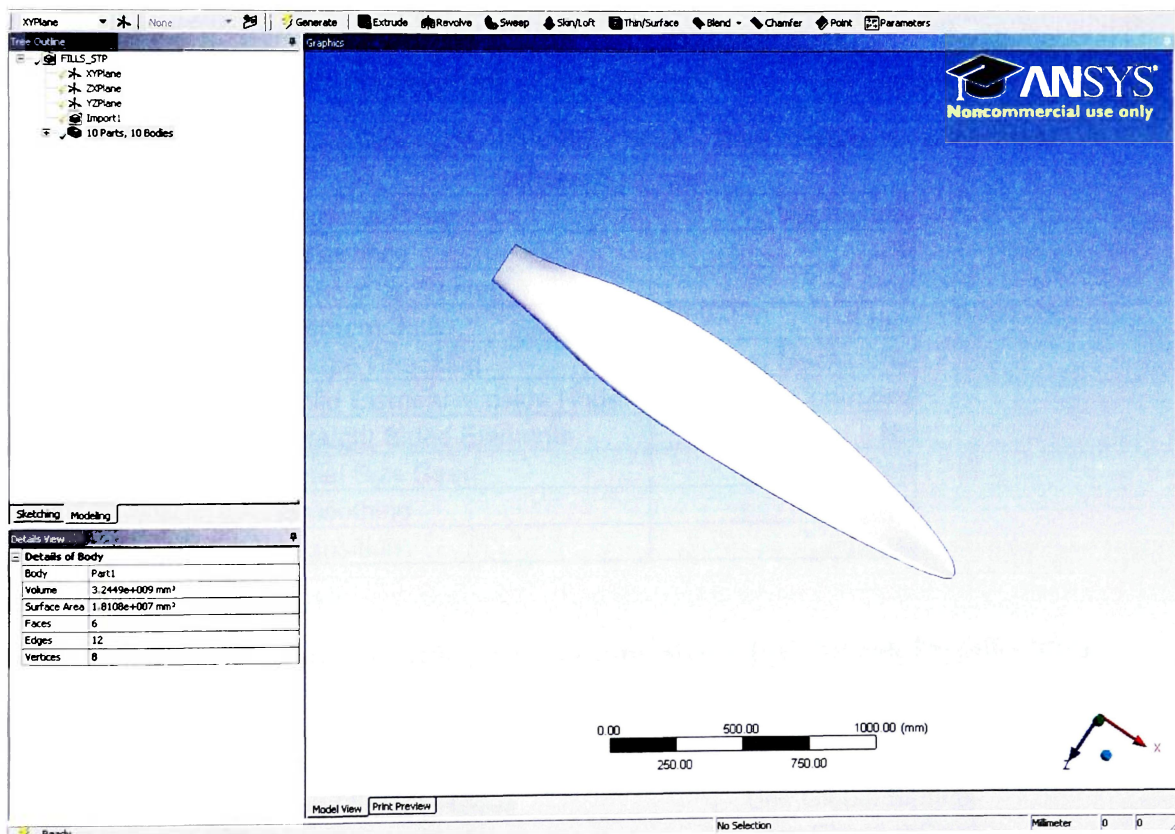


Figure 34: High Altitude Propeller Blade in DesignModeler

#### 4.3.3.5. Simulation

The blade geometry is imported into Simulation from DesignModeler. For structural analysis, a new static structural analysis is added to the model. The propeller is only constrained at the hub, so a fixed support is only placed at the hub of the blade. Since no CFD results are made available for the current blade geometry, no CFX pressure load is applied to the blade.

Nevertheless, Figure 35 illustrates the mesh generated for the structural analysis. Table 25, Table 26, and Table 27 show the general mesh, mesh method, and face sizing settings of the propeller blade, respectively.

**Table 25: General Settings for Structural Mesh – High Altitude Propeller Blade**

<b>General Settings</b>	
Physical Preference	Mechanical
Relevance	100
Relevance Center	Fine
Element Size	6 mm
Shape Checking	Standard Mechanical
Solid Element Midside Nodes	Program Controlled
Straight Sided Elements	No
Initial Size Seed	Part
Smoothing	High
Transition	Fast

**Table 26: Mesh Method Settings for Structural Mesh – High Altitude Propeller Blade**

<b>Mesh Method -- Patch Independent</b>	
Method	Tetrahedrons
Algorithm	Patch Independent
Element Midside Nodes	Use Global Setting
Defined By	Max Element Size
Max Element Size	6 mm
Define Defeaturing Tolerance	No
Curvature and Proximity Refinement	Yes
Min Size Limit	3 mm
Span Angle	Fine
Minimum Edge Length	25.155 mm

**Table 27: Face Sizing Settings for Structural Mesh – High Altitude Propeller Blade**

Face Sizing	
Location	Hub and Shroud
Type	Element Size
Element Size	3 mm
Edge Behavior	Curv/Proximity Refinement

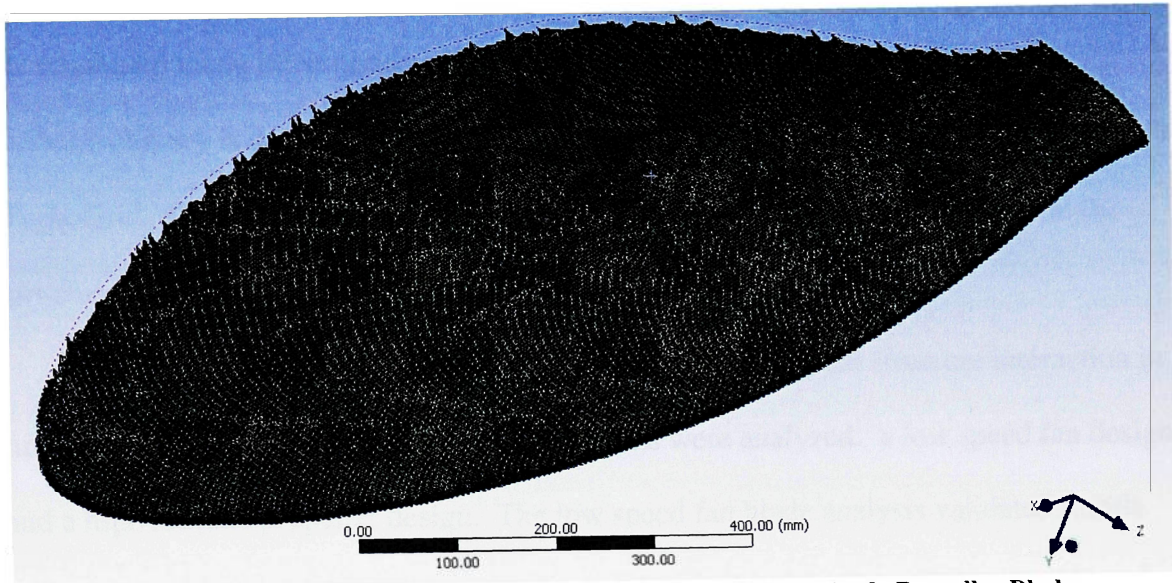


**Figure 35: Structural Mesh Created in Simulation – High Altitude Propeller Blade**

From Figure 35, the mesh does not cover the entire trailing edge of the blade. The trailing edge of the blade is very thin, so Simulation has difficulty meshing it. When the maximum and minimum size parameters change to smaller values, Simulation is not able to mesh the blade. Since a smaller mesh size is not allowed and the current mesh does not cover the entire blade, the next step to change the mesh is to modify the geometry of the blade so the trailing edge is not too thin. One way to modify the geometry is to trim and round off the trailing edge of the blade, so it does not end as a sharp point with very little thickness.

## 5. CONCLUSIONS AND RECOMMENDATIONS

Combining CFD and structural analysis is essential when designing turbomachinery and optimizing its performance. The fluid structure interaction process in ANSYS Workbench provides an environment where CFD and structural analysis may be combined using interconnected programs. Within ANSYS Workbench, the turbomachinery is designed or imported into BladeModeler, and meshed in CFX-Mesh or TurboGrid. CFD analysis is performed in CFX and Simulation is used to perform the structural analysis.

To develop a process within ANSYS Workbench for fluid structure interaction in turbomachinery, two turbomachinery applications were analyzed: a low speed fan design and a high altitude propeller design. The low speed fan blade analysis validated results with the previous study [5]. The current research used Model 1 from Reference [5] and followed the ANSYS Workbench approach specified in Figure 1, which employed BladeGen, BladeEditor, CFX-Mesh, CFX, DesignModeler, and Simulation software components. Note that some of the programs now available ANSYS Workbench were also used in the previous research (BladeGen and CFX).

Comparing the previous CFD results with the current CFD predictions, the ANSYS Workbench environment process was able to successfully perform the CFD analysis on the fan blade. The differences between CFD results in the previous and current research were less than 1% (Table 7). With no structural analysis performed in Reference [5], the current research conducted the structural analysis of the fan blade using two different materials: Polyethylene and ABS plastic. Comparing results for the two plastics (Table 14), both the maximum shear stress and maximum equivalent stress

agreed within 5%. On the other hand, the predicted maximum total deformations showed a difference of 88%. This indicates that different types of plastic create very different deformations, and the proper choice is clearly very important in the overall design study.

For the high altitude propeller blade analysis, the blade was created using a model from NASA's ERAST study that also performed CFD analysis on a high altitude propeller blade [9]. The chord and pitch angle distributions along the span of the blade were used to create a 3D CAD blade model in the current analysis. Two analyses were performed on the blade design: a preliminary design using a blade element theory spreadsheet used to calculate the blade's performance variables and a fluid structure interaction analysis in ANSYS Workbench. The results from the blade element theory spreadsheet showed high errors. The high errors were possibly attributed to the fact that the spreadsheet used a NACA 4412 airfoil for performance predictions, while the high altitude propeller blade employed an Eppler 387 airfoil.

Next, analysis on the high altitude propeller blade was attempted using the ANSYS Workbench environment. However, problems arose while importing the blade model into ANSYS due to the fact that BladeGen appeared to be not well-suited for highly twisted propeller blades. Neither importing method, importing the blade using BladeGen's Data Import Wizard nor creating a meanline file of the blade, worked in the process. Instead, a 3D CAD model of the blade and its surrounding fluid domain was imported into DesignModeler and CFX-Mesh created an unstructured mesh of the blade and fluid domain.

Since the propeller blade was not created in BladeGen, BladeEditor was not used to automatically mesh the blade and the mesh was manually created in CFX-Mesh.

When running CFD analysis in CFX, an error occurred indicating two isolated volumes in the mesh. With this error, CFX was not able to run and no CFD results were produced. No structural analysis was run on the propeller because the loading on the blade for structural analysis should be based on the CFD results that were not made available. Even though no structural analysis was completed, the structural mesh was created for illustration.

Analyzing the two turbomachinery applications, ANSYS Workbench proves to be a useful tool for combining CFD and structural analysis in one design environment.

However, with the problems in the propeller blade analysis, some possible recommendations follow to help eliminate the encountered problems:

1. Use correct airfoil properties for an Eppler 387 airfoil (i.e. coefficient of lift, coefficient of drag, and coefficient of lift slope) in order to implement in the blade element theory spreadsheet. Also, include the correct Reynolds number correction in the spreadsheet for the operating low Reynolds number of the blade.
2. Research the CFX error message of having two isolated volumes in the blade and fluid domain model.
  - a. Investigate the current boundary conditions set in CFX-Pre to see if they are correct for the current blade and fluid domain model.
  - b. Reevaluate the 3D CAD model design for use in ANSYS Workbench. Instead of connecting just the fluid domain curves to create one geometry in CATIA, connect the blade surface and the fluid domain so everything is in one geometry.



3. Modify the blade trailing edge geometry, so the structural mesh covers the entire blade. Trim and round off the trailing edge to increase its thickness.
4. Instead of using CFX-Mesh to mesh the propeller blade after it is imported into DesignModeler, use TurboGrid, GAMBIT, or ANSYS ICEM to mesh the blade for CFD analysis.
5. Contact L. Danielle Koch to gather the propeller blade's missing information, including the angular velocity of the blade and the blade tip geometry.

Even though the fluid structure interaction process in ANSYS Workbench works and the low speed fan blade analysis is complete, some suggestions are listed to improve and enhance the analysis process:

1. Research and apply the correct plastic of the low speed fan blade for structural analysis. As the results show, the type of plastic for the low speed fan blade changes the maximum total deformation of the blade.
2. Incorporate the two-way coupling feature for fluid structure interaction in ANSYS Workbench. This creates a multi-field solver that solves the CFD and structural analysis simultaneously.
3. Use DesignXplorer in ANSYS Workbench to create an optimization analysis of the CFD and structural analysis.

## REFERENCES

- [1] ANSYS BladeModeler. ANSYS, Inc. January 11, 2007.
- [2] Robinson, Chris and Peter Came. “CFX Shortens Fan Design Time From Three Months to One.” CFX Update No. 23, Summer 2003.
- [3] Arnal, Michel, Christian Precht, and Thomas Sprunk. “Fluid Structure Interaction Makes for Cool Gas Turbine Blades.” ANSYS Advantage Vol. 1, Issue 1, 2007.
- [4] Elder, Robin, Ian Woods, and Simon Mathias. “Streamlined Flutter Analysis.” ANSYS Advantage Vol. 1, Issue 3, 2007.
- [5] Idahosa, Uyi. An Automated Optimal Design of a Fan Blade using an Integrated CFD/MDO Computer Environment. MS Thesis. Embry-Riddle Aeronautical University. Daytona Beach, Florida. December 2005.
- [6] San Diego Plastics, Inc. “ABS Plastic.” <<http://www.sdplastics.com/abs.html>>
- [7] Goodfellow. “Polyacrylonitrile-butadiene-styrene (ABS) – Material Information.” <<http://www.goodfellow.com/csp/active/static/A/Polyacrylonitrile-butadiene-styrene.HTML>>
- [8] The British Plastics Federation. “ABS – Acrylonitrile Butadiene Styrene Plastic.” 2003. <[http://www.bpf.co.uk/bpfindustry/plastics\\_materials\\_Acrylonitrile\\_Butadiene\\_Styrene\\_ABS.cfm](http://www.bpf.co.uk/bpfindustry/plastics_materials_Acrylonitrile_Butadiene_Styrene_ABS.cfm)>
- [9] Koch, L. Danielle. Design and Performance Calculations of a Propeller for Very High Altitude. MS Thesis. Case Western Reserve University. Cleveland, Ohio. February 1998. NASA TM-1998-206637.
- [10] Adkins, C.N. and R.H. Liebeck. “Design of Optimum Propellers.” New York: American Institute of Aeronautics and Astronautics. 1983. AIAA 1983-190-516.
- [11] “1976 Standard Atmosphere Properties.” Last updated on March 25, 2008. <<http://www.luizmonteiro.com/StdAtm.aspx>>
- [12] Eastlake, Charles. Blade Element Theory Spreadsheet.
- [13] Usher, Colin. “Airfoil Calculator Eppler 387.” 2007. <<http://www.colinusher.info/Model%20Aircraft/aerofoils.html> >
- [14] Rhode, PhD, Axel. CATIA Macro.
- [15] “Meanline Data File Format (rtzt).” ANSYS BladeGen On-Line Help Contents.
- [16] Anderson, Jr., John D. Fundamentals of Aerodynamics. Third Edition. New York: McGraw-Hill, 2001.

## APPENDIX A – LOW SPEED FAN BLADE CFD RESULTS

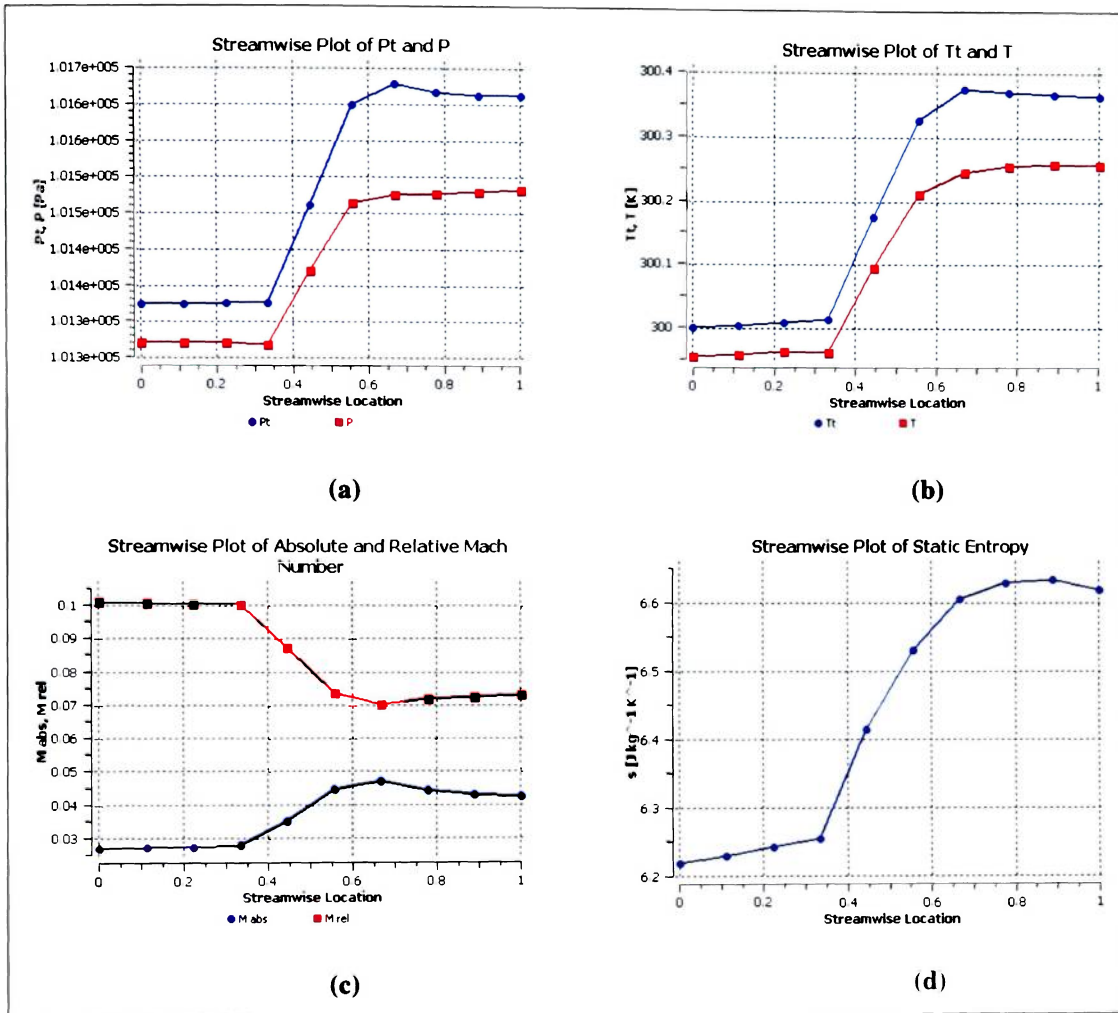
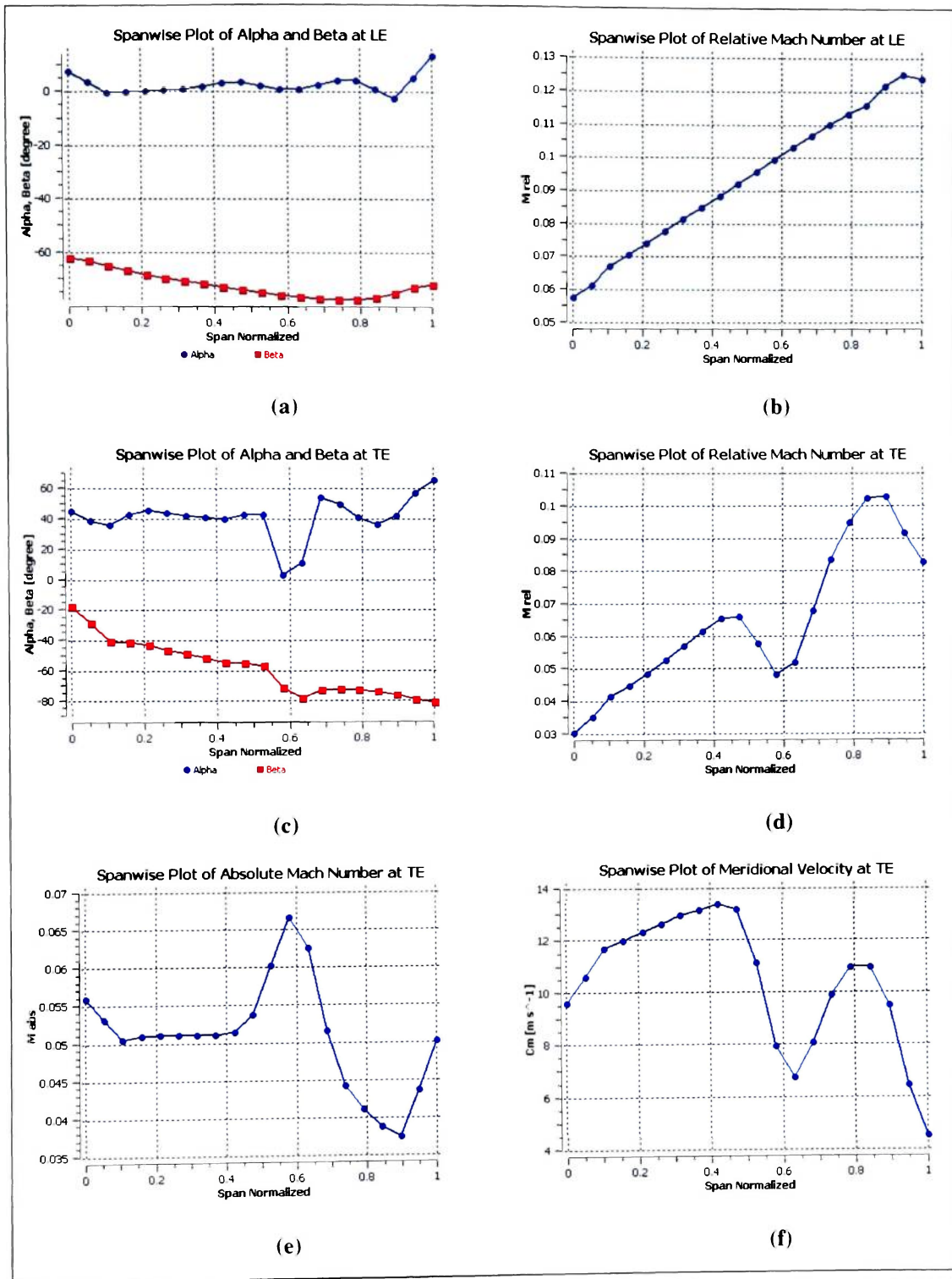
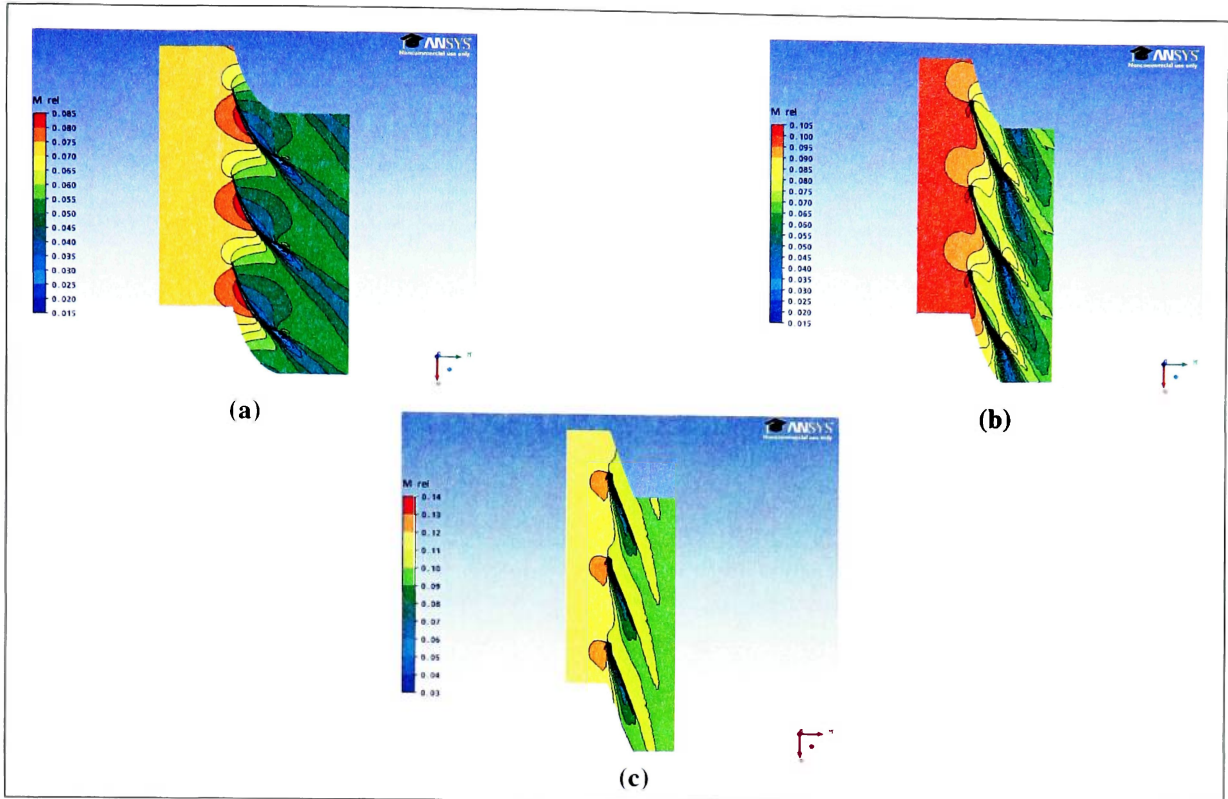


Figure 36: Low Speed Fan Blade CFX Results – Streamwise Plots: (a) Pt and P, (b) Tt and T, (c) Absolute and Relative Mach Number, and (d) Static Entropy



**Figure 37: Low Speed Fan Blade CFX Results – Spanwise Plots: (a) Alpha and Beta at LE, (b) Relative Mach Number at LE, (c) Alpha and Beta at TE, (d) Relative Mach Number at TE, (e) Absolute Mach Number at TE, and (f) Meridional Velocity at TE**



**Figure 38: Low Speed Fan Blade CFX Results – Contour of Relative Mach Number at (a) 20% Span, (b) 50% Span, and (c) 80% Span**

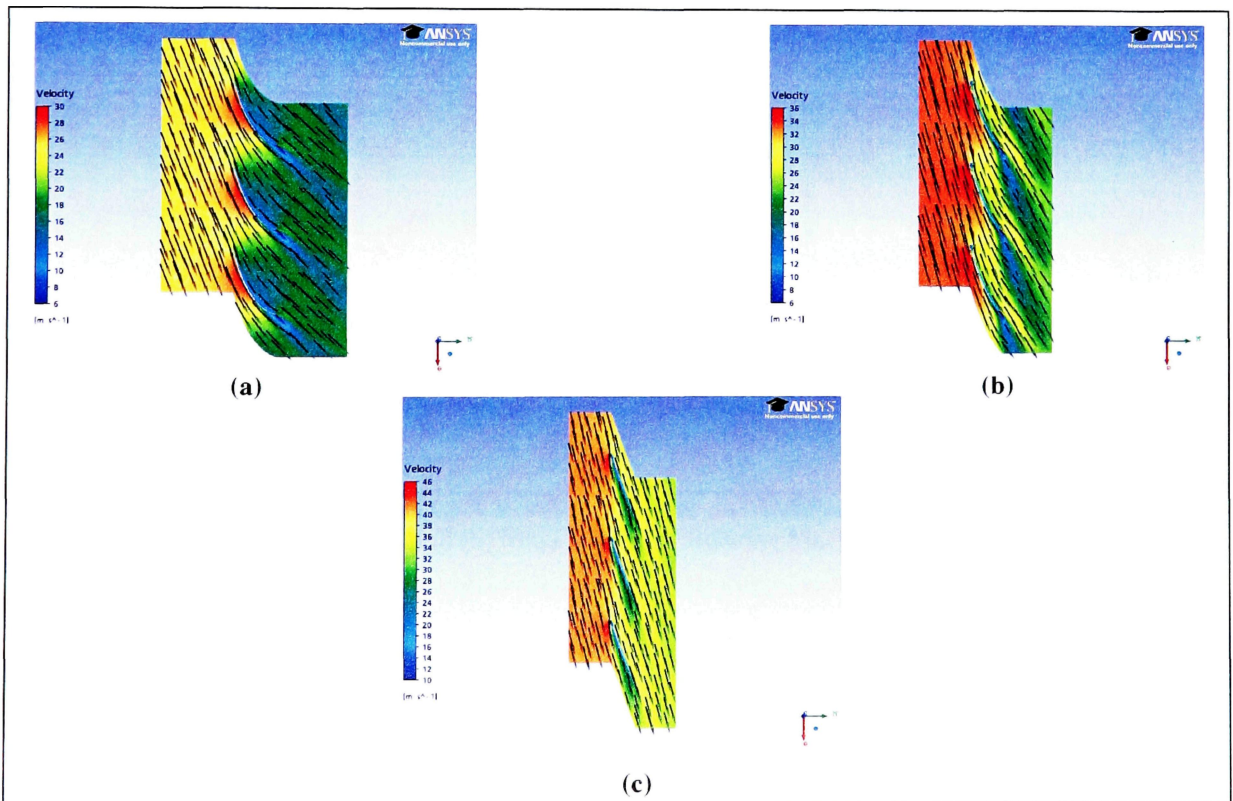


**Figure 39: Low Speed Fan Blade CFX Results – Velocity Vectors at (a) 20% Span, (b) 50% Span, and (c) 80% Span**



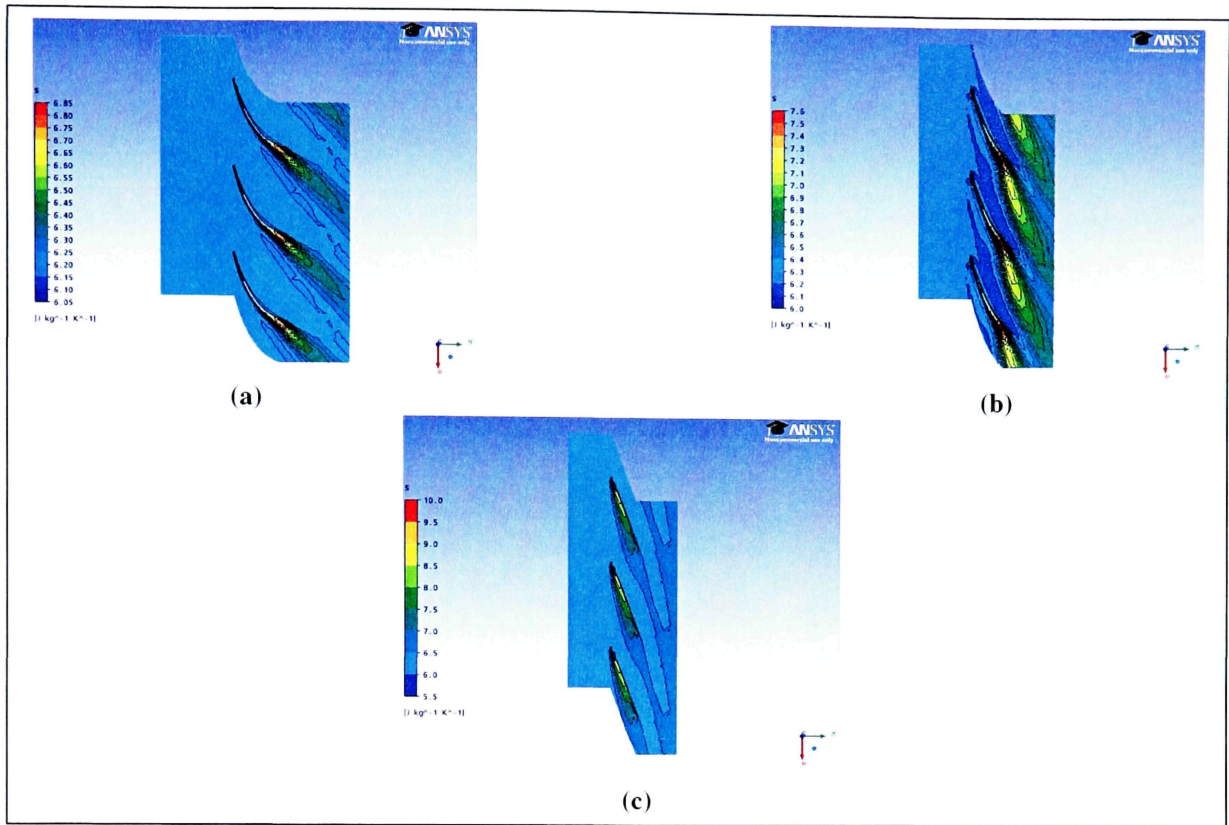


Figure 40: Low Speed Fan Blade CFX Results – Contour of Specific Entropy at (a) 20% Span, (b) 50% Span, and (c) 80% Span

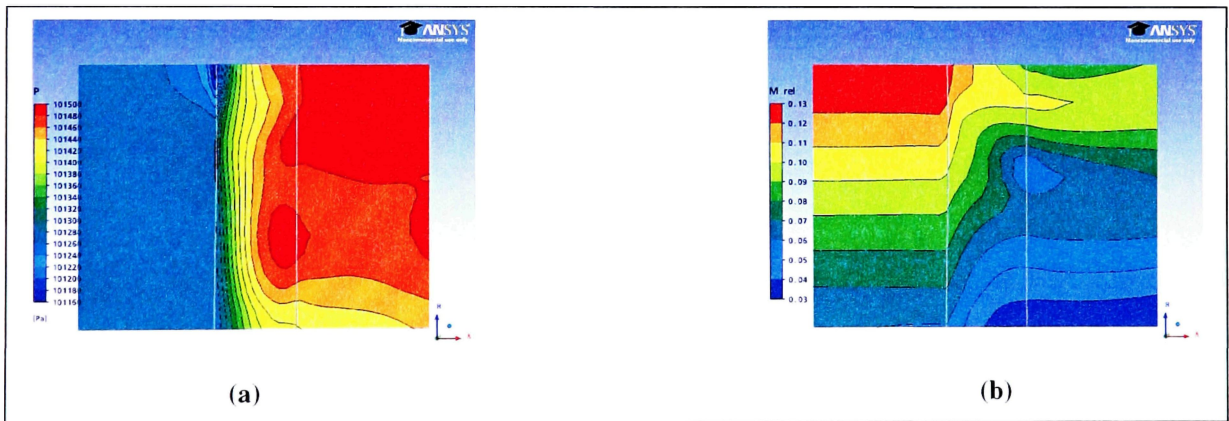


Figure 41: Low Speed Fan Blade CFX Results – Contour on Meridional Surface of (a) Mass Averaged Pressure and (b) Mass Averaged Relative Mach Number

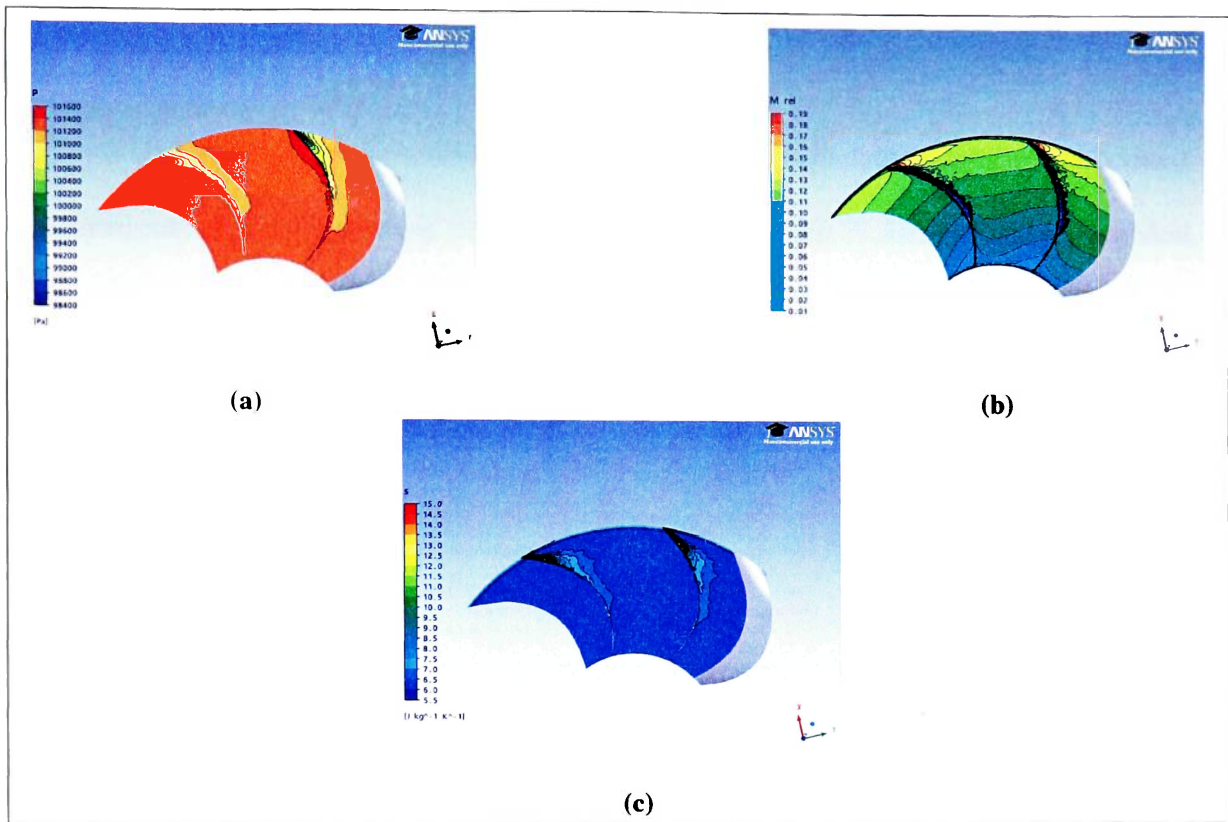


Figure 42: Low Speed Fan Blade CFX Results – Contour at Blade LE of (a) Pressure, (b) Relative Mach Number, and (c) Specific Entropy

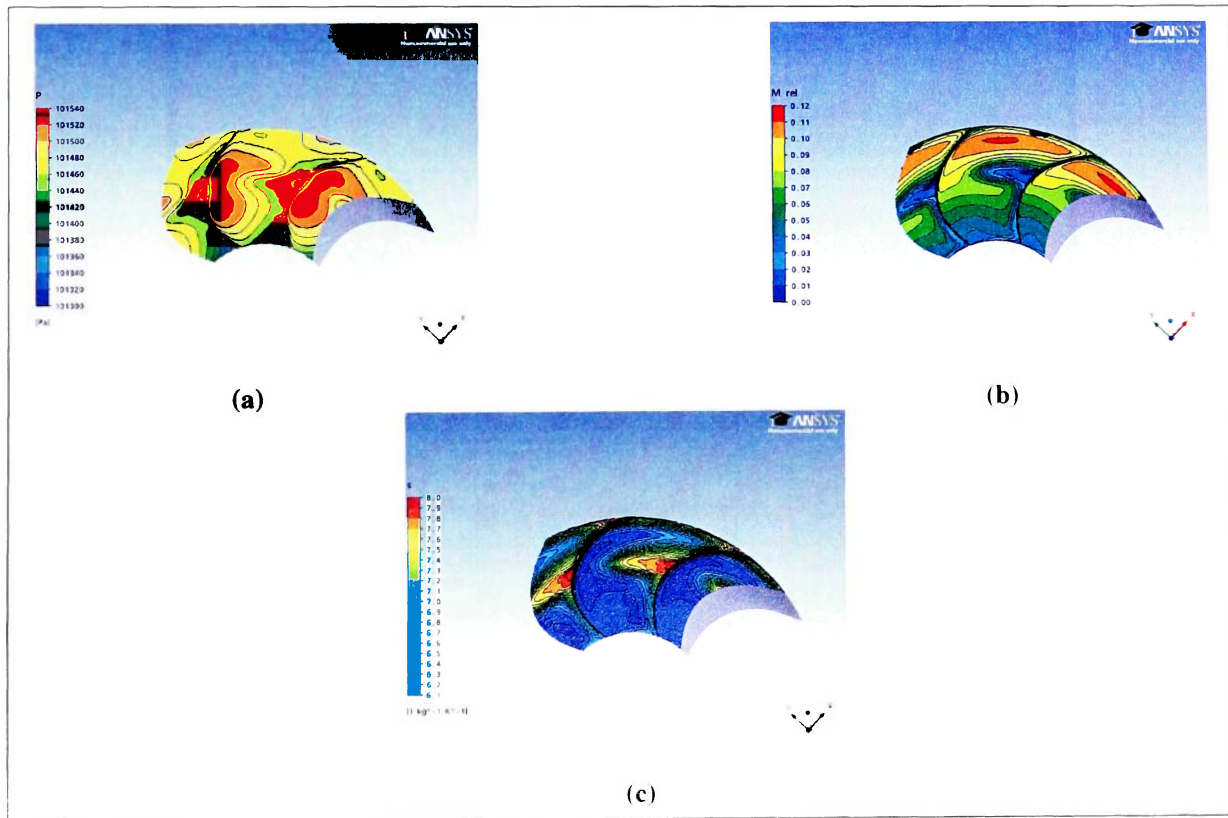


Figure 43: Low Speed Fan Blade CFX Results – Contour at Blade TE of (a) Pressure, (b) Relative Mach Number, and (c) Specific Entropy

## APPENDIX B – ATMOSPHERE SOURCE

Using the atmosphere website [11], the altitude at which the propeller is operated is typed into the corresponding field and the atmospheric data is automatically calculated.

The following figure gives a sample of the standard atmospheric data from the website:

1976 Standard Atmosphere Properties (0-86 km)		<input checked="" type="checkbox"/> Show additional decimal point	Clear
<b>Variables</b>			
Geometric Altitude (Z)	25908.0 [m]	85000 [ft]	16.0985 [sm]
Geopotential Altitude (H)	25802.8 [m]	84654.9 [ft]	16.0331 [sm]
Lapse rate ( $\lambda$ or $L_{\lambda}$ )	0.0010 [K/m]	0.30480 [°C/1000 ft]	
Temperature Ratio ( $\theta$ )	0.772004		
Molecular Temperature ( $T_w$ )	222.4528 [K]	-50.6972 [°C]	
	400.4151 [°R]	-59.2549 [°F]	
Kinetic Temperature (T)	222.4528 [K]	-50.6972 [°C]	
	400.4151 [°R]	-59.2549 [°F]	
Mean Molec. Wt. Ratio ( $M/M_0$ )	1.0000000		
Mean Molecular Weight (M)	28.9644 [kg/kmol] or [lb/lbmol]		
Pressure Ratio ( $\delta$ )	2.19023e-2		
Pressure (P)	2.21925e+3 [Pa] or [N/m <sup>2</sup> ]	6.55345e-1 [in Hg]	
	2.21925e+1 [hPa] or [mbar]	1.66458e+1 [mmHg] or [torr]	
	4.63501e+1 [lb <sub>f</sub> /ft <sup>2</sup> ]	3.21875e-1 [lb <sub>f</sub> /in <sup>2</sup> ]	
Density Ratio ( $\sigma$ )	2.83708e-2		
Density ( $\rho$ )	3.47542e-2 [kg/m <sup>3</sup> ]	6.74342e-5 [slug/ft <sup>3</sup> ]	
Gravitational Accel. Ratio ( $g/g_0$ )	0.99190		
Gravitational Acceleration (g)	9.72720 [m/s <sup>2</sup> ]	31.9134 [ft/s <sup>2</sup> ]	
Dynamic Viscosity Ratio ( $\mu/\mu_0$ )	8.12194e-1		
Dynamic Viscosity ( $\mu$ )	1.45332e-5 [kg/(m·s)]	3.0353e-7 [slug/(ft·s)]	
Kinematic Viscosity Ratio ( $\eta/\eta_0$ )	2.86278e+1		
Kinematic Viscosity ( $\eta$ )	4.18172e-4 [m <sup>2</sup> /s]	4.50117e-3 [ft <sup>2</sup> /s]	
Speed of Sound Ratio ( $C_s/C_{s0}$ )	8.78637e-1		
Speed of Sound ( $C_s$ )	298.995 [m/s]	980.955 [ft/s]	581.200 [Kts]
Pressure Scale Height ( $H_s$ )	6564.66 [m]	21537.60 [ft]	4.079092 [sm]
Number Density (N)	7.22595e+23 [1/m <sup>3</sup> ]	2.55182e+25 [1/ft <sup>3</sup> ]	
Mean Air-Particle Speed ( $v$ )	403.246 [m/s]	1322.986 [ft/s]	783.848 [Kts]
Mean Collision Frequency ( $\nu$ )	1.72471e+8 [1/s]		
Mean Free Path (L)	2.33805e-6 [m]	7.67078e-6 [ft]	1.45280e-9 [sm]
Therm. Cond. Ratio ( $k_p/k_{p0}$ )	7.89393e-1		
Therm. Conductivity Coeff. ( $k_p$ )	1.99921e-2 [W/(m·K)]	1.24480e-4 [BTU/(ft·s·°R)]	
Mole Volume ( $v_m$ )	8.33408e+2 [m <sup>3</sup> /kmol]	5.20280e+1 [ft <sup>3</sup> /lbmol]	

Figure 44: Sample of Atmospheric Data Table



Sample of Spreadsheet

**Prop with tip loss (no duct)**

C.N. Eastlake, 8/5/2004.

Engine/prop Data	
Engine HP	<b>85</b>
N	<b>3</b>
R (ft)	<b>7.55</b>
Prop RPM	<b>860.35</b>
Fwd speed (kts)	<b>232.48</b>

**Meekins design, Revision 2**

Calculated Prop Data	
A (ft <sup>2</sup> )	178.9
$\Omega$ (rad/s)	90.09
$\Omega R$ (ft/s)	679.80
Fwd speed (ft/s)	392.4

Atmospheric Data (@ 85,000 ft)	
$\rho$ (slug/ft <sup>3</sup> )	<b>6.74E-05</b>
$V_{sound}$ (ft/sec)	<b>980.96</b>
$\rho/\mu$ (sec/ft <sup>2</sup> )	<b>222.17</b>

Echo of prop output data from results page	
Thrust	70
Total HP	47.1
% power	55.5
$\eta_{PROP}$	1.055

Notes:

1. **Bold font** indicates required input data.
2. Analysis is combined momentum theory and blade element theory presented in classic helicopter rotor texts. Focus changed from helicopter rotor to propeller in forward flight. For helicopter rotor, vertical climb speed is entered in forward speed cell (B10).
3. Drag coefficient equation was changed from that for NACA 0012 to NACA 4412.
4. Compressibility correction is now made to drag coefficient (limit = 0.1) and lift curve slope (limit = 7/rad).
5. Reynolds number correction is now made to drag coefficient, using a base Rn=3,000,000.
6. Calculated max lift coefficient is limited to a cutoff value of 1.4 at Rn=3,000,000. Rn correction is made to the limit.
7. Tip losses are calculated, which inherently presumes a free prop (not inside a duct).
8. Lift curve slope input is 2-D airfoil value and again inherently presuming free prop, an aspect ratio correction is calculated.
9. Pitch increment to simulate controllable pitch prop is entered on Results sheet, cell E16, and is automatically transferred to the column above.
10. Sea level standard atmospheric conditions are assumed for input data. Data for any other altitude may be entered instead.

$r = \sqrt{R}$	Prop					$\theta$ (rad)	$M$	$\text{sqrt}(l M^2)$	incomp 2D			incomp 3D			Intermediate steps in induced velocity calculation			
	chord (in)	Chord (ft)	Bavelinc $\theta$ (deg)	Echo of $\Delta\theta$ (deg)	Zero lift 4OA (deg)				$C_{l\alpha}$ (1/rad)	$C_{l\alpha}$ (1/rad)	$C_{l\alpha}$ (1/rad)	$\sigma = Nc/\pi R$	$\phi$ (rad)	I	II	III	IV	
0.1	6.40	0.5331	78.5	0.40	-2.30	1.4040	0.069	0.998	6.28	5.07	5.08	0.0675	1.3962	210.752	-201.534	2648.118	14.538	
0.15	7.22	0.6015	76.5	0.40	-2.30	1.3677	0.104	0.995	6.28	5.07	5.10	0.0761	1.3138	212.615	-113.503	2347.196	16.402	
0.2	9.19	0.7655	73.3	0.40	-2.30	1.3131	0.139	0.990	6.28	5.07	5.12	0.0969	1.2359	217.089	35.359	1844.225	20.876	
0.25	11.48	0.9569	69.8	0.40	-2.30	1.2513	0.173	0.985	6.28	5.07	5.15	0.1211	1.1639	222.308	32.897	1475.380	26.095	
0.3	13.45	1.1210	66.5	0.40	-2.30	1.1931	0.208	0.978	6.28	5.07	5.19	0.1419	1.0980	226.781	94.232	1259.471	30.568	
0.4	16.24	1.3533	60.0	0.40	-2.30	1.0804	0.277	0.961	6.28	5.07	5.28	0.1713	0.9822	233.118	195.150	1043.198	36.905	
0.5	17.39	1.4490	54.2	0.40	-2.30	0.9786	0.347	0.938	6.28	5.07	5.41	0.1834	0.8837	235.728	272.832	974.308	39.515	
0.6	17.39	1.4490	49.6	0.40	-2.30	0.8986	0.416	0.909	6.28	5.07	5.58	0.1834	0.7994	235.728	340.628	974.308	39.515	
0.7	16.40	1.3670	45.0	0.40	-2.30	0.8186	0.485	0.874	6.28	5.07	5.80	0.1730	0.7249	233.491	386.671	1032.766	37.278	
0.75	15.42	1.2850	42.9	0.40	-2.30	0.7823	0.520	0.854	6.28	5.07	5.94	0.1626	0.6906	231.255	405.243	1098.687	35.041	
0.8	14.27	1.1893	41.3	0.40	-2.30	0.7532	0.554	0.832	6.28	5.07	6.09	0.1505	0.6587	228.645	426.782	1187.088	32.432	
0.9	10.50	0.8749	38.1	0.40	-2.30	0.6986	0.624	0.782	6.28	5.07	6.49	0.1107	0.5974	220.071	462.444	1613.697	23.858	
0.95	7.71	0.6425	36.7	0.40	-2.30	0.6732	0.658	0.753	6.28	5.07	6.74	0.0813	0.5669	213.734	477.061	2197.375	17.521	
0.977	5.25	0.4374	37.1	0.40	-2.30	0.6804	0.677	0.736	6.28	5.07	6.89	0.0554	0.5493	208.142	511.510	3227.394	11.929	
0.992	3.28	0.2734	36.7	-0.40	-2.30	0.6732	0.687	0.726	6.28	5.07	6.98	0.0346	0.5373	203.669	515.196	5163.831	7.456	
1.0	0.98	0.0820	36.7	0.40	-2.30	0.6732	0.693	0.721	6.28	5.07	7.00	0.0104	0.5268	198.450	522.823	17212.769	2.237	

↓	avg chord	0.8988	↑
			Pitch $\Delta\theta$
			0.40

Thrust/Power Calculations	
B	0.9462
$(C_T)_{no1sec}$	1.3011 02
$(AC_T)_{1P}$	5.0851 04
$C_T$	1.2501 02
T (lb)	69.7
$C_{m1}$	4.5671 04
$(C_Q)_{n1}$	6.4891 03
$(\Delta C_Q)_{11}$	1.0271 04
$C_{m2}$	6.3861 03
$C_Q$	6.8431 03
Total HP	47.15
% power	55.47
$\eta_{PROP}$	1.0547

$i, (i \in S)$	$i + V_i$	$\alpha (r, d)$	$\alpha (d, c)$	$m_{comp}$ $C_d$	$comp_{c, visible}$ $C_i$	Resultant V Rn	$C_{int}$ for Rn $C_a$	$C_i$	$dC_i/dw$	$dC_{cp}/dr$	$dC_{cp}/dr$	$dC_{cp}/dr$	$dC_{cp}/dr$	$dC_{cp}/dr$	$dC_{cp}/dr$
7.07	385.36	0.0078	0.45	0.0084	0.0084	4.717E+04	0.0193	0.0399	1.346E+05	6.515E+07	1.879E+06	6.217E+06	8.831E+08	1.206E+06	
4.42	388.00	0.0539	3.09	0.0100	0.0100	5.418E+04	0.0224	0.2747	2.352E+04	2.881E+06	4.636E+05	2.503E+05	3.018E+07	5.893E+06	
1.71	390.72	0.0772	4.42	0.0111	0.0112	7.063E+04	0.0237	0.3954	7.660E+04	9.191E+06	1.893E+04	6.175E+05	7.919E+07	1.713E+05	
1.92	394.35	0.0874	5.01	0.0116	0.0118	9.092E+04	0.0238	0.4502	1.704E+03	2.249E+05	4.958E+04	1.213E+04	1.706E+06	3.833E+05	
6.26	398.69	0.0952	5.45	0.0121	0.0123	1.101E+05	0.0239	0.4934	3.150E+03	4.574E+05	1.038E+03	5.125E+04	8.739E+06	1.914E+04	
14.97	407.39	0.0982	5.63	0.0123	0.0128	1.435E+05	0.0235	0.5182	7.100E+03	1.290E+04	2.790E+03	9.431E+04	1.980E+05	3.993E+04	
21.85	414.28	0.0949	5.44	0.0123	0.0131	1.671E+05	0.0233	0.5131	1.176E+02	2.670E+04	5.197E+03	1.502E+03	3.753E+05	6.980E+04	
27.00	419.43	0.0993	5.69	0.0127	0.0139	1.822E+05	0.0244	0.5535	1.827E+02	4.836E+04	8.763E+03	2.066E+03	6.134E+05	1.023E+03	
29.06	421.49	0.0937	5.37	0.0126	0.0144	1.873E+05	0.0251	0.5437	2.304E+02	7.432E+04	1.169E+02	1.198E+03	4.066E+05	6.145E+04	
28.90	421.32	0.0916	5.25	0.0126	0.0147	1.837E+05	0.0258	0.5441	2.488E+02	8.833E+04	1.259E+02	1.315E+03	4.841E+05	6.876E+04	
28.49	420.92	0.0945	5.41	0.0129	0.0155	1.772E+05	0.0273	0.5759	2.774E+02	1.053E+03	1.461E+02	2.860E+03	1.183E+04	1.523E+03	
23.78	416.21	0.1013	5.80	0.0138	0.0177	1.413E+05	0.0325	0.6570	2.946E+02	1.313E+03	1.584E+02	1.393E+03	6.540E+05	7.496E+04	
18.73	411.16	0.1062	6.09	0.0145	0.0192	1.079E+05	0.0374	0.7158	2.626E+02	1.304E+03	1.415E+02	6.658E+04	3.398E+05	3.580E+04	
14.18	406.60	0.1131	7.51	0.0164	0.0223	7.498E+04	0.0467	0.8666	2.290E+02	1.206E+03	1.229E+02	2.683E+04	1.490E+05	1.436E+04	
9.22	401.65	0.1359	7.78	0.0157	0.0217	4.738E+04	0.0497	0.8165	1.389E+02	8.378E+04	7.401E+03	7.298E+05	4.738E+06	3.830E+05	
2.92	395.35	0.1464	8.39	0.0143	0.0198	1.430E+04	0.0577	0.6987	3.626E+03	2.993E+04	1.910E+03				

## Spreadsheet Equations

The following equations are ones that are not explained in Preliminary High Altitude Propeller Blade Design section. These equations are taken directly from the spreadsheet.

### **Span Increment Calculated Values**

#### Non-dimensional Radial Position / Span Location

$$r = \frac{y}{R}$$

#### Corrected Pitch Angle

$$\theta = \theta_b + \Delta\theta - \alpha_{L=0}$$

#### Mach Number

$$M = r \frac{\Omega R}{a}$$

#### Compressibility Correction Factor

$$C_{cf} = \sqrt{1 - M^2}$$

#### Incompressible 3D Coefficient of Lift Slope

$$(C_{L\alpha})_{incom,3D} = (C_{L\alpha})_{incom,2D} \frac{R / C_{avg}}{2 + R / C_{avg}}$$

#### Compressible 3D Coefficient of Lift Slope

$$(C_{L\alpha})_{com} = \begin{cases} \frac{(C_{L\alpha})_{incom,3D}}{C_{cf}} & \text{if } (C_{L\alpha})_{com} < 7 \\ 7 & \text{otherwise} \end{cases}$$

### Solidity

$$\sigma = \frac{Nc}{\pi R}$$

### Flow Angle

$$\phi = \tan^{-1} \left( \frac{V}{r \Omega R} \right)$$

### Induced Velocity with Intermediate Equations

$$v_i = I \left( -1 + \sqrt{1 + \frac{II}{III + V_f + IV}} \right)$$

$$I = \frac{V_f}{2} + \frac{\sigma(C_{L\alpha})_{incom,3D} \Omega R}{16}$$

$$II = 2\theta r \Omega R - V_f$$

$$III = \frac{4V_f^2}{\sigma(C_{L\alpha})_{incom,3D} \Omega R}$$

$$IV = \frac{\sigma(C_{L\alpha})_{incom,3D} \Omega R}{16}$$

### Tangential Velocity

$$V = v_i + V_f$$

### Angle of Attack

$$\alpha = \theta - \phi$$

### Incompressible Drag Coefficient

$$(C_d)_{incom} = 0.008251 + 0.003014C_L + 0.01678C_L^2 - 0.01972C_L^3 + 0.01029C_L^4$$

### Compressible Drag Coefficient

$$(C_d)_{com} = \frac{(C_d)_{incom}}{C_{cf}}$$

### Reynolds Number

$$R_n = \frac{\rho}{\mu} c \sqrt{(r\Omega R)^2 + V_f^2}$$

### Compressible Drag Coefficient with Reynolds Number Correction

$$(C_d)_{Rn} = \begin{cases} (C_d)_{com} \left( \frac{3,000,000}{R_n} \right)^{0.2} & \text{if } (C_d)_{Rn} < 0.1 \\ 0.1 & \text{otherwise} \end{cases}$$

### Coefficient of Lift

$$C_L = \begin{cases} (C_{L\alpha})_{com} \alpha & C_L < 1.4 \left( \frac{R_n}{3,000,000} \right)^{0.13} \\ 1.4 \left( \frac{R_n}{3,000,000} \right)^{0.13} & \text{otherwise} \end{cases}$$

### Coefficient per Unit Radius for Thrust

$$\frac{dC_T}{dr} = \frac{\sigma}{2} r^2 C_L$$

### Coefficient per Unit Radius for Profile Torque

$$\frac{dC_{Q_p}}{dr} = \frac{\sigma}{2} r^3 (C_d)_{Rn}$$

### Coefficient per Unit Radius for Induced Torque

$$\frac{dC_{Q_i}}{dr} = \frac{dC_T}{dr} \phi r$$

## Other Calculated Values

### Blade Surrounding Area

$$A = \pi R^2$$

### Tip Loss Distance

$$B = 1 - \frac{\sqrt{2(C_T)_{no\ loss}}}{N}$$

### Thrust Coefficient with No Tip Loss

$$(C_T)_{no\ loss} = \sum_i^{k-1} \left( \frac{dC_T}{dr} \right)_{trap_i}$$

### Thrust Coefficient Tip Loss

$$(\Delta C_T)_{tip\ loss} = \frac{1}{2} \left[ \left( \frac{dC_T}{dr} \right)_{r=1.0} + \left[ \left( \frac{dC_T}{dr} \right)_{r=1.0} - SLOPE \left( \left( \frac{dC_T}{dr} \right)_{r=0.9} : \left( \frac{dC_T}{dr} \right)_{r=1.0}, r_{0.9} : r_{1.0} \right) (1-B) \right] \right] (1-B)$$

*SLOPE* is a function in Microsoft Excel that calculates the slope of the linear regression line between the selected points

### Thrust Coefficient

$$C_T = (C_T)_{no\ loss} - (\Delta C_T)_{tip\ loss}$$

### Thrust

$$T = C_T \rho A (\Omega R)^2$$

### Profile Torque Coefficient

$$C_{Q_i} = \sum_i^{k-1} \left( \frac{dC_{Q_i}}{dr} \right)_{trap_i}$$

### Induced Torque Coefficient with No Tip Loss

$$(C_{Q_i})_{no\ loss} = \sum_i^{k-1} \left( \frac{dC_{Q_i}}{dr} \right)_{trap_i}$$

### Induced Torque Coefficient Tip Loss

$$(\Delta C_{Q_i})_{tip\ loss} = (1 - B) \left( \frac{dC_{Q_i}}{dr} \right)_{r=1.0}$$

### Induced Torque Coefficient

$$C_{Q_i} = (C_{Q_i})_{no\ loss} - (\Delta C_{Q_i})_{tip\ loss}$$

### Torque Coefficient

$$C_Q = C_{Q_e} + C_{Q_i}$$

### Total Power

$$(HP)_{Total} = \frac{1}{550} C_Q \rho A (\Omega R)^3$$

### Percent of Power

$$\% Power = 100 \frac{(HP)_{Total}}{(HP)_e}$$

### Propeller Efficiency

$$\eta_{prop} = \frac{T V_f}{550 (HP)_{Total}}$$



## APPENDIX D – ANSYS, INC. BLADEGEN EMAIL

The following is an email sent by ANSYS, Inc. representative Mihajlo Ivanovic explaining the reason the high altitude propeller blade is not able to be imported into ANSYS Workbench through BladeGen using the Data Import Wizard or the meanline file:

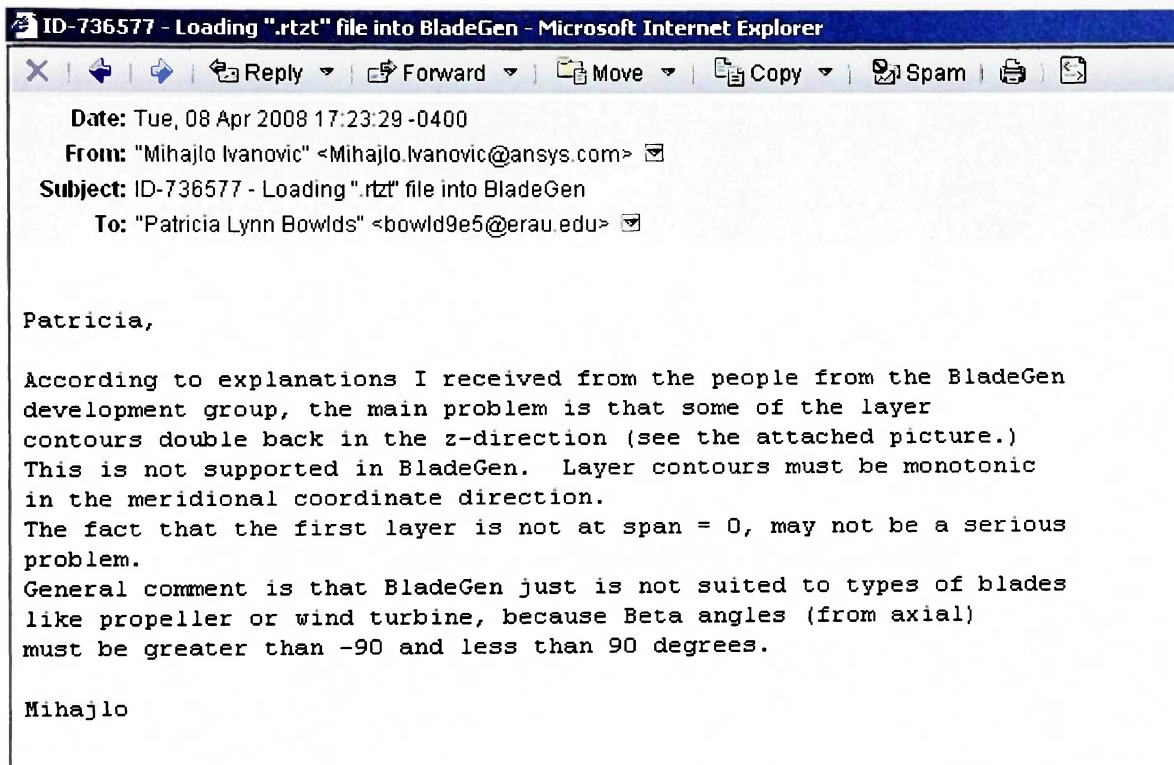


**Figure 45: Propeller Blade Importing Error Email Explanation from ANSYS, Inc.**